NSTX Upgrade

DISRUPTION ANALYSIS OF PASSIVE PLATES, VACUUM VESSEL AND COMPONENTS

NSTXU-CALC-12-01-01

Rev 1

April , 2011

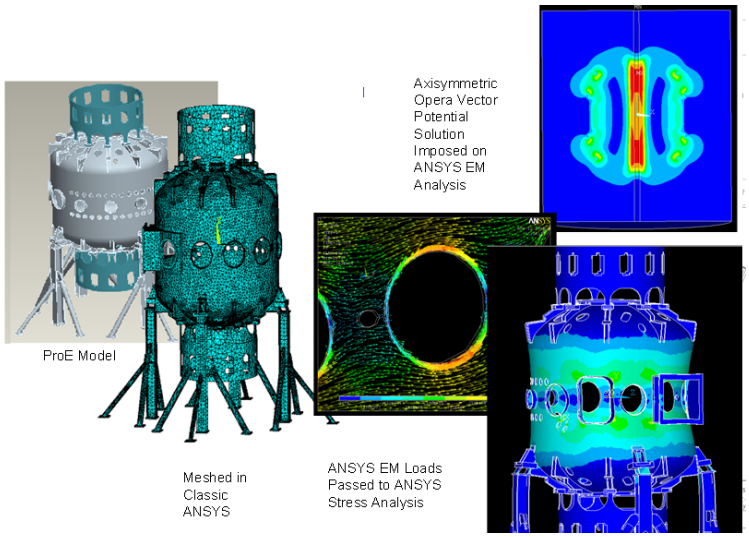

Prepared By:

Peter Titus,
Contributing Authors: A.Brooks, Srinivas Avasarala, J. Boales PPPL Mechanical Engineering

Reviewed By:

Peter Titus, Branch Head, Engineering Analysis Division

Reviewed By:

Phil Heitzenroeder, Head, Mechanical Engineering

PPPL Calculation Form

Calculation # NSTXU-CALC-12-01-01 Revision # 00 ____ WP #, 1672
(ENG-032)

Purpose of Calculation: (Define why the calculation is being performed.)

To provide guidance on passive plate and divertor hardware upgrades needed to survive upgrade disruption loads. In addition, the vessel, and a number of other vessel internal components are analyzed for disruption loads.

References (List any source of design information including computer program titles and revision levels.)

These are included in the body of the calculation, in section 6.3

Assumptions (Identify all assumptions made as part of this calculation.)

This calculation is based on transfer of Vector Potential (VP) data from an OPERA disruption simulation. The OPERA simulation is axisymmetric and relatively simple with respect to it's modeling of conducting structures near the plasma. An assumption is made that the complicated hardware of the passive plates, antennae. diagnostics tiles etc do not substantially alter the electromagnetic environment of the disruption, beyond what is represented in the OPERA model.

Calculation (Calculation is either documented here or attached)

These are included in the body of the following document

Conclusion (Specify whether or not the purpose of the calculation was accomplished.)

For the fast quench disruptions, the passive plate hardware require upgrades to resist the larger disruption loads from the upgrade increases in plasma current and toroidal field. Slow translations of the plasma near the surface of the secondary passive plate are more severe. The bolts and passive plates are overstressed for these cases assuming .5% damping.

Cognizant Engineer's printed name, signature, and date:

Phil Heitzenroreder: _____

I have reviewed this calculation and, to my professional satisfaction, it is properly performed and correct.

Checker's printed name, signature, and date

Pete Titus: _____

2.0 Table of Contents

4.0 Executive Summary

The objective of this analysis is to estimate and assess the stresses in the vacuum vessel, selected internal components, and passive plates caused by the plasma disruption. Bake-out stresses on the passive plates have been considered in the original design and are addressed in calculation #NSTX-CALC-11-6. [1]

Mid-plane disruptions and quenches are manageable. For these events, the loads required some modest upgrades of the mounting hardware. The slow VDE's may be more severe for the secondary passive plate. These appear to be generating large counter currents in the plate as the plasma approaches it. - as would be expected from passive plates. The background fields were input too high for the secondary passive plate, and as of April 21 2011, the slow VDE's are being re-run.

Development of this procedure began in Summer 2009 and was worked on by Srinivas Avasarala, Ron Hatcher.\, Art Brooks, Larry Bryant, and Joseph Boales. Early test runs are included in Section 7 as illustrations of the procedure

The Vector Potential solution for a 2D axisymmetric simulation of disruption in OPERA is imposed on the 3-D model in ANSYS to obtain the eddy currents and Lorentz forces. A static and dynamic stress pass is then run and the stresses are computed. A number of other calculations address components not covered in this calculation. Some components like the vessel port region, and the bellows, are considered in this calculation, and in greater depth in other calculations. The divertor tiles, diagnostic shutters are some of the components addressed in other calculations. The primary purpose of this calculations was to address the passive plates. Other components have been added because the procedures developed for the passive plates are useful for many components.

Figure 4.0-1 View of Passive Plates and Lower Divertor During an Outage. Divertor Tiles have been removed an a protective cover is on the secondary passive plate

Vector potentials obtained from OPERA are arranged in 80x80 tabular form so that they can be fed into ANSYS. The first 11 tables are considered for the study and these tables are spaced 0.5 ms apart. Macros are developed that read these values into ANSYS. The meshes in OPERA and ANSYS are dissimilar, but since ANSYS interpolates the tables between two adjacent indices, proper indexing of the coordinates yields a reasonable approximation of the Vector Potentials. The element type used was SOLID 97 and the material properties used are that of Stainless Steel except for the passive plates which are made up of Copper. This model is then solved for eddy currents and Lorentz forces..

The model is then converted into a structural model by switching the SOLID 97s into SOLID 45s. For the test cases, eleven load steps, 5ms apart are written for the stress pass. Later analyses use up to 45 steps. Forces are read from the earlier E-mag results by using LDREAD command and both the static and dynamic analyses are performed. A 0.5% damping factor is used in the dynamic run.

The procedure has been multiply checked. In section 7 of this calculation the consistency with the OPERA analysis was checked. Poloidal and toroidal field plots were checked. In section 7.6.1, results were compared with disruption simulations done only in ANSYS for the HHFW antenna. Results for the mid plane disruption were similar. In section 9.2.2 the total currents in the major components of the toroidal elements that would inductively pick up the plasma current, were summed. These included the vessel, the passive plates and the centerstack casing. They approximately add to the plasma current. This should be the case for inductively coupled closely nested current loops.

Stress Summary (Dynamic Unless Otherwise Noted)

Component	Section	Damp	Disruption	Stress	Allowable
Vessel At Port Ligaments Near Bay L NB and Thom Scattering Ports		.5%	Mid Plane Disruption	40 MPa	40 MPa*
Vessel Support Column Intersection with Vessel		.5%	Mid Plane Disruption	40 MPa	40 MPa*
Secondary Passive Plate		.5%	Mid Plane Disruption	90 MPa	171 MPa
Secondary Passive Plate			Fast Quench Plasma 4	180 MPa	171 MPa
Secondary Passive Plate		.5%	P1-P5 Slow	360 MPa	***
Tresca from Shear Stress in Passive Plate Counter-bore	9.5	.5%	Fast Quench Plasma 4	232 MPa	171 MPa
Centerstack Casing (No Halo)	11.2	.5%	Mid Plane Disruption	1 MPa	1 MPa*
TAE Antenna Moly Shield	14.0	.5%	Mid-Plane Disruption	200	600 Yield

* These are values passed on to other calculations to be added to normal operational loads. Comparison with the allowable needs to be performed in these calculations.
*** Being Re-run with correct background field.

5.0 Digital Coil Protection System.

There is no input to the DCPS planned for disruption loading of components. The loading calculated for the vessel, passive plates and other components in this calculation is based on the maximum toroidal field for the upgrade, and the maximum poloidal fields for the 96 scenarios specified in the design point spreadsheet.

6.0 Design Input

6.1 Criteria

Stress Criteria are found in the NSTX Structural Criteria Document. Disruption specifications are outlined in the GRD -Ref [7] and are discussed in more detail in section 6.5

6.2 References

[1] Structural Analysis of NSTX Passive Plates and Support Structures, NSTX CALC 11-06, Brad Nelson, B. Gorenson, June 8 1998

[2] Disruption specification J. Menard spreadsheet: disruption_scenario_currents_v2.xls, July 2010. NSTX Project correspondence, input to Reference [1]

[3] "Characterization of the Plasma Current quench during Disruptions in the National Spherical Torus Experiment" S.P. Gerhardt, J.E. Menard and the NSTX Team Princeton Plasma Physics Laboratory, Plainsboro, NJ, USA Nucl. Fusion 49 (2009) 025005 (12pp) doi:10.1088/0029-5515/49/2/025005

[4] ITER material properties handbook, ITER document No. G 74 MA 15, file code: ITER-AK02-22401.

[5] Disruption Analysis Of Vacuum Vessel and Passive Plates NSTX-CALC-12-001-00, S. Avasarala

[6] NSTX Disruption Simulations of Detailed Divertor and Passive Plate Models by Vector Potential Transfer from OPERA Global Analysis Results P. H. Titus[a], S. Avasaralla, A.Brooks, R. Hatcher 2010 SOFT Conference, Porto Portugal October 20110

[7] NSTX Upgrade General Requirements Document, NSTX_CSU-RQMTS-GRD Revision 0, C. Neumeyer, March 30, 2009

[8] Inductive and Resistive Halo Current s in the NSTX Centerstack, A.Brooks, Calc # NSTX-103-05-00

[9] OPERA 2D Disruption Analyses, R. Hatcher, NSTX upgrade calculation #NSTXU-CALC- NSTXU-CALC-12-03-00

[10] NSTX HHFW (High Harmonic Fast Wave) Eddy Current Analysis for Antenna NSTX-CALC-24-03-00 Jan 10, 2011, Han Zhang, PPPL

[11] email from Michael Bell estimating loads on the TAE antenna, Appendix G.

[12] Modeling of the Toroidal Asymmetry of Poloidal Halo Currents in Conducting Structures N. Pomphrey, J.M. Bialek_, W. Park Princeton Plasma Physics Laboratory,

[13] NSTX Halo Current Analysis of Center Stack NSTX-133-05-00-April 13, 2010Art Brooks

[14] Center Stack Casing Bellows, NSTXU-CALC-133-10-0 by Peter Rogoff.

[15] Neutral Beam Armor Backing Plate NSTXU-CALC-24-02-00, Larry Bryant

[16] Diagnostics Review and Database NSTXU-CALC-40-01-00, Joseph Boales

[17]Vessel Port Re-work for NB and Thompson Scattering Port, Calculation number NSTXU-CALC-24-01-00

6.3 Photos and Drawing Excerpts

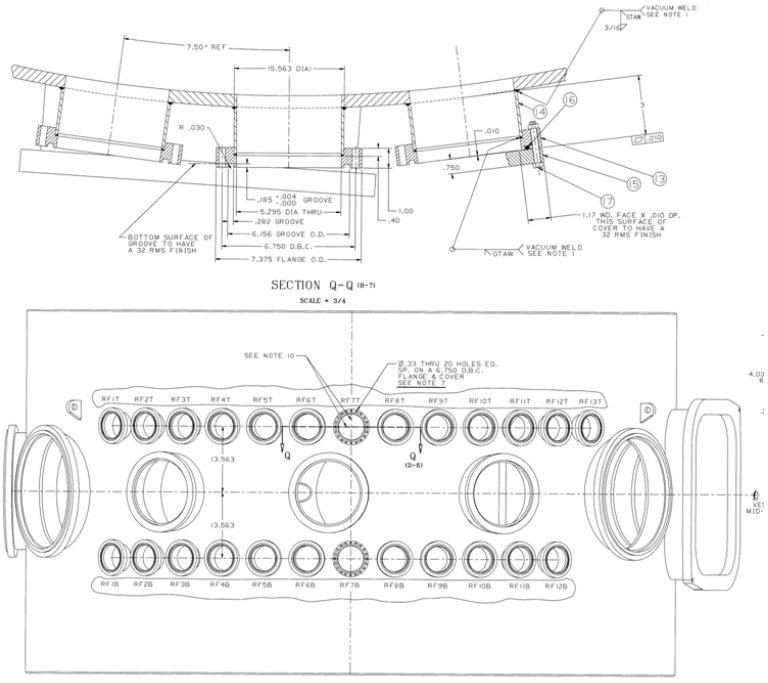

Figure 6.4-1 Vessel Cylindrical Shell Elevation

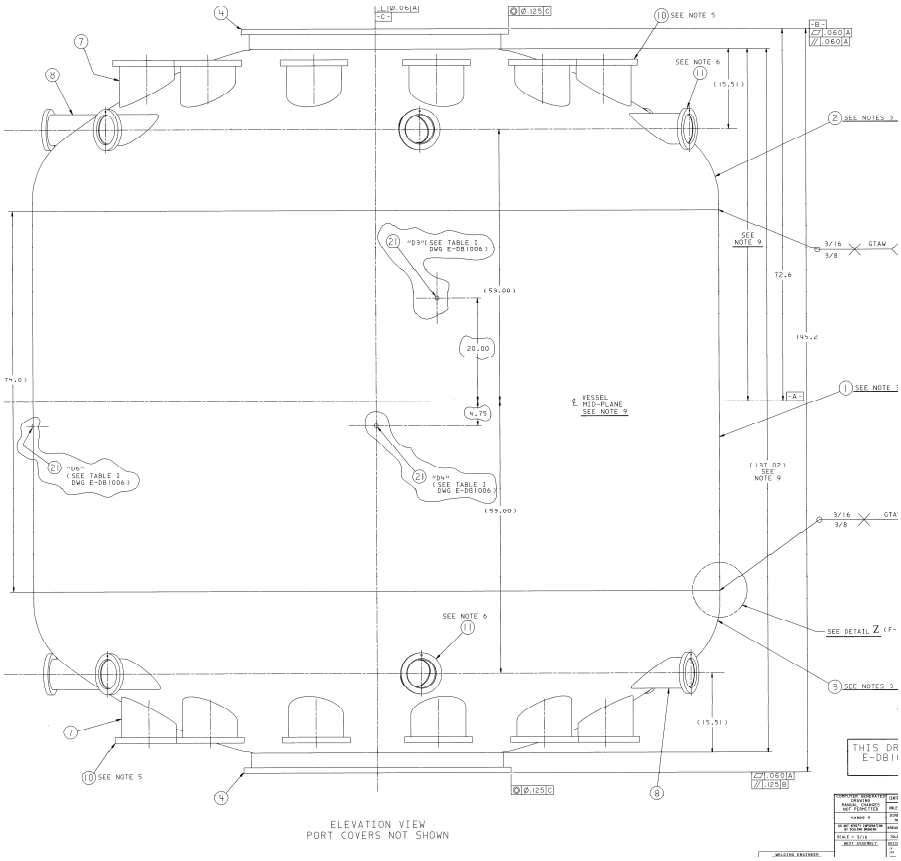

Figure 6.4-2 Vessel Elevation

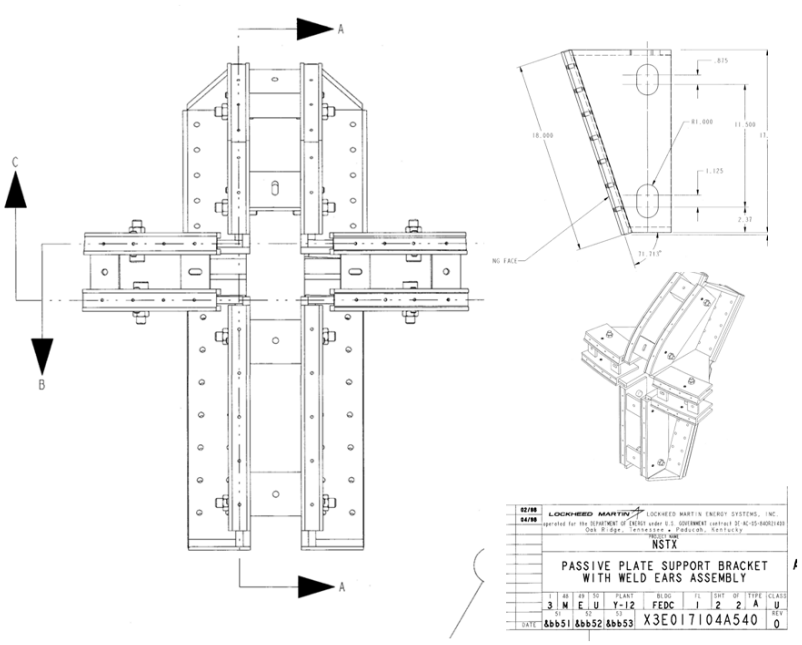

Figure 6.4-3 Passive Plate Bracket

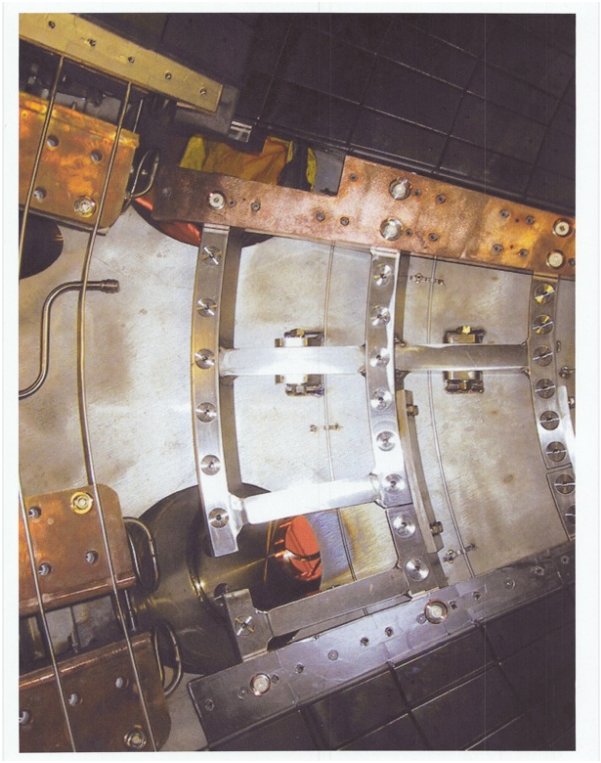

Figure 6.4-4 Lower Outer Divertor "Barbeque" Rails

6.4 Materials and Allowables

Vessel Shell – 304 Stainless 45 ksi Yield, 30 ksi Near Welds

05/19/1998 13:53 6174728409 NEWENGLANDSTEELTANK PAGE 03

Avesta Sheffield

Avesta Sheffield Plate Inc.

Certificate of Analysis and Tests

OUR ORDER 106101 - 01 HEAT & PIECE 87893-3B 5/13/98

SOLD TO: PROCESS SYSTEMS INTERNATIONAL 20 WALKUP DRIVE WESTBOROUGH MA 01581

SHIP TO: NEW ENGLAND STEEL TANK 111 BROCK ROAD SOUTH QUINCY MA 02169 737001-06

PSI MIC NO. P5627

YOUR ORDER & DATE

558635 3/18/98 TAG# PART #V077P001

ITEM DESCRIPTION

HEAT & PIECE 87893 - 3B 3A
WEIGHT 3092
FINISH 1
GRADE 304 UNS-S30400
DIMENSIONS .625 X 76.000 X 212.000 EXACT

SPECIFICATIONS

THE PRODUCTS LISTED ON THIS MILL TEST REPORT SATISFY PREFERENCE CRITERION B AS DEFINED IN ARTICLE 401 OF THE NORTH AMERICAN FREE TRADE AGREEMENT. COUNTRY OF ORIGIN IS USA

ASTM A240-96A ASMESA240-96AD
NO WELD REPAIR ON MATERIAL
ASTM A262-93A PRAC A

ASTM A480-96,ASMESA480-96AD
MAG PERM <1.05 ASTM A342 (6)
ASTM A262-93A PRAC E

PLATES & TEST PCS SOLUTION ANNEALED @ 1950 DEGREES FARENHEIT MINIMUM. THEN WATER COOLED OR RAPIDLY COOLED BY AIR
FREE OF MERCURY CONTAMINATION
HOT ROLLED, ANNEALED & PICKLED (HRAP)

MECHANICAL & OTHER TESTS

HARDNESS RB	81	
GRAIN SIZE	5	
YIELD STRENGTH (PSI)	45254	✓
TENSILE STRENGTH (PSI)	91368	✓
BEND	OK	✓
INTERGRANULAR CORROSION	OK	
ELONGATION % IN 2"	63.6	✓
REDUCTION OF AREA %	72.5	

Centerstack Casing

INCONEL 625

Test Temperature, °F(°C)	Ultimate Tensile Strength, ksi (MPa)	Yield Strength at 0.2% offset,ksi (MPa)	Elongation in 2" percent
Room	138.8 (957)	72.0 (496)	38
200	133.3 (919)	67.3 (464)	41
400	129.4 (892)	62.2 (429)	44
600	125.6 (866)	59.5 (410)	45
800	122.2 (843)	59.2 (408)	45

The passive Plates are made of CuCr1Zr UNS.C18150. Chromium Zirconium Copper C18150 is a copper alloy with high electrical conductivity, hardness, and ductility, moderate strength, and excellent resistance to softening at elevated temperatures. The addition of 0.1% zirconium (Zr) and 1.0% chromium (Cr) to copper results in a heat treatable alloy which may be solution treated and subsequently aged to produce these desirable properties. NSTX Bake-out temperature is 350 degrees C. The softening temperature of properly heat treated C18150 rod exceeds 500°C as compared to unalloyed pure copper which softens at 200°C, and silver bearing coppers which soften at 350°C.

From Ref [1] **Table 4 Material properties assumed for analysis**

Property	units	304L sst [7]		Cu-Cr-Zr, (18150) Solution annealed and aged [6]	
		150 C (302 F)	350 C (662 F)	150 C (302 F)	350 C (662 F)
Young's modulus (temp effect < 5%)	psi	28 E6	28 E6	17 E6	17 E6
Min Tensile strength	psi	70,000 (RT)	--	49,000	38,000
Min. Yield Strength	psi	25,000 (RT)	--	40,000 276 MPa	34,000 234 MPa
Sm		15, 300	13,700	16,500 114 MPa	13,000
1.5Sm				171 MPa	
3Sm				341 MPa	
Coeff of therm expansion	in/in-F	0.96 E-5	0.96 E-5	0.98 E-5	0.98 E-5
Thermal Conductivity	BTU/ hr-ft-F	9.4	9.4	208	202

According to the NSTXU criteria as currently written, the Sm for CuCrZr should be the lesser of 2/3 yield or 26.6ksi/184 MPa or 24.5ksi/169 MPa - or Sm = 24.5ksi/169 MPa

Tensile Property (average) [4]

Material	Yield strength (MPa)	UTS (MPa)	Average over
Low strength (L)	78	248	3
Intermediate strength (I)	199.4	318.6	3
High strength (H)	297	405.3	5

This is from the ITER Materials Database and the NSTX allowable would be the lesser of 202 or 198 MPa.

6.5 Disruption Specs:

The requirements for disruption analysis are outlined in the NSTX Upgrade General Requirements Document [7]. The latest (August 2010) disruption specification were provided by Jon Menard as a spreadsheet: disruption_scenario_currents_v2.xls.[2] This reference includes a suggested tile phasing of the inductively driven currents and the halo currents.

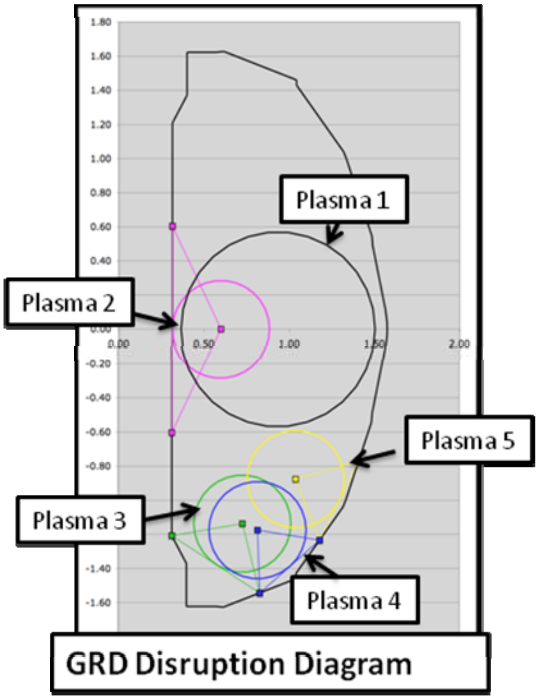

New High Priority Disruption Analyses
Centered disruption, fast quench
Initiated shifted to CS, fast quench, no halo
Inward drift to CS, very slow quench, halo
Initiated shifted down to inboard, fast quench, no halo
Vertical drift to inboard, very slow quench, halo
Initiated shifted down to middle, fast quench, no halo
Vertical drift to middle, very slow quench, halo
Initiated shifted down to outboard, fast quench, no halo
Vertical drift to outboard, very slow quench, halo

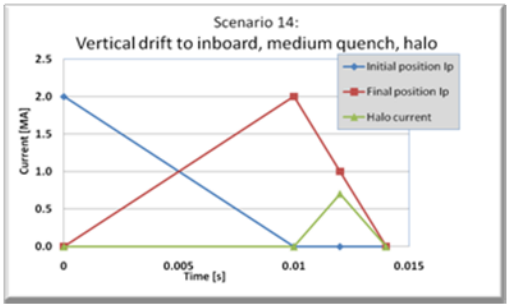

	Plasma 1	Plasma 2	Plasma 3	Plasma 4	Plasma 5
	Centered	Offset, Midplane	Offset, Inboard	Offset, Central	Offset, Outboard
Center of plasma (r,z) [m]	0.9344	0.5996	0.7280	0.8174	1.0406
	0.0000	0.0000	-1.1376	-1.1758	-0.8768
Minor radius of plasma [m]	0.5696	0.2848	0.2848	0.2848	0.2848

Criteria from the GRD:

Current and field directions (referring to Figure 2.2-2) shall be as follows; Plasma current Ip into the page (counter-clockwise in the toroidal direction, viewed from above) Halo current exits plasma and enters the structure at the entry point, exits the structure and re-enters the plasma at the exit point (counter-clockwise poloidal current, in the view of the figure) Toroidal field into the page (clockwise in the toroidal direction, viewed from above)

For the halo currents a toroidal peaking factor of 2:1 shall be assumed in all cases. Thus the toroidal dependence of the halo current is $[1 + \cos(\phi - \phi_0)]$, for $\phi = 0$ to 360° where ϕ is the toroidal angle.

Table 2-2 - Plasma Disruption Specifications

	Centered	Offset, Midplane	Offset, Inboard	Offset, Central	Offset, Outboard
Center of plasma (r,z) [m]	0.9344	0.5996	0.7280	0.8174	1.0406
	0.0000	0.0000	-1.1376	-1.1758	-0.8768
Minor radius of plasma [m]	0.5696	0.2848	0.2848	0.2848	0.2848
Current Quench					
Initial plasma current [MA]	2	2	2	2	2
Linear current derivative [MA/s]	-1000	-1000	-1000	-1000	-1000
VDE/Halo					
Initial plasma current	2	0	0	0	0
Final plasma current [MA]	0	2	2	2	2
Linear current derivative [MA/s]	-200	200	200	200	200
Halo current [MA]	n.a	20%=	35%=	35%=	35%=
		400kA	700kA	700kA	700kA
Halo current entry point (r,z) [m]	n.a	0.3148	0.3148	0.8302	1.1813
		0.6041	-1.2081	-1.5441	-1.2348
Halo current exit point (r,z) [m]	n.a	0.3148	0.8302	1.1813	1.4105
		-0.6041	-1.5441	-1.2348	-0.7713

7.0 Analysis Procedure and Test Runs

The analysis procedure is discussed in a more concise fashion in a SOFT paper, ref. [6]. Ron Hatcher's disruption analyses [9] were used to provide a vector potential "environment" for a model of all the components affected by the disruption. Sri Avasarala developed a procedure which starts with Ron Hatcher's OPERA disruption simulation, and transfers the axisymmetric vector potential results into a 3 D electromagnetic (EM) model of the vessel and passive plates. Background toroidal and poloidal fields are applied by superimposing appropriate vector potential distributions. The macros used to impose the background fields were supplied by Art Brooks. With modest changes, any of the vessel internal components can be evaluated with this procedure. Originally the OPERA analyses included poloidal fields that were selected to be worst case loading for a specific component - initially for the passive plates, but to be able to used the OPREA data more generically for other components, the opera analysis was revised to use no added background fields, but simply to develop the poloidal field changes from the disruption. Background fields are added in the ANSYS analysis.

7.1 Opera Analyses

OPERA axisymmetric analyses utilize a specialized formulation of the VP degree of freedom. Computations are done with r*A theta as the solution degree of freedom. The resulting VP solution must be divided by the radius of the coordinate point before passing this to the 3D ANSYS EM analysis. Figure 7.3-1 shows an ANSYS reconstruction of the NSTX poloidal fields from the OPERA to ANSYS VP data transfer.

An email from Bob Pillsbury:

```
The 2D OPERA default potential is r*A-theta - they call it "modified
potential".It is definitley an axisymmetric formulation.  Are you
thinking of converting to cartesian components and applying to 3D
structures? It's a kludge, but if that's the only way to get close...
Not sure if it helps, but I think it's not a real problem to do the
math in OPERA and output Ax and Ay. BTW - you can ask for a potential
of A-theta, but VF recommends the other.
Regards
Bob:
```

The VDE specified by the CDR GRD did not include a final quench – This was a reasonable assumption for a fast VDE (a flux conserved solution would attempt to preserve the original flux state of the centered mid-plane plasma). In later analyses a final quench was added.

7.2 Preparation and Use of the Table Data

Vector potentials obtained from OPERA are arranged in 81x81 tabular form so that they can be mapped into ANSYS as table data. Data transfer is done in a cylindrical coordinate system with only r-z coordinate results from the 2D analysis mapped to the 3D model.

*dim,vect%inum%,table,81,81,1,x,z,,5 ! Specifies a 81X 81 parameter table

*tread,vect%inum%,'VecPot_case_%inum%','txt' ! Reads the table text file into the table

A typical number of time points extracted from the OPERA analysis produced 44 tables The time points represented by the tables are input with a parameter set. . Macros are developed that read these table values into ANSYS. The meshes in OPERA and ANSYS are dissimilar, but since ANSYS interpolates the tables between two adjacent indices, proper indexing of the

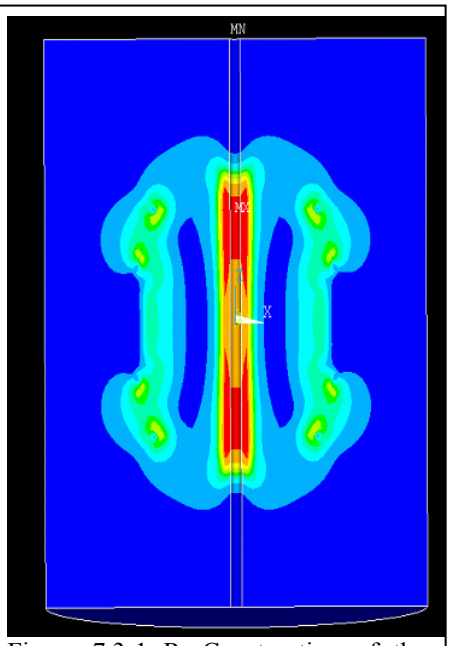

Figure 7.3-1 Re-Construction of the OPERA Poloidal Field in ANSYS using a wedge of elements after reading in an OPERA vector Potential Result.

coordinates yields a reasonable approximation of the VP. The ANSYS EM element type used was SOLID 97 which is converted to SOLID 45 for the structural analyses. The lower order elements are needed to support the EM ANSYS vector potential analysis. Higher order elements use boundary element formulations and are not consistent with the OPERA vector potential results.

7.3 Application of the Background Fields.

The poloidal background fields are extracted from separate analyses of the scenarios, or operating experience. Figure 7.3-2 shows maps of enveloped poloidal fields from all (96) design equilibria for the planned upgrade of NSTX. The poloidal and toroidal background fields are converted to VP gradients. The resulting VP values are superimposed on the VP values from the OPERA analysis.

$$\mathbf{B} = \nabla \times \mathbf{A} = \frac{1}{r}\begin{vmatrix} u_r & u_\theta & u_z \\ \frac{\partial}{\partial r} & \frac{\partial}{\partial \theta} & \frac{\partial}{\partial z} \\ A_r & rA_\theta & A_z \end{vmatrix}$$

The above equation can be solved for the VP for a constant field in any one of the directions. An expression of the total field in terms of VP is obtained by superposition. While the expressions are linear in A and B, they are coupled in the coordinate directions, so that the presence of a radial field induces a non uniform vertical field. The specified field can be obtained only over a limited range from the field point chosen.

```
!       ANSYS Commands

!d,i,ay,vect%inum%(x,z) ! Interpolates and applies the Vector Potential on the node

d,i,ay,BackBz*x/2-BackBr*(z-z0)+vect%inum%(x,z) ! Intrepolates and applies the Vector Potential on the node

!       Applying the Toroidal Field

d,i,az,-0.5*BR*log(x*x) ! applies vector potential for toroidal magnetic field
```

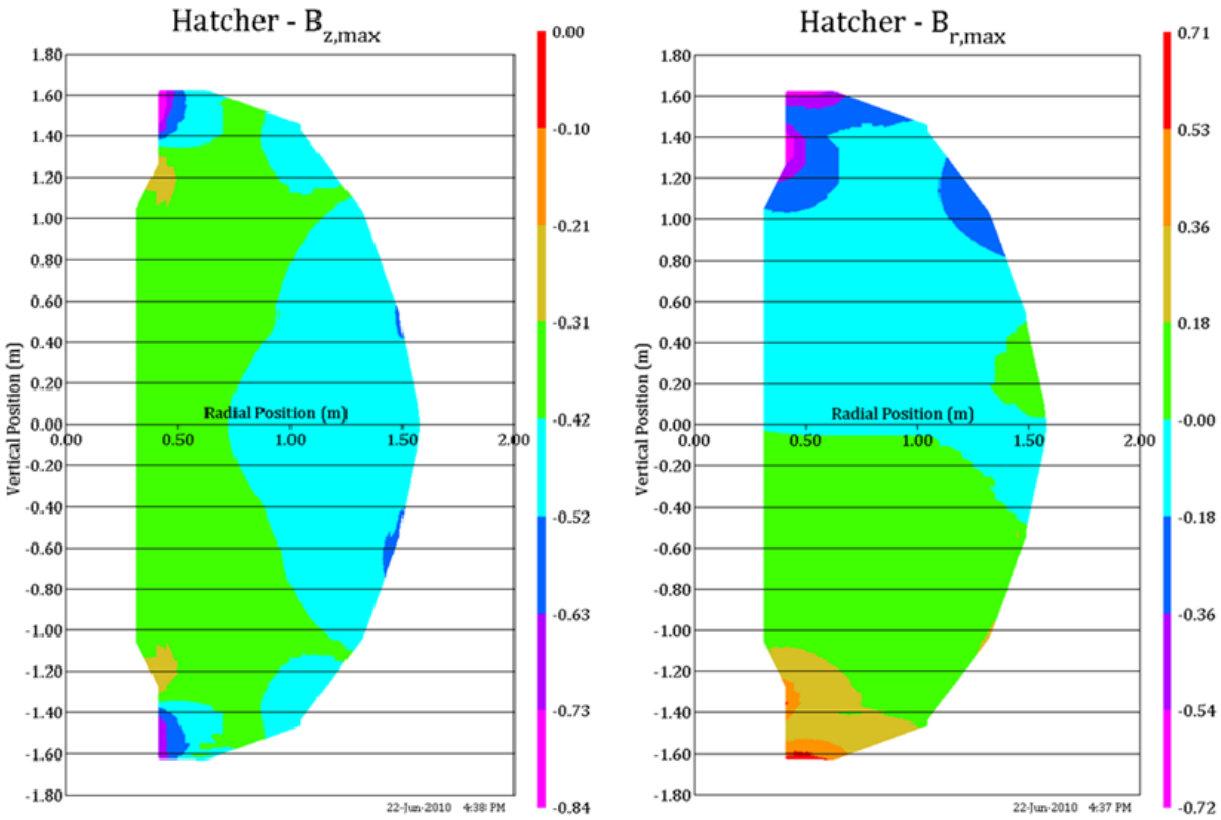

Fig.7.3-2 Maximum Poloidal Field Magnitudes for All NSTX Upgrade Planned Scenarios (R. Hatcher Data, J Boales Plot). More included in Appendix E. This is used to select the worst poloidal field for the component being considered.

7.4 ANSYS 3D Model

The ANSYS EM analysis is transient analysis that must track the time points and VP from the OPERA transient analysis

In order to obtain tractable models of the components, yet still capture the effect of shared currents with the vessel, symmetry and cyclic symmetry can be used. On poloidal cuts of the system, the volt degree of freedom is coupled across cyclic symmetry faces using the ANSYS CPCYL command. Where current transfer is small for example across the equatorial plane of the vessel, volt degrees of freedom are allowed to "float"..

Concurrently with the addition of halo currents, the EM model is solved for eddy currents and Lorentz forces, which are saved in the results file for input to the structural analysis.

7.5 Addition of Halo Loads

Halo currents are applied at the appropriate entry and exit points specified in the GRD by a nodal amp "force" ANSYS command. Entry is modeled with positive nodal currents and exit is modeled as negative nodal currents. Halo current flow needs to be considered in choosing the symmetry boundary conditions In the passive plate model presented in section 9, the symmetry sector is 60 degrees/lower half, and the halo current specified in the GRD is multiplied by the peaking factor, then divided by 6. The symmetry conditions imposed in the passive plate model actually model identical halo currents in the top and bottom of the vessel, and a toroidal distribution of currents uniformly multiplied by the peaking factor.

Halo currents are added in the transient ANSYS analysis. The halo current distribution between the entry and exit points will have resistive and inductive components. The inductive vs. resistive distribution of Halo currents has been studied by A. Brooks for the NSTX center stack casing[4]. Halo currents were

modeled initially as poloidal. currents in the plasma Then interrupted with entry and exit points on the casing and peaking factors in accordance with the GRD. Early analyses of the current distributions in the NSTX centerstack casing claimed a resistive re-distribution that improved the peaking factor[12]. The A.Brooks analysis showed that an initial inductive distribution that maintained the peaking factor throughout the height of the centerstack and then produced a resistive re-distribution. The decision is to retain the peaking factor in the halo current distribution, but with an appropriate time duration. In the procedure outlined here, the distribution of entry and exit nodes are chosen to retain the peaking factor.

There is also the question of timing of the inductive currents from the plasma quench and the halo current peak. Some guidance in the time phasing of these current peaks is provided in [2] and figure 7.5-1. Time duration of the loading is important in properly simulating the dynamic response.

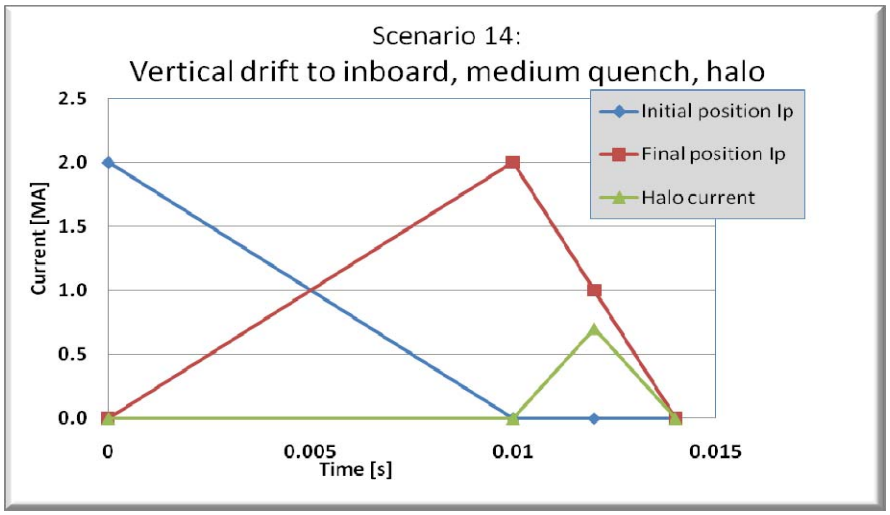

Figure 7.5-1Time phasing of the plasma current changes that induce currents in the vessel and vessel components, and the halo currents. From J. Menard

7.6 Procedure Test Run

7.6.1 The Solid Model:

The solid model of the Vessel, Port Extensions legs and umbrella structure are processed in both Pro-E and ANSYS to merge components, to yield a simpler model for FEA. The umbrella structure is modeled as a separate solid to incorporate the sliding joint at a later stage in analysis. At the time the test runs were made, the solid model of the passive plates had not been prepared. A simple representation of the passive plates was added for the test runs.

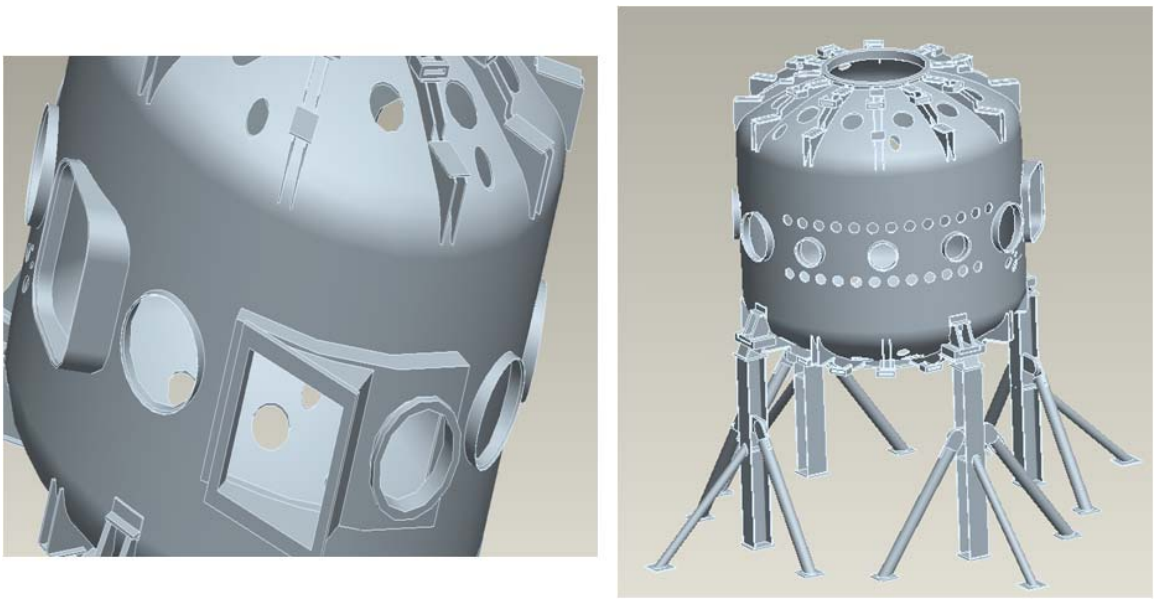

Figure 7.6.1-1 Neutral Beam Ports (left) Vessel and Supports (Right)

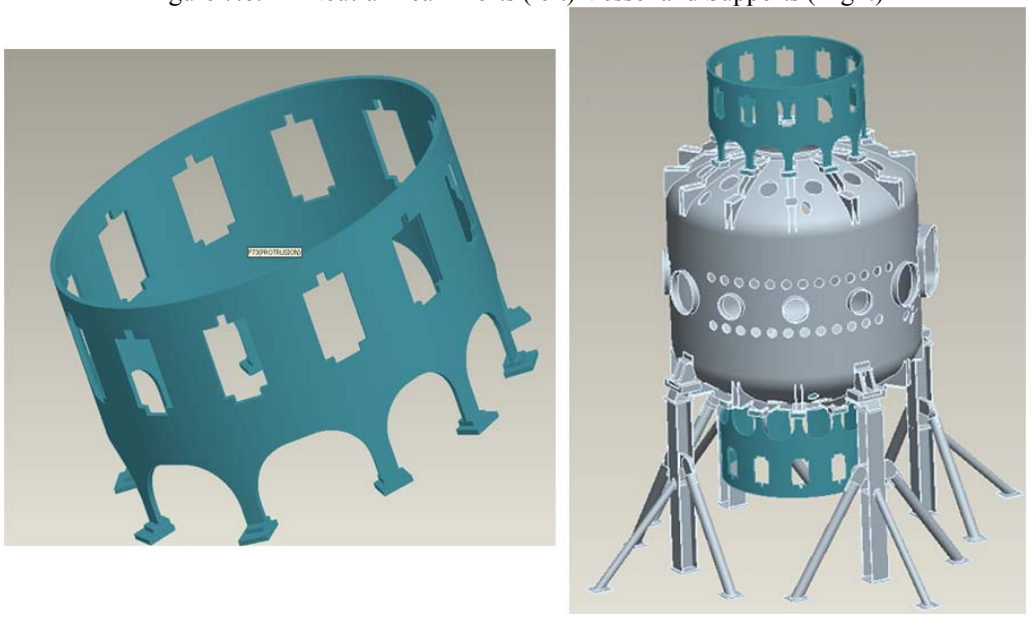

Figure 7.6.1-2 Umbrella Structure (Left) Vessel With Umbrella Structure (Right)

7.6.2 Finite Element Model

The solid models of the vessel, umbrella structure, port extensions and support legs are imported from Pro-E. The model retains all the complex 3-D geometry but the port extensions, legs and the vessel are merged together to form one solid. The umbrella structure is a separate solid. This model is meshed with 8 node bricks in workbench and the mesh is carried into ANSYS classic. To get around the DOF compatibility issues, the mesh is rebuilt in ANSYS classic, retaining the number of nodes and elements and the connectivity.

The model is meshed in ANSYS- Workbench with an 8-node brick element and the mesh is transferred to ANSYS-Classic. The preferred element type is SOLID 97 because of its capability to handle Vector Potentials. However, there were some DOF compatibility issues when the mesh is transferred to ANSYS-

Classic. Several methods to circumvent this obstacle, like using the CDWRITE and CDREAD commands failed. The mesh was reconstructed in ANSYS retaining the same nodes, elements and the connectivity. The Model has 216112 elements and 76436 nodes.

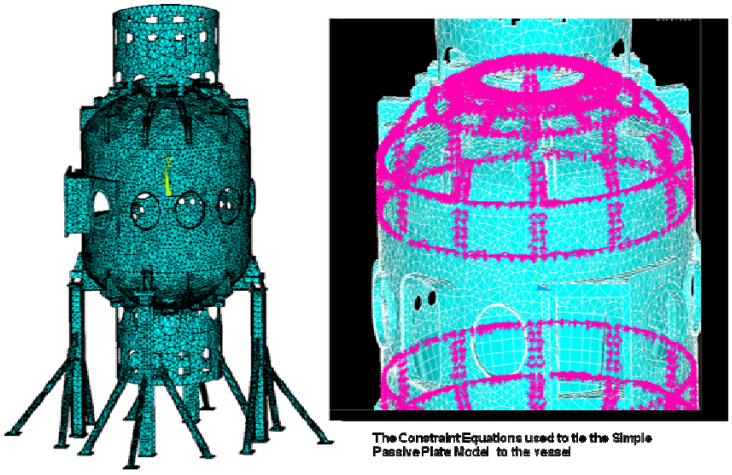

Figure 7.6.2-1 Finite Element Model

An approximate FE model of the passive plates is built based on the 2-D OPERA model and an earlier axisymmetric model of the vessel. This model could not be glued to the vessel because of the difference in dimensions. Hence, the CEINTF command was used to tie the passive plates to the vessel both electrically and structurally.

Table 7.6.2-1 Passive Plate and Outboard Divertor Coordinates

Primary Passive Plate Coordinates	Secondary Passive Plate Coordinates	Outboard Divertor Coordinates
X=1.3600 Y=1.0056	X=1.0640 Y=1.4447	x=0.6208 y=1.6390
X=1.5092 Y=0.5530	X=1.3399 Y=1.0543	x=1.2056 y=1.4092
X=1.5213 Y=0.5569	X=1.3503 Y=1.0617	x=1.2149 y=1.4185
X=1.3720 Y=1.0095	X=1.0744 Y=1.4520	X=1.0744 Y=1.4520

Registration of the OPERA passive plates and ANSYS passive plates is important. Effects of the currents flowing in the passive plates need to be captured consistently in the OPERA and ANSYS EM analysis. If the change in vector potential due to the passive plates in the OPERA model is not positioned directly on the ANSYS passive plates, the eddy currents may not be driven in a consistent manner.

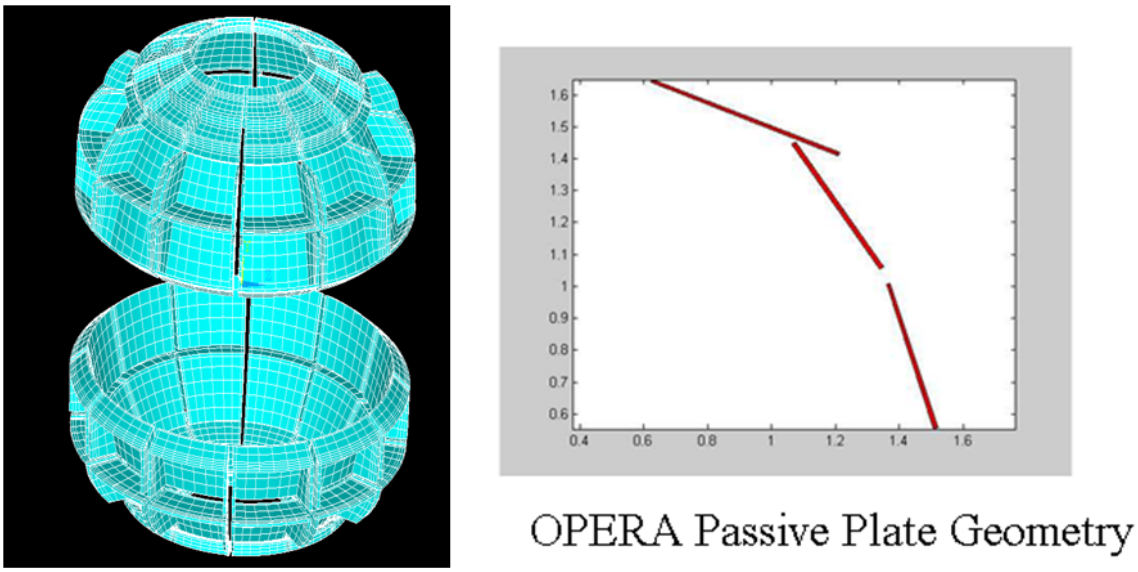

Figure 7.6.2-2: The Simple FEA Model of the passive plates.

A vector potential gradient was then applied on this model to see if the model works. Eddy currents and Lorentz forces obtained agreed qualitatively with what would be expected from a mid-plane quench.. An approximate model of the passive plates, in agreement with the 2-D model used in OPERA, was modeled in ANSYS. This is tied to the vessel using constraint equations. The degree of freedom coupled is Volt during the E-mag run and Displacement during the structural run.

7.6.3 Application of the Vector Potential and Reading the Vector Potential Data From the OPERA Results

Charlie Neumeyers group, and Ron Hatcher have the responsibility to run the NSTX disruption simulations, but the Analysis Branch has to qualify all the nuts and bolts and welds and brackets, so the OPERA vector potential solution is transferred to an ANSYS model with all the detail and then the EM transient is run with the proscribed A's. They are converted to cylindrical coordinates and A's are superimposed for the toroidal field (Rons analysis doesn't have it) then get Lorentz Forces and stresses. -

Before taking the analysis further the model is tested—a Vector Potential gradient is applied to see if it yielded eddy currents and Lorentz forces as expected. The model worked as expected.

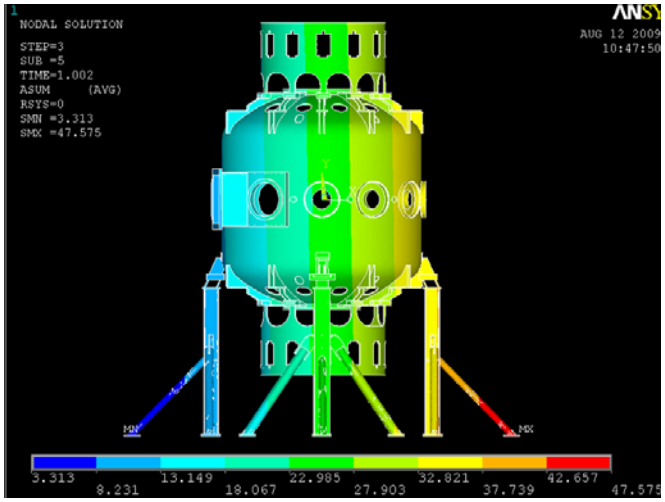

Figure 7.6.3-1 Vector Potential gradient.

For the MIT C-Mod Divertor Upgrade, the PPPL Engineering Analysis Branch is doing a similar analysis. An ANSYS coarse disruption model is used to pass A's to a detailed model of the divertor hardware. For C-Mod, both analyses are 3D, so the 1/r correction is not needed here. The correction to Ron's OPERA result in ANSYS by dividing the A's by r. In later analyses, Ron Hatcher includes the r correction in the data.

The vector potentials from OPERA, which are generated in cylindrical coordinate system, are arranged in a matrix format to be compatible with ANSYS requirements. MATLAB is used to achieve this in the test runs by S. Avasarala. In later analyses Ron Hatcher used the output formatting features of OPERA to create the needed tables. . These values are imposed on the nodes using TREAD command. ANSYS uses linear interpolation and will use an approximated vector potential on nodes that are not coincident with the nodes is OPERA. A toroidal field is also applied along with the values from OPERA. Before running the disruption simulation on the vessel, the vector potentials are applied on a hollow cylinder and the poloidal and toroidal fields are plotted.

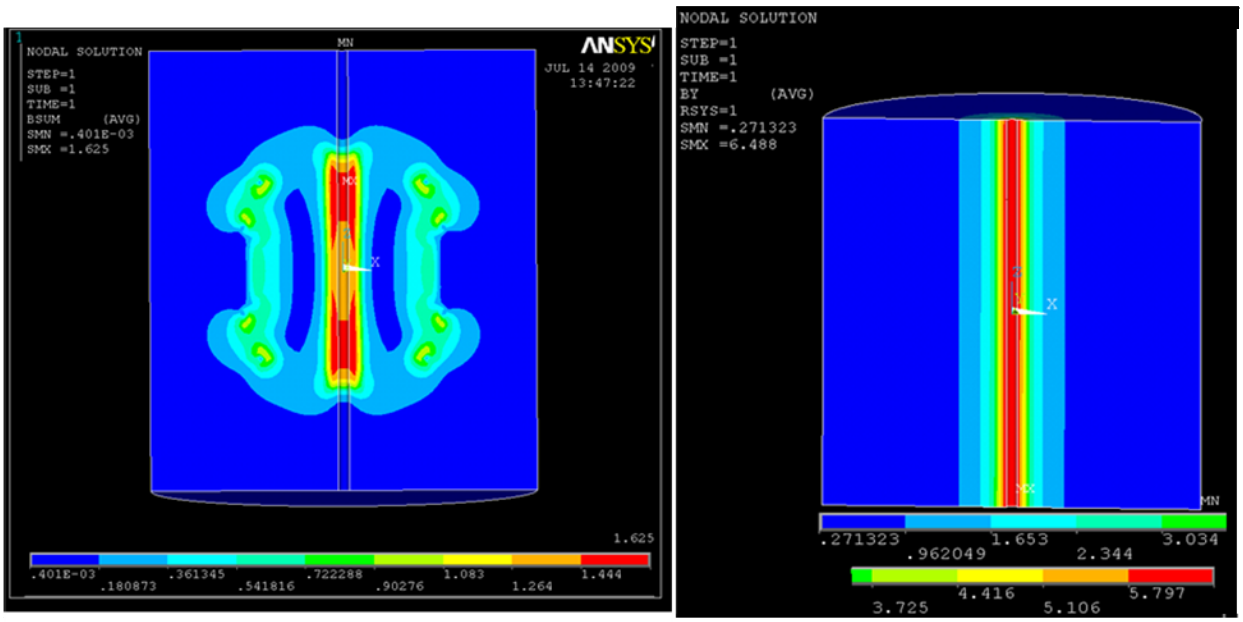

Figure 7.6.3-2 Field plots - Poloidal Created by an ANSYS Interpretation of OPERA input, and Toroidal from A.Brooks Macro

7.6.4 Test Case Disruption Simulation

OPERA results in this first test case, are spaced 0.5 ms apart and hence the load steps in ANSYS are written 0.5 ms apart too. Only the first load step was written at 10 sec to allow for the model to settle and not produce any currents due to the steep change in vector potentials over a short period. A total of 11 load steps are written for the plasma quench. The vector potential boundary conditions are then applied to the model in an ANSYS E-mag analysis.

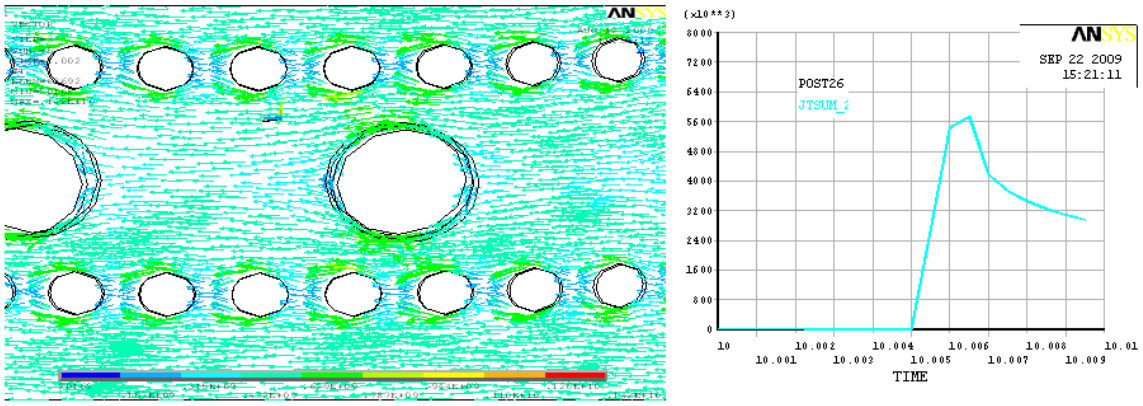

Figure 7.6.4-1 Current Densities

The above figure shows that the currents are maximum at time =10.0065 seconds.It also shows expected "Bunching" above ports

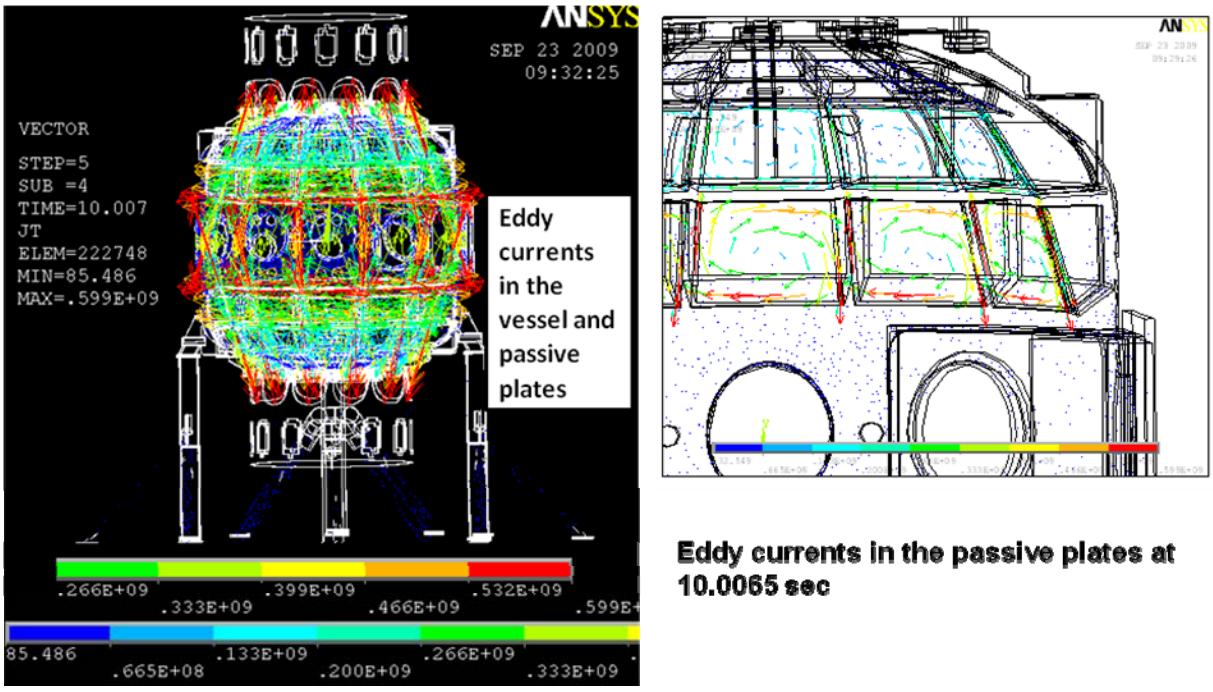

Figure 7.6.4-2 Passive Plate Eddy Currents

The above figure shows that the eddy currents in Cu are larger compared to those in the stainless steel. Also the eddies in the plates are evident. The analysis procedure produces appropriate poloidal currents that the axisymmetric OPERA model does not include.

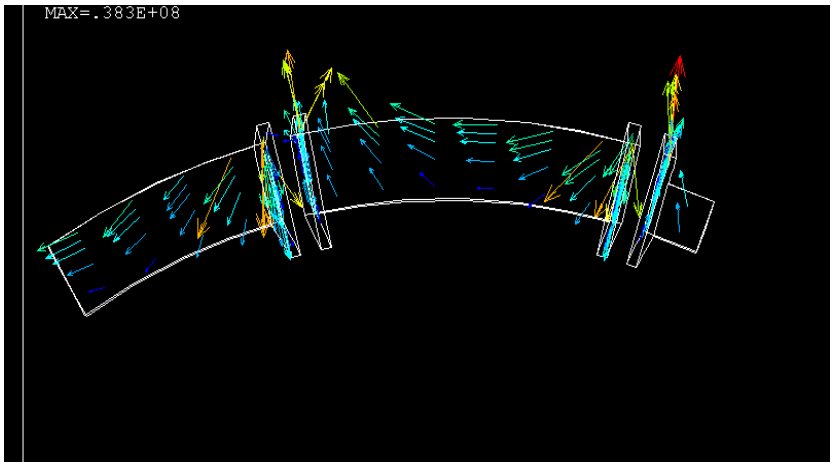

Figure 7.6.4-3Eddy currents flowing in and out of the passive plates

The above figure shows the eddy currents making a loop from the vessel into the passive plates and then back into the vacuum vessel. This indicates that the constraint equations have tied the plates to the vessel as expected. Also, this confirms that the analysis procedure develops realistic three dimensional currents in the toroidally discontinuous structures. The OPERA model that serves as the source of the disruption electromagnetic "environment" is axisymmetric and does not have three dimensional current distributions. The OPERA model must adjust the toroidal resistance of the corresponding complex structures to simulate the toroidal currents that develop during the disruption.

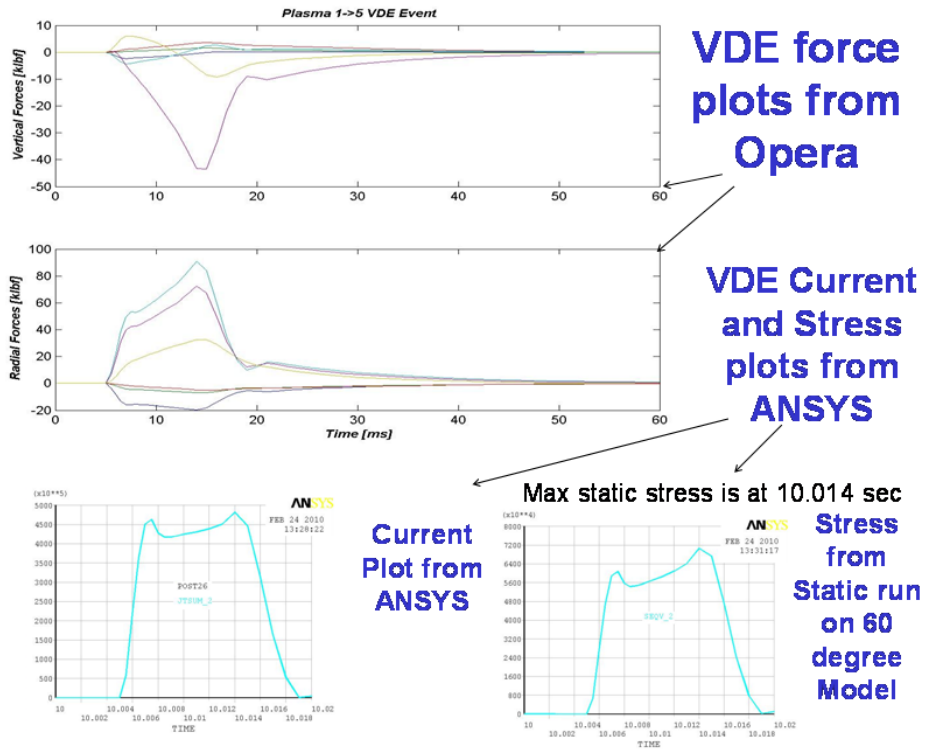

Figure 7.6.3-4 VDE Comparison Between OPERA and ANSYS Results

S. Avasarala ann R. Hatcher ran a VDE case and compared results, in Feb 2009. Current and force profiles are similarly shaped. This was an attempt at doing a "sanity check" on whether data was being successfully transferred from OPERA to ANSYS

7.6.5 Comparison of Bdots with Disruption analysis of the HHFW Antenna

Three nodes on the vessel are picked to compare the rate of change of Vertical Bs with the values obtained from the disruption analysis on the RF antenna. The disruption in both the cases is 2 MA in 1ms.

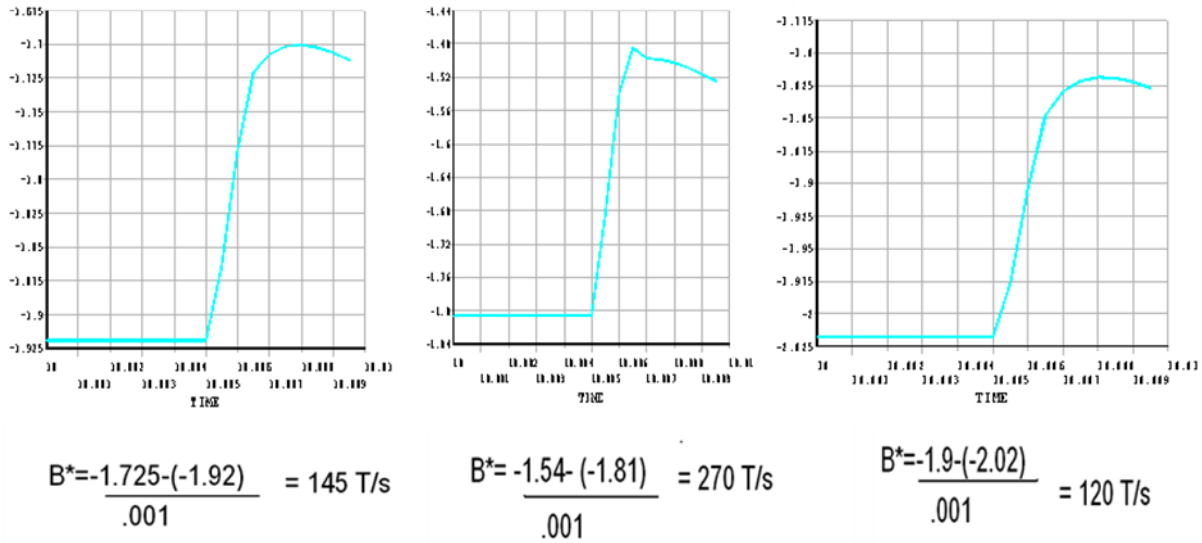

Figure 7.6.5-1 Vertical B values on three nodes on the vessel surface

From Han Zhang's HHFW Antenna Analysis

	above antenna			inside antenna			below antenna		
time (s)	BZ_2	BZ_3	BZ_4	BZ_5	BZ_6	BZ_7	BZ_8	BZ_9	BZ_10
1.00E-03	-6.43E-02	-4.53E-02	-5.10E-02	-0.153989	-0.18615	-0.158143	-5.65E-02	-6.59E-02	-5.47E-02
1.09E-03	-4.03E-02	-2.75E-02	-3.30E-02	-0.151737	-0.183004	-0.15682	-3.33E-02	-4.72E-02	-3.76E-02
1.18E-03	-1.66E-02	-9.03E-03	-1.41E-02	-0.145861	-0.175897	-0.15132	-1.04E-02	-2.74E-02	-1.94E-02
1.27E-03	7.06E-03	9.86E-03	5.22E-03	-0.135675	-0.165017	-0.1415	1.26E-02	-7.03E-03	-6.26E-04
1.36E-03	3.08E-02	2.92E-02	2.50E-02	-0.121633	-0.150762	-0.127905	3.56E-02	1.39E-02	1.87E-02
1.45E-03	5.46E-02	4.87E-02	4.51E-02	-0.104215	-0.134021	-0.111012	5.87E-02	3.53E-02	3.84E-02
1.55E-03	7.84E-02	6.86E-02	6.55E-02	-8.39E-02	-0.115067	-9.13E-02	8.17E-02	5.71E-02	5.85E-02
1.64E-03	0.102127	8.86E-02	8.61E-02	-6.11E-02	-9.44E-02	-6.92E-02	0.10475	7.91E-02	7.89E-02
1.73E-03	0.12588	0.108719	0.106917	-3.63E-02	-7.21E-02	-4.50E-02	0.12777	0.101344	9.95E-02
1.82E-03	0.149592	0.128977	0.127823	-9.53E-03	-4.86E-02	-1.90E-02	0.150742	0.123768	0.120255
1.91E-03	0.173284	0.14935	0.148872	1.87E-02	-2.40E-02	8.49E-03	0.1737	0.146364	0.141214
2.00E-03	0.196926	0.169782	0.169984	4.83E-02	1.57E-03	3.73E-02	0.196604	0.169059	0.162282
	Bz_dot (T/s) in cylindrical coordinate								
	263.90	195.77	198.37	24.77	34.61	14.55	255.14	205.85	187.70
	260.65	203.44	207.71	64.64	78.18	60.51	252.53	217.48	200.33
	260.88	207.86	212.75	112.06	119.69	108.03	252.81	224.26	206.59
	261.37	212.39	217.85	154.48	156.82	149.56	253.34	230.77	213.04
	261.45	215.31	221.25	191.62	184.17	185.84	253.38	235.16	216.57
	261.36	217.91	224.24	223.19	208.29	216.62	253.30	239.01	220.76
	261.32	219.90	226.52	250.63	226.87	243.39	253.23	242.19	224.03
	261.31	221.81	228.68	273.54	245.70	266.31	253.25	244.85	226.50
	260.86	222.86	229.99	294.02	258.68	285.85	252.72	246.69	228.69
	260.64	224.13	231.56	311.09	270.91	302.23	252.56	248.58	230.57
	260.09	224.77	232.26	325.13	280.99	316.41	251.97	249.67	231.77

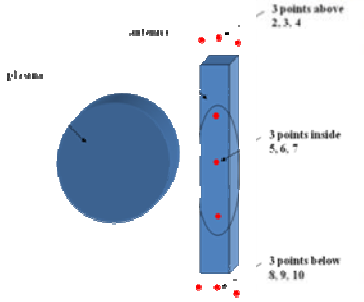

Figure 7.6.4-2: Vertical Bdots from the Disruption analysis on RF antenna, Ref [10]

Han Zhang's HHFW analysis is a mid-plane disruption similar to the Plasma 1 quench simulated by R. Hatcher. In the comparison above, only the equatorial plane Bdot is at the same coordinate, and the results agree. for that point.

7.7 Structural Test Runs

7.7.1 Damping

The damping value used in the structural dynamic analysis has a significant impact on the results. In these NSTX calculations, a conservative 0.5% damping is used. The figure below is a collection of some other damping value guidance from fission and fusion reactor sources. Larger damping values than 0.5% could be justified for the worst of the disruptions in NSTX, but if the response is fully elastic, and the vessel velocities remain small, 0.5% is approriate

Fission Reactor Experience

Regulatory Guide 1.61 - Damping Values for Seismic Design of Nuclear Power Plants

Table 1 Damping Values[1] (Percent of Critical Damping)

[1] Table 1 is derived from the recommendations given in Reference 1.
[2] In the dynamic analysis of active components as defined in Regulatory Guide 1.48, these values should also be used for SSE.
[3] Includes both material and structural damping. If the piping system consists of only one or two spans with little structural damping, use values for small meter piping.

Structure or Component	Operating Basis Earthquake or 1/2 Safe Shutdown Earthquake[2]	Safe Shutdown Earthquake
Equipment and large-diameter piping systems[3], pipe diameter greater than 12 in	2	3
Small-diameter piping systems, diameter equal to or less than 12 in.	1	2
Welded steel structures	2	4
Bolted steel structures	4	7
Prestressed concrete structures	2	5
Reinforced concrete structures	4	7

Fusion Reactor Experience (ITER) Vessel Loads Spec

Magnetic Damping is important in the ITER vessel dynamic analyses. Magnetic damping is conservatively neglected in the NSTX analyses

Horizontal Support due to Magnetic Coupling

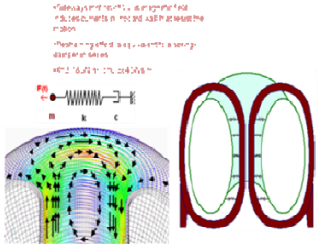

7.7.2 Static Analysis Results for the Test Case:

The EM model is used for the structural model after conversion of element type from 97 to 45 and addition of appropriate displacement constraints. Material properties used are that of Stainless Steel except for the passive plates which are made up of a high strength copper. If only static analysis results were used, the conclusion would be that the passive plates are significantly overstressed. A dynamic analysis is needed to properly simulate the response of the passive plates.

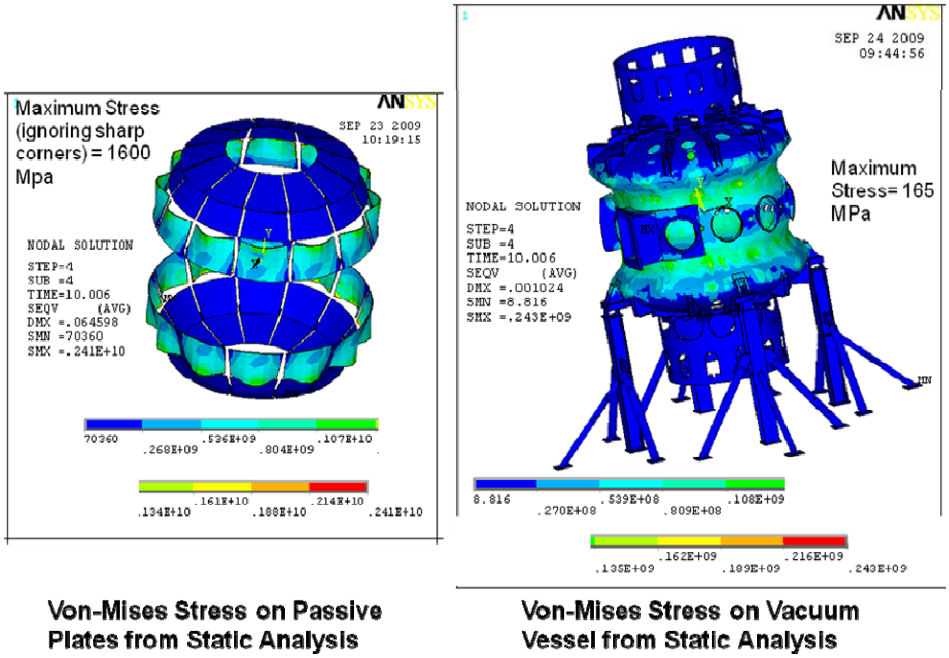

Von-Mises Stress on Passive Plates from Static Analysis

Von-Mises Stress on Vacuum Vessel from Static Analysis

Figure 7.7.2-1 Von-Mises Stress on Passive Plates from Static Analysis

7.7.3 Dynamic Analysis Results for the Test Case:

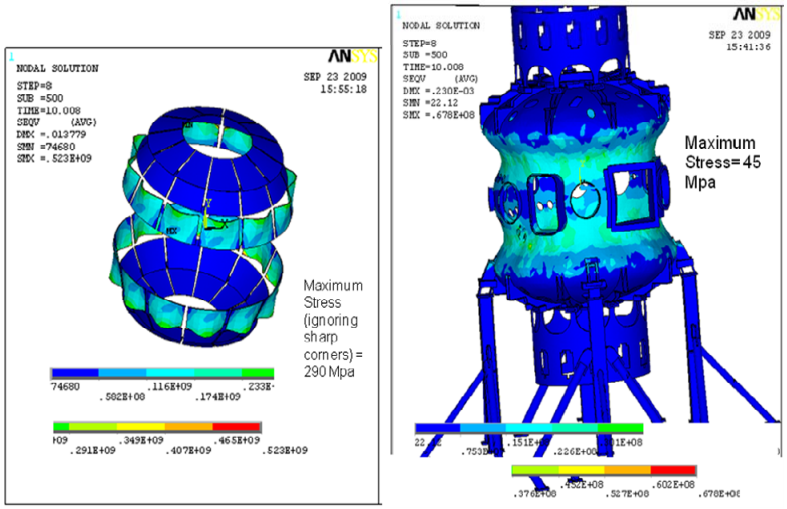

Von-Mises Stress on Passive Plates from Dynamic Analysis

Von-Mises Stress on Vacuum Vessel from Dynamic Analysis

Figure 7.7.3-1 Von-Mises Stress on Passive Plates from Dynamic Analysis

The dynamic response is substantially below that for the static analysis. This is relied on to qualify the passive plates and bolting. It also raised the issue as to whether the fastest quench in fact caused the worst loading. As a result some of the slow VDE/quench cases were run.

7.7.4 Comparison of Dynamic and Static Analyses

Four regions are selected on the vacuum vessel and the passive plates to compare displacements and stresses.

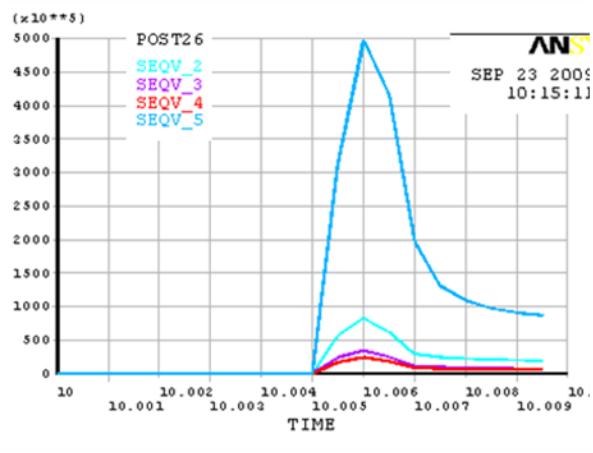

Stress from static analysis on nodes 47059,29593,19132 and 76456

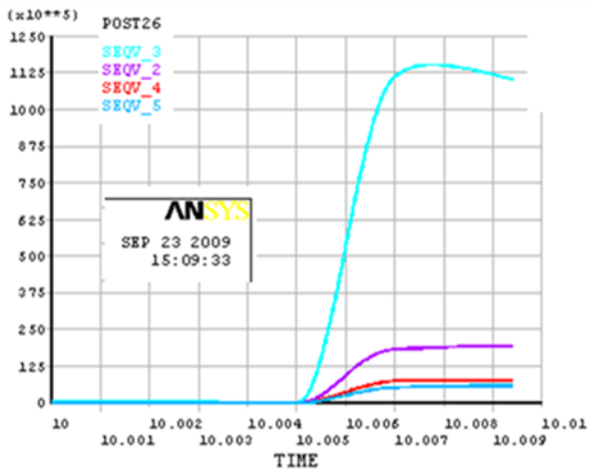

Stress from dynamic analysis on nodes 47059,29593,19132 and 76456

Figure 7.7.4-1 Stress from Static and Dynamic Analysis on nodes 47059,29593,19132 and 76456

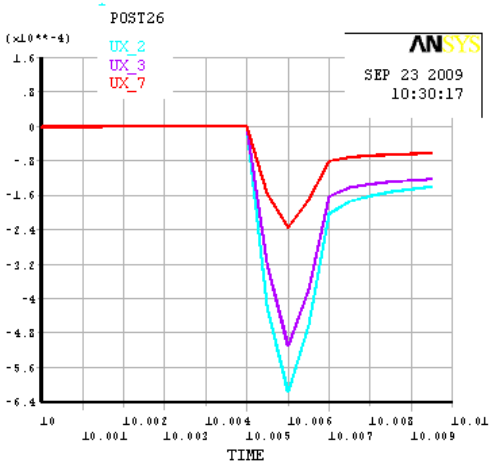

Displacements from static analysis on nodes 47059,29593 & 19132.

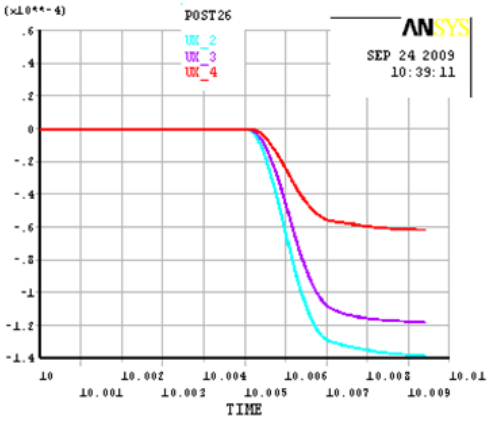

Displacements from Dynamic analysis on nodes 47059,29593 & 19132

Figure 7.7.4-2 Displacements from Static and Dynamic Analysis on nodes 47059,29593,19132 and 76456

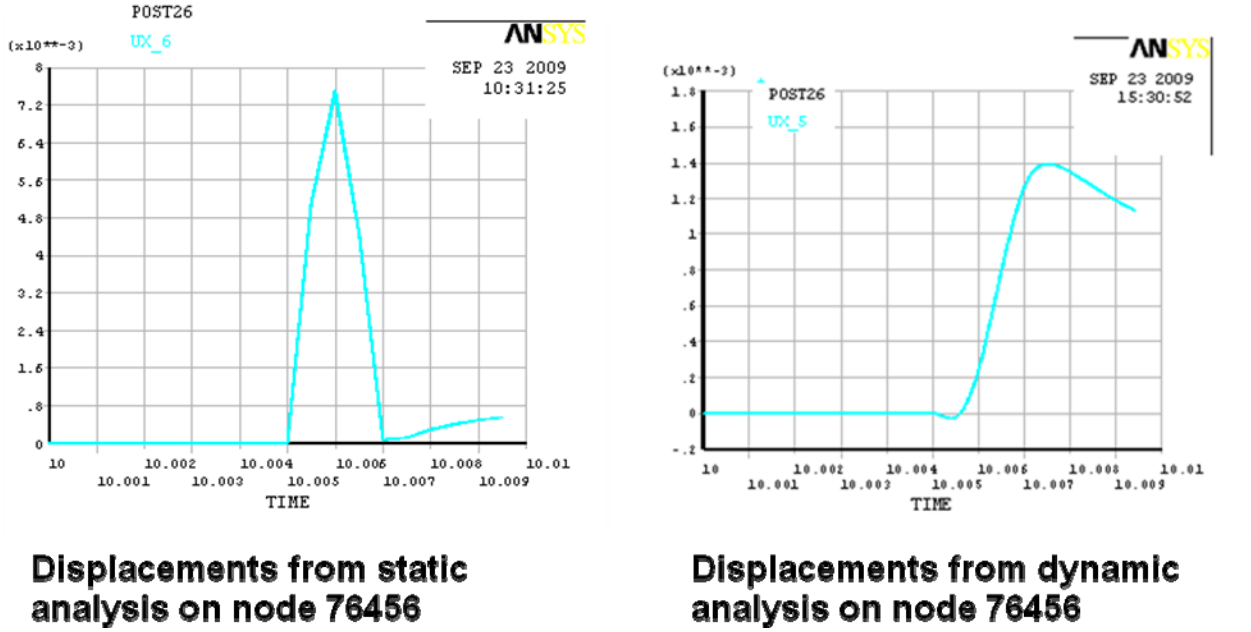

Figure 7.7.4-3 Displacements from Static and Dynamic Analysis on node 76456

8.0 Global Vacuum Vessel
8.1 Mid-Plane Disruption

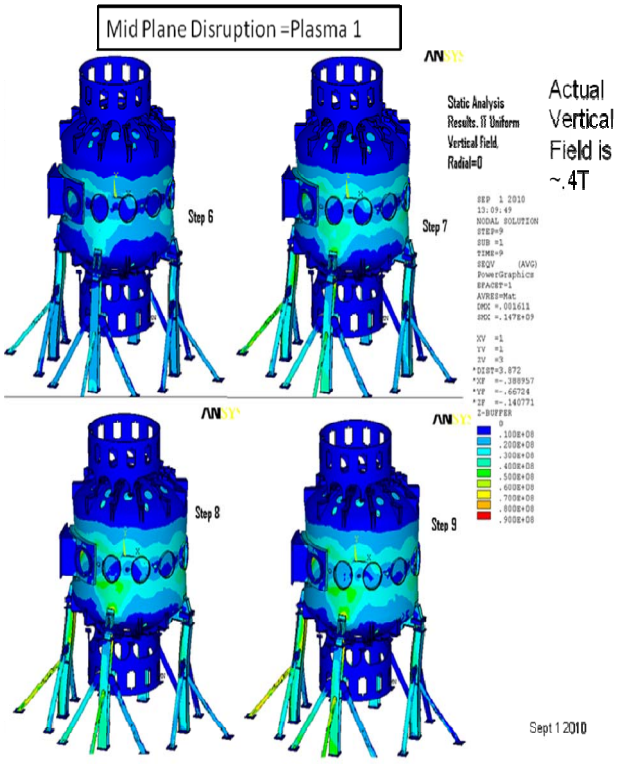

8.1.2 Mid Plane Disruption Currents and Stresses Near Bay L,

The primary responsibility for qualifying this area of the vessel is found in reference [17], "Vessel Port Rework for NB and Thompson Scattering Port". Results are included here for comparison.

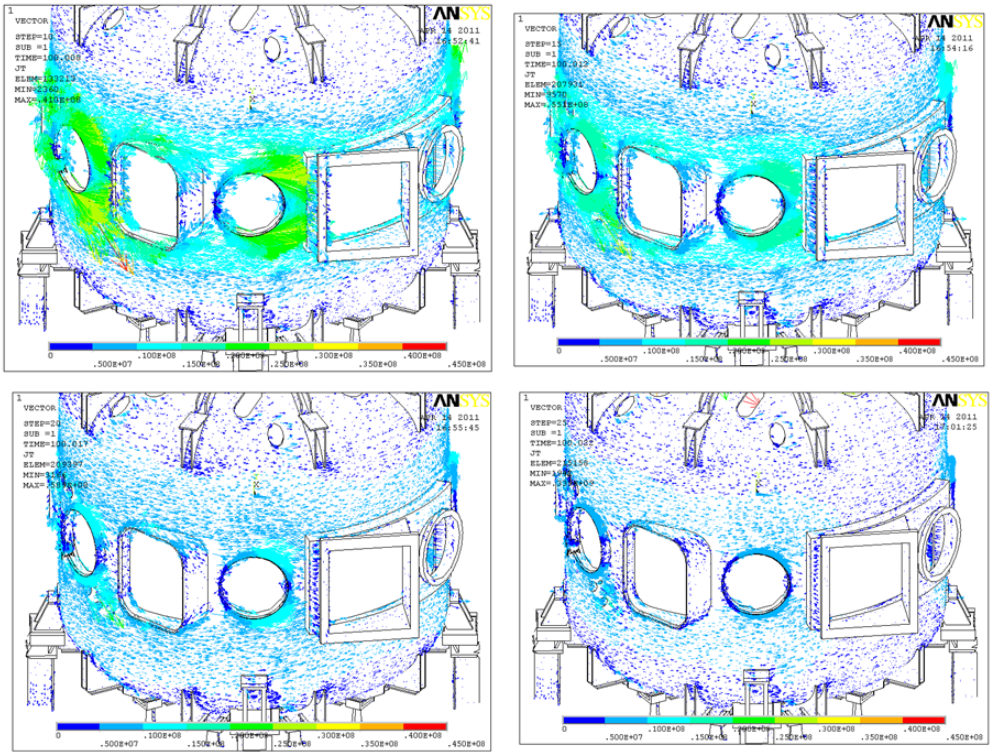

Figure 8.1.2-1 Current Densities in the NB/Thompson Scattering Port Area

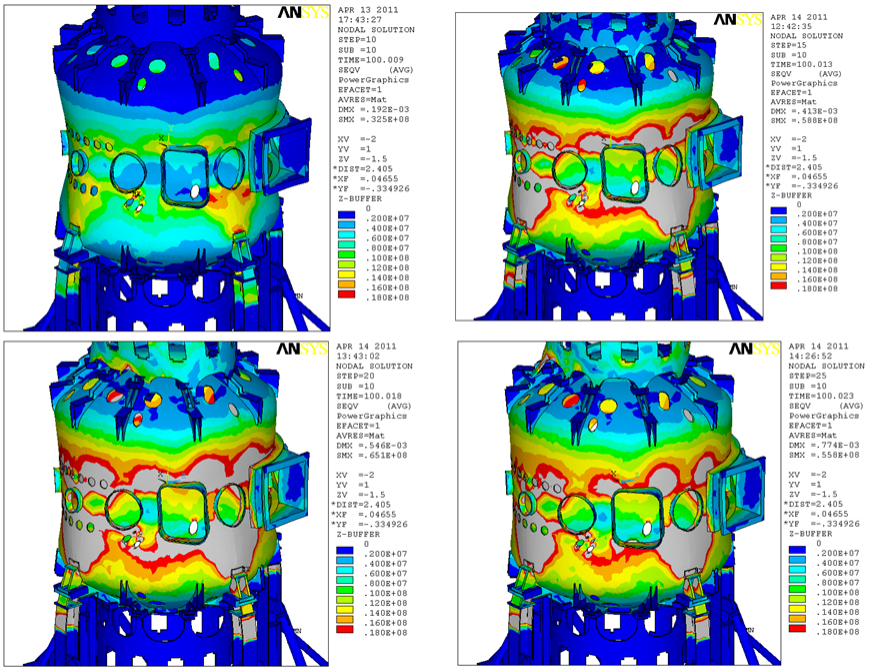

Figure 8.1.2-2 Von Mises Stresses (Contoured for a Max=18 MPa) in the NB/Thompson Scattering Port Area

8.3 Vessel Response to a Plasma 4 Quench

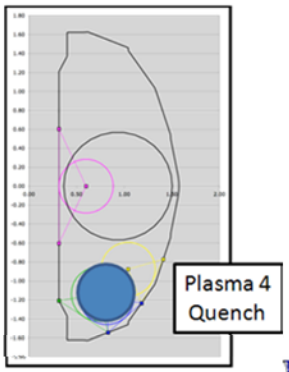

Plasma4 Quench Analysis of the Vessel

PP and Full Vessel Have not Been Integrated, But the Shielding Effect of the PP is included in the OPERA Analysis

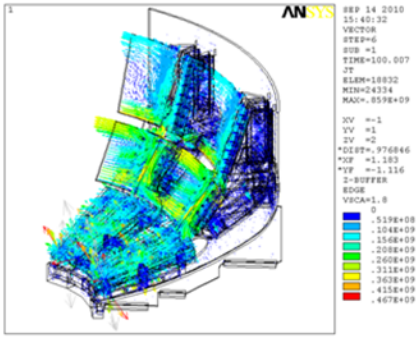

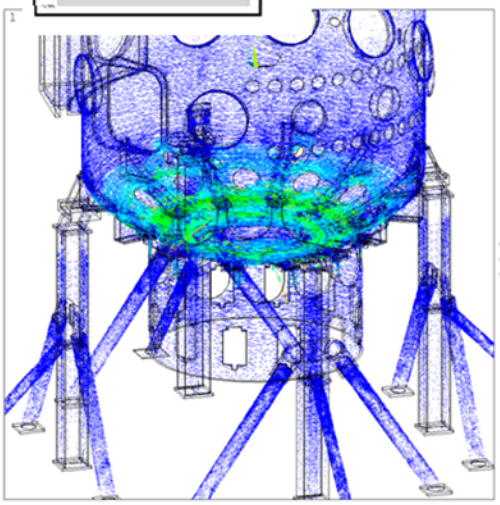

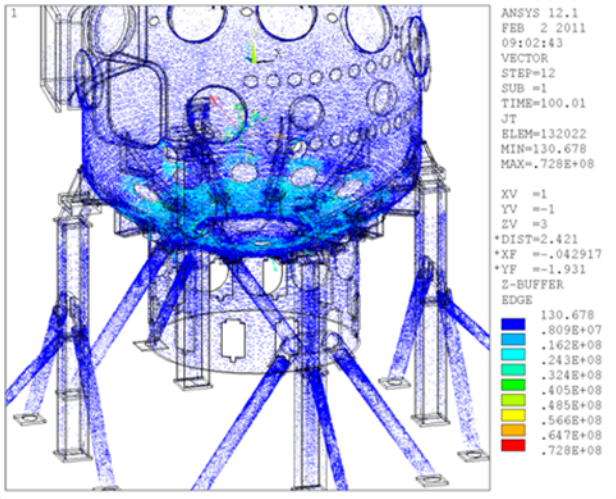

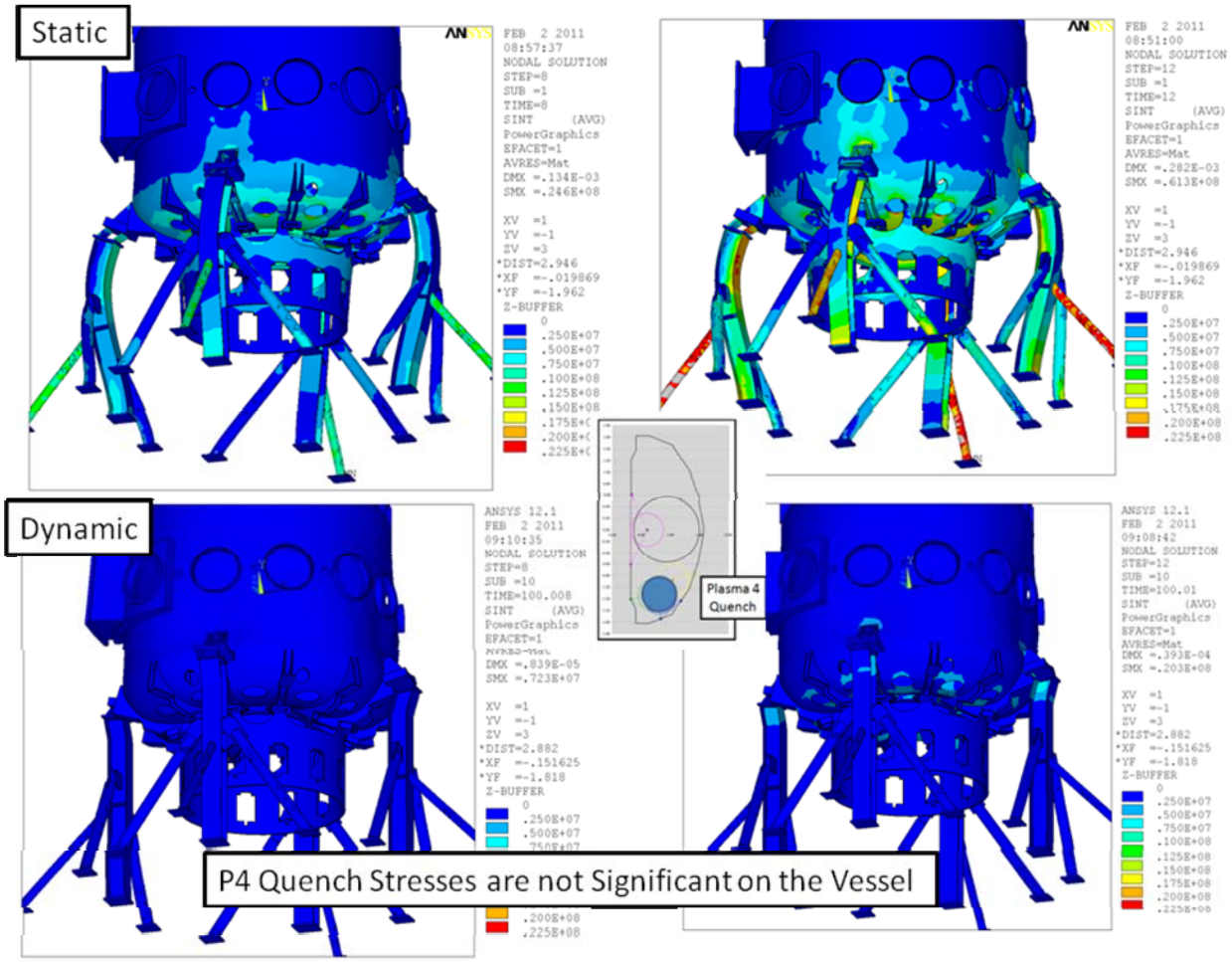

8.4 Estimate of Disruption Accelerations at the Lowe Head Nozzles

Diagnostics mounted on the heads of the vacuum vessel will experience some dynamic excitation at their mounting location. The Plasma 4 Quench results were post processes in the area near the lower vertical nozzles. Vertical displacement plots from the dynamic analysis were obtained, and the peak velocity estimated from the slope. The velocity divided by the time needed to develop the velocity yielded an estimate of the acceleration. Only .05 g's was obtained, which is modest compared with gravity loads, and has no structural consequence. It may have some impact on the resolving power of the diagnostic if data is needed during the disruption.

Dynamic Disruption Displacements at Lower Nozzle

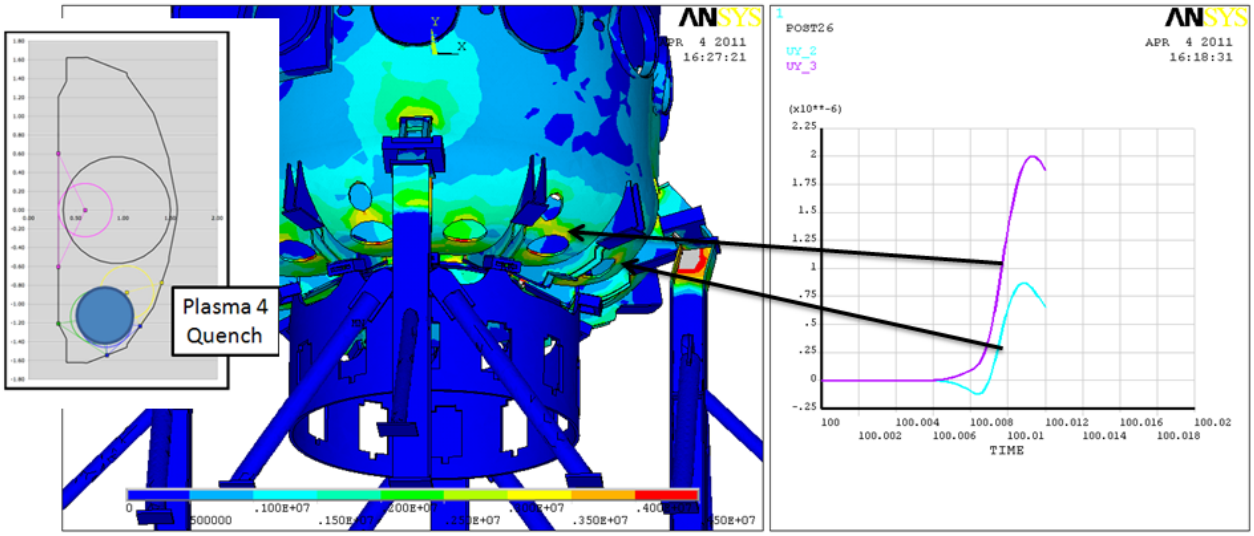

Peak Velocity is Approx 1e-6/.001= 1e-3 m/sec
This develops over About 2 milli-sec. The acceleration
= .5 m/sec^2 = .5/9.8 = .05 g

8.5 Vessel Support Leg Analyses

8.5.1 Drawing Excerpts and Photos

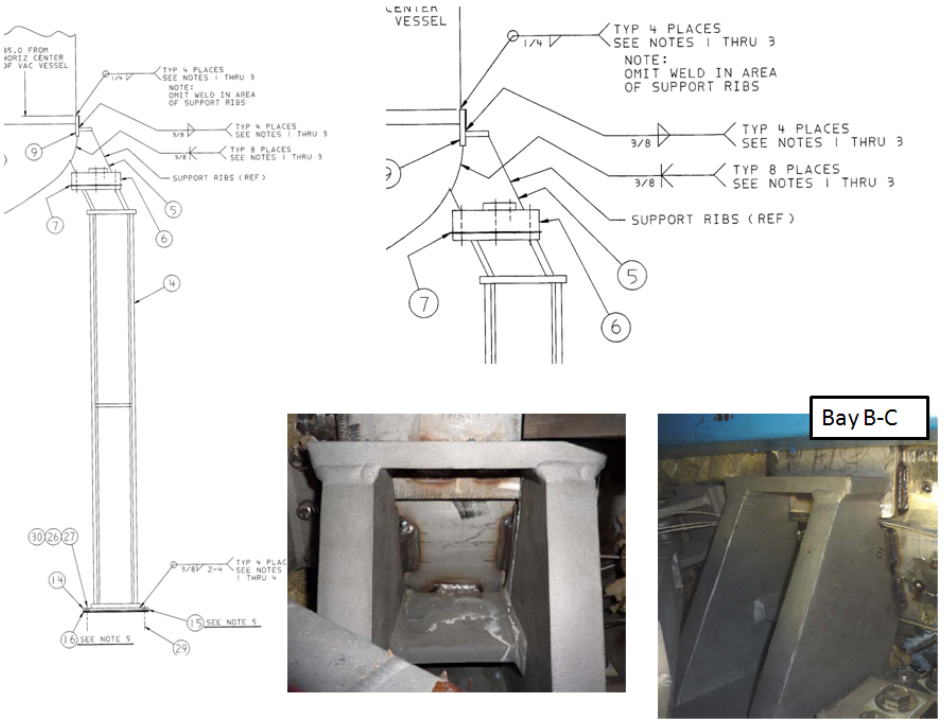

8.5.2Vessel Stresses Near the Column Supports

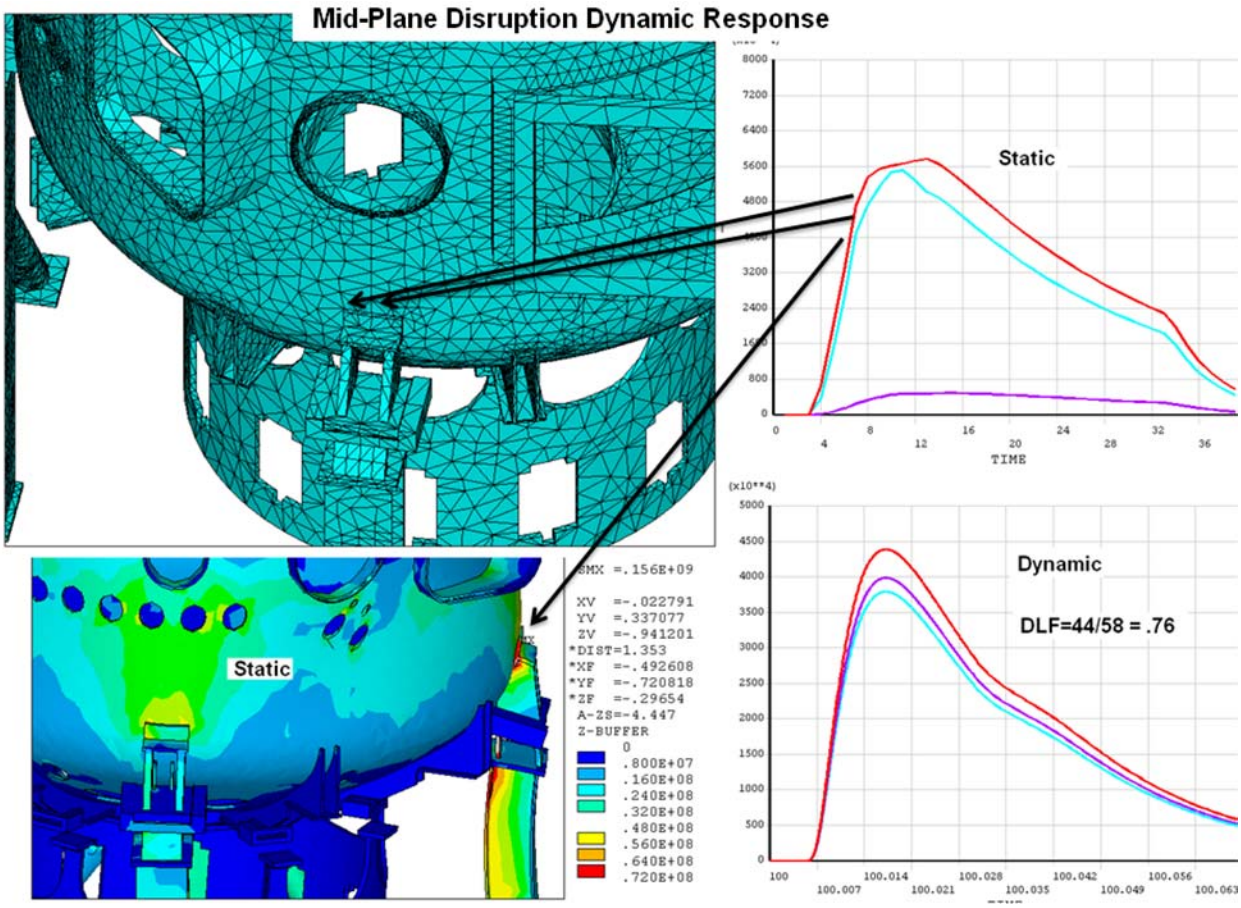

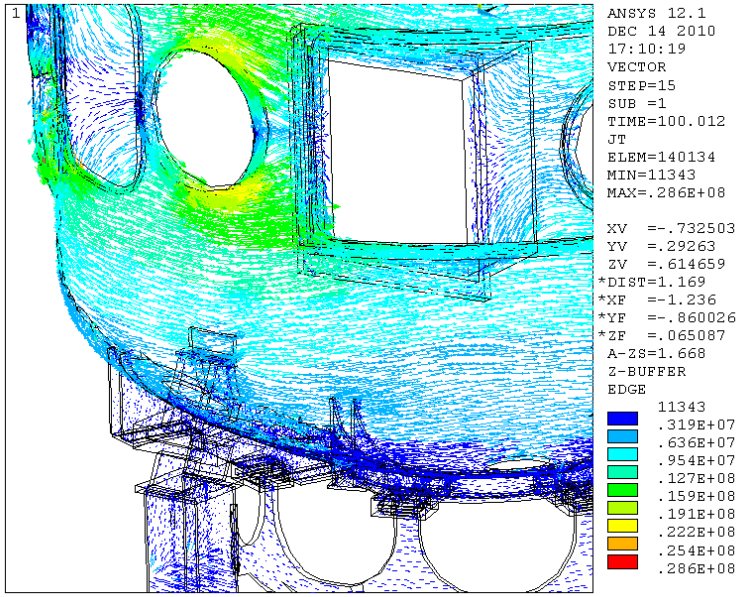

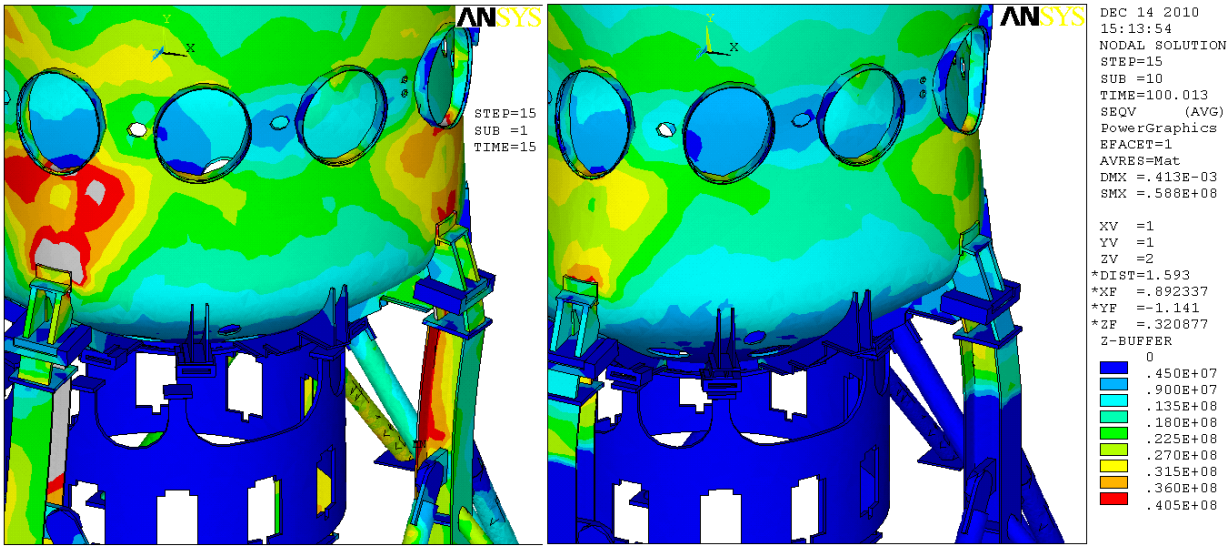

Static Dynamic

9.0 Passive Plate Disruption Analyses With Halo Currents

The Passive Plates are copper and are close to the plasma. They currently pick up large currents and are expected to see even larger currents and loads during the upgrade operation. In the test cases discussed in section 7, the passive plates were simply modeled because a solid model was not available. The passive plates were supplied by ORNL and the design drawings were entered into the NSTX Pro-E solid model of the machine in the summer of 2009. This work was done by Bruce Paul, with S. Avasarala interacting in the process to allow a meshable continuous solid. In order to facilitate creation of cyclic symmetry in ANSYS, 30 degrees of the desired section was created and reflected so that the nodes on the cyclic symmetry face would line-up. The model was still not fully merged at the backing plates, and a swept mesh was created that had reasonable bolt elements and would merge with the rest of the model.

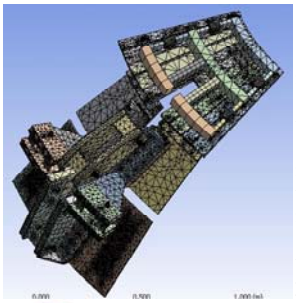

30 degree ProE model was meshed and then reflected to fit vessel 60 degree sector model. The vessel was added to model current sharing. Reflection was done to allow precise CP command coupling

Incorporation of the Detailed ProE model

To manage model size, 60 degree cyclic symmetry and up-down symmetry is used.

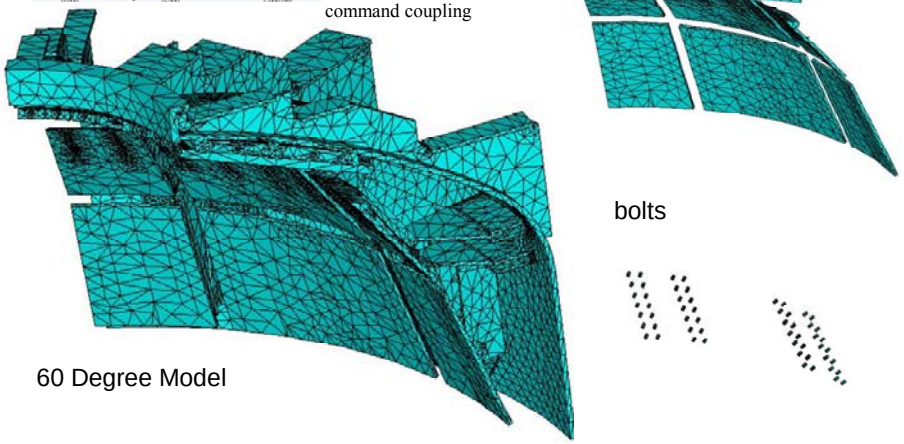

Figure 9.0-1 The ProE model and its Conversion to a meshed ANSYS cyclic Symmetry Model

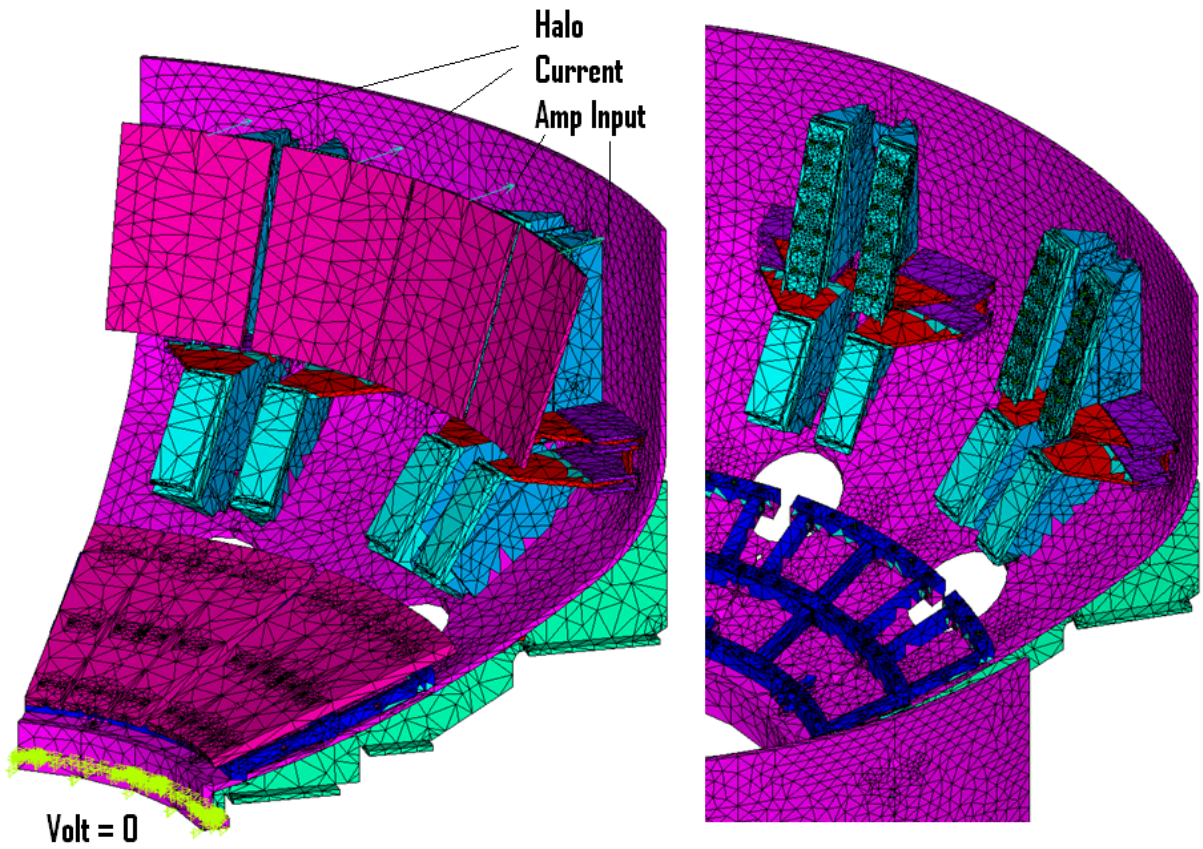

Figure 9.0-2 Halo Current Input Electromagnetic Model as of July 15th 2010. The secondary passive plates are not yet included

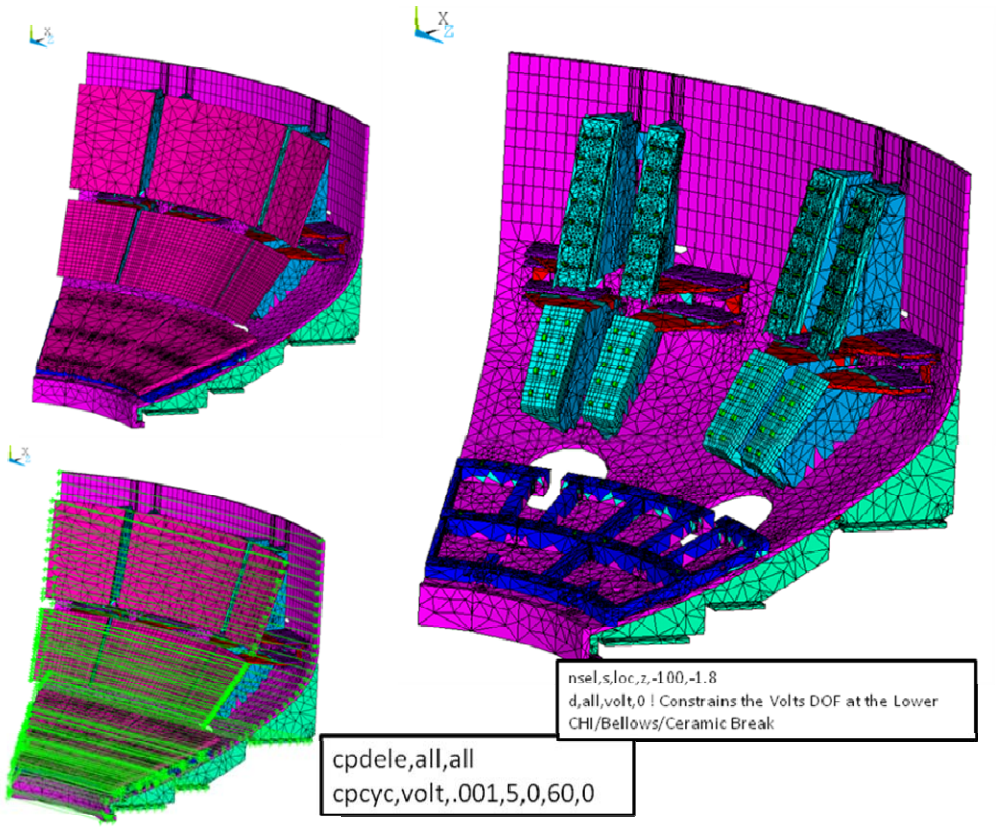

Figure 9.0-3 Halo Current Input Electromagnetic Model. The secondary passive plates have been added

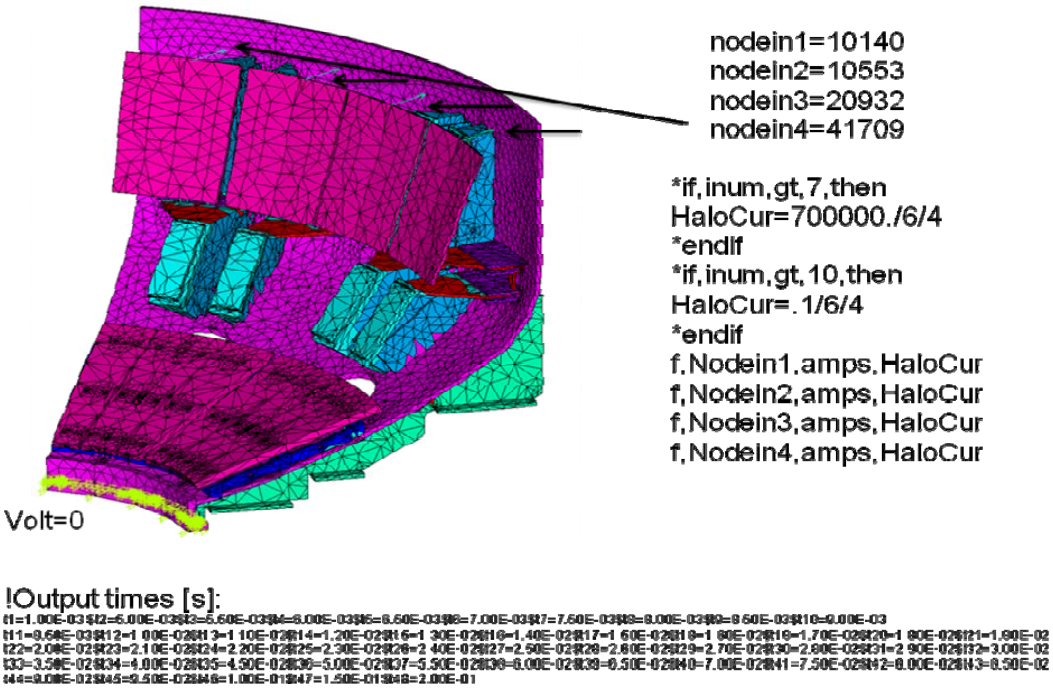

Figure 9.0-3 Halo Current Input Electromagnetic Model. Halo Current Input

9.1 Drawing Excerpts and Photos

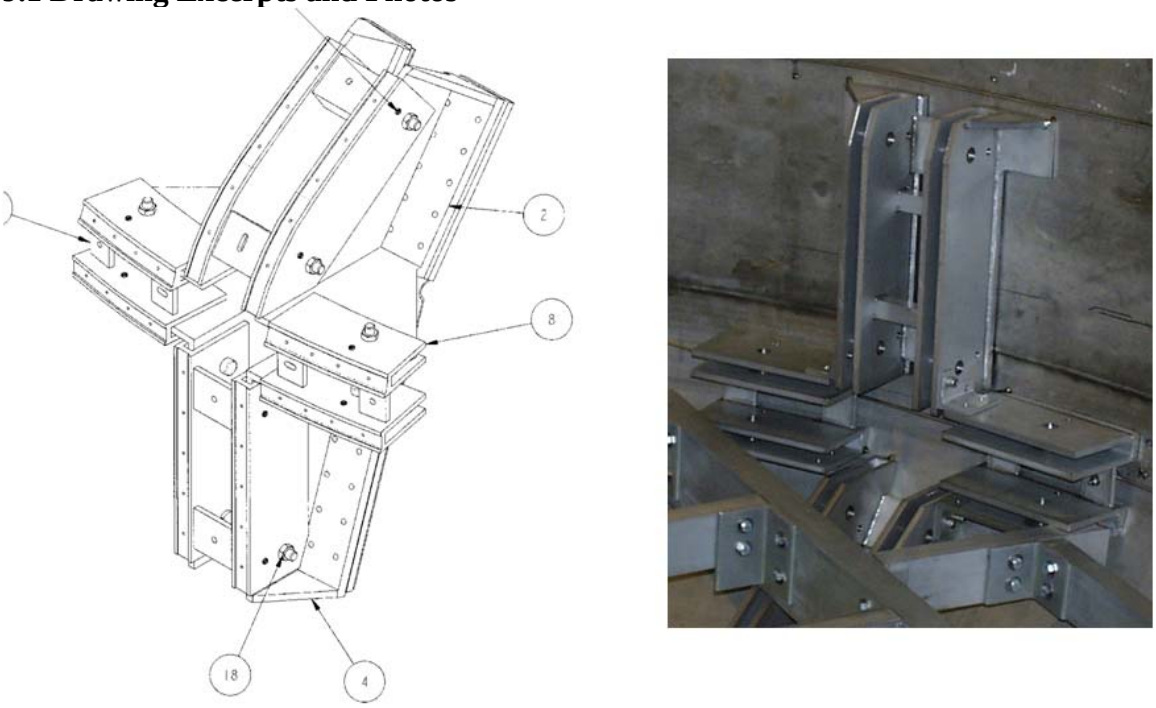

Figure 9.1-1 Bracket as it appears on the ORNL Drawing, and a photo of the bracket during installation. Not that the perimeter welds that connect the bracket to the vessel wall have not yet been made.

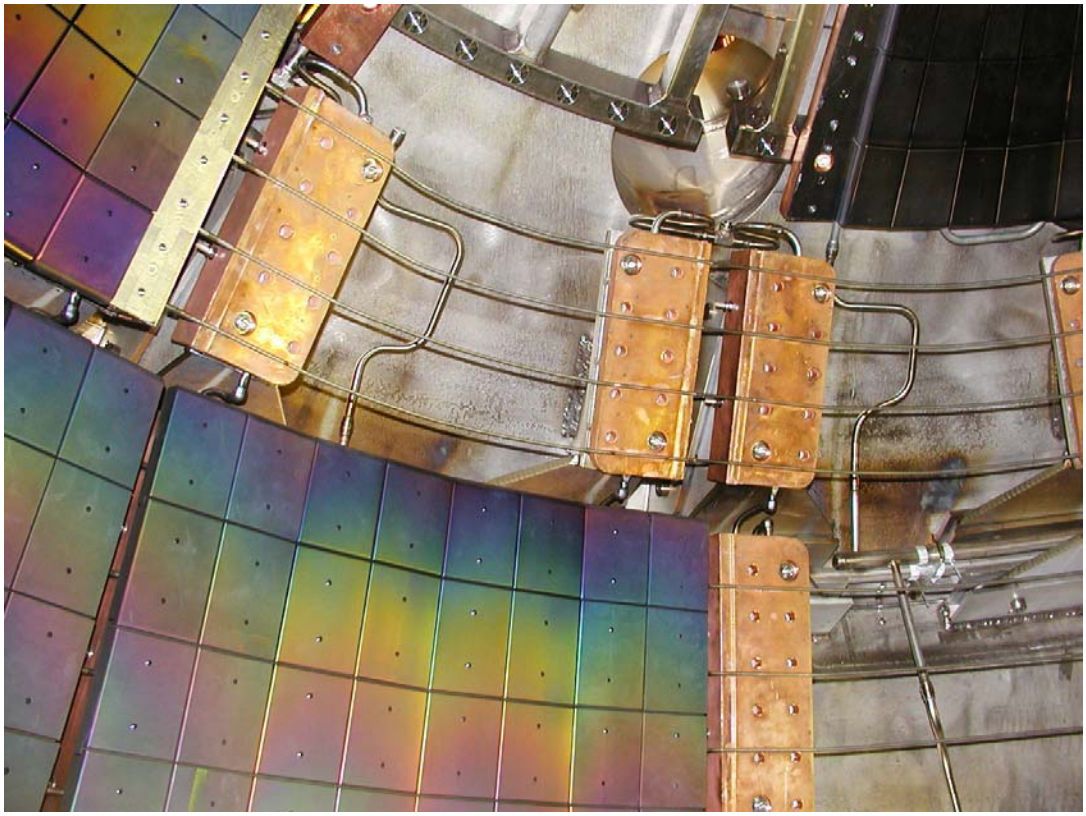

Figure 9.1-2 Bracket Bolt Surface of the Upper Secondary Passive Plate. - with the plate removed.

9.2 Passive Plates Loaded by a Mid-Plane Disruption

9.2.1 With and Without Halo Currents

The model was run with and without halo currents with the mid-plane disruption. In July 2010,the secondary passive plate had not been meshed. so the model was run without it to see the effects of the halo currents entering the passive plates and traveling through the vessel wall. Plots of with and without halo currents are shown below in figures 9.2-1 and 2

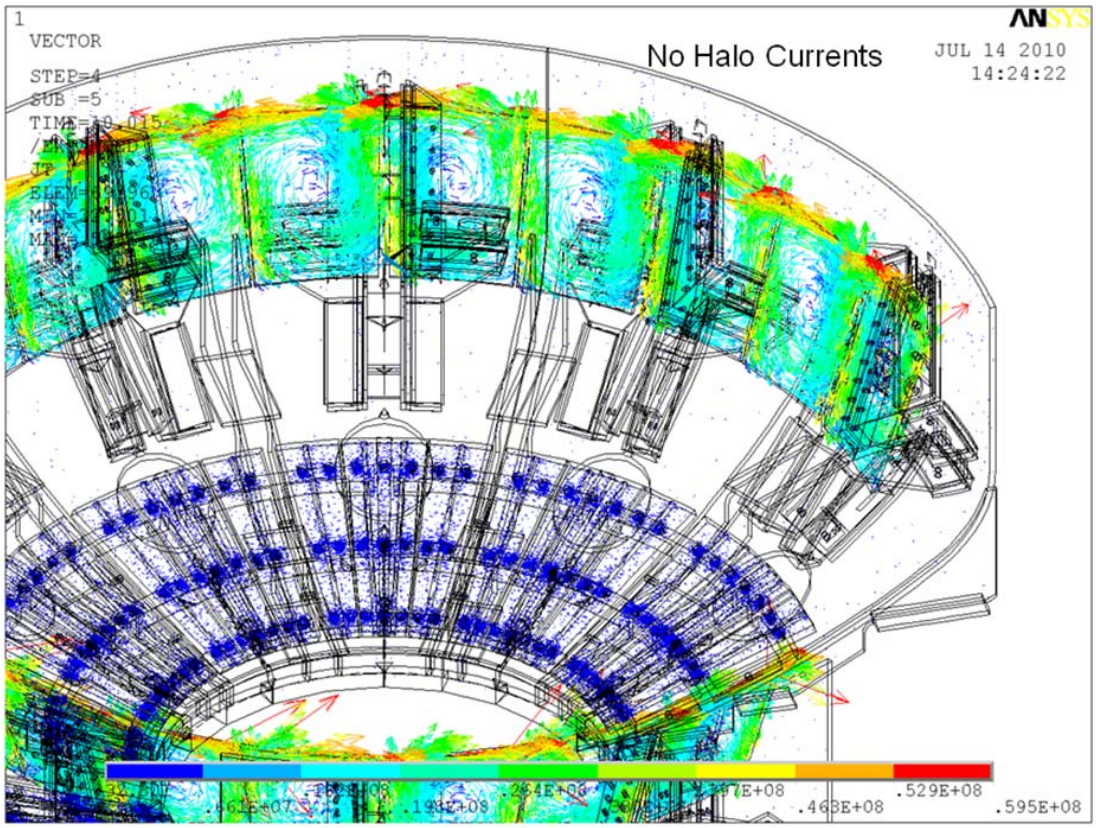

Figure 9.2-1 Results without halo currents

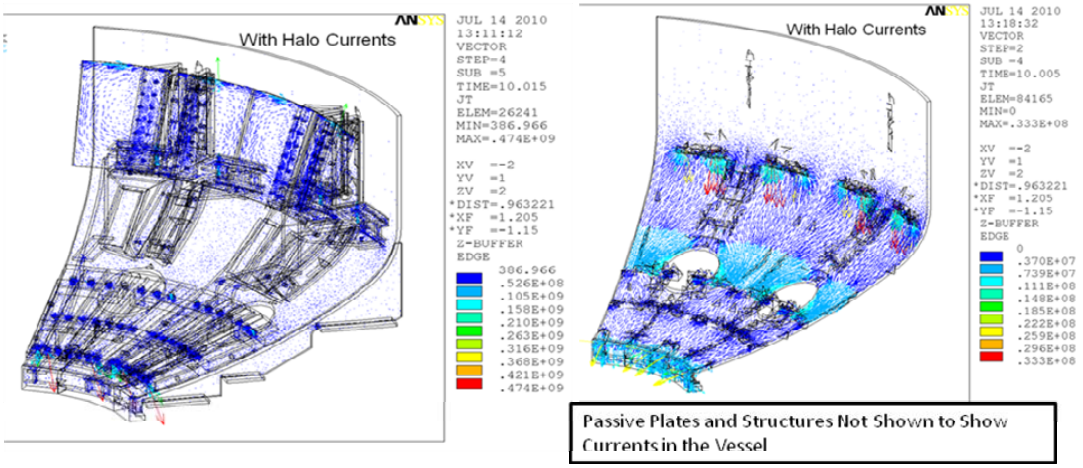

Figure 9.2-2 Results with halo currents

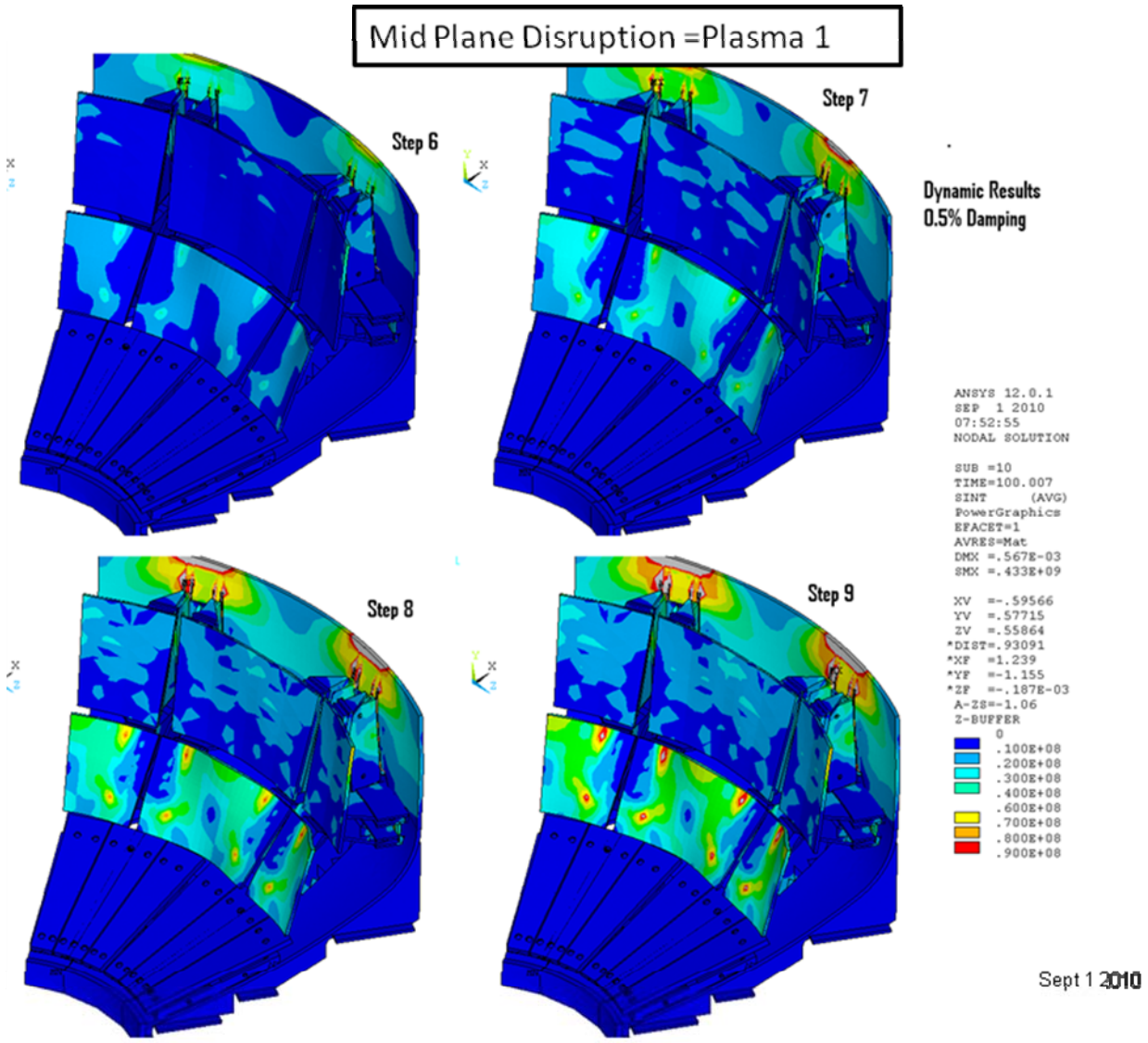

Figure 9.2-1 Static Stress in the middle of the Passive Plate

9.2.2 Currents Flowing in the Passive Plates, Mid-Plane Disruption, Plasma 1

The OPERA axisymmetric Analysis produces only toroidal currents.The results of the Opera/ANSYS disruption simulation show eddy currents in the plates. In the ANSYS results there is a clear net toroidal current in the primary passive plates represented by larger current densities at the top of the plate than at the bottom. Based on the top and bottom current densities, at the time in the disruption that produced the largest current densities , the conduction cross section of the primary passive plates and an assumed triangular current density distribution:

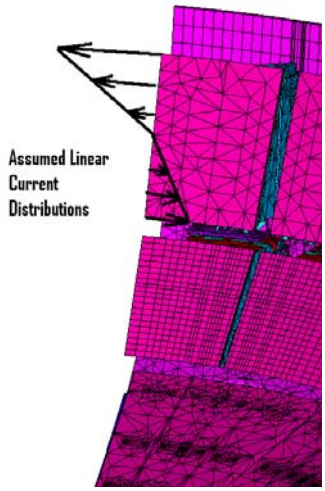

Figure 9.2.2-1

Fraction of IP flowing in the Primary Passive Plates is:

(.467e9-.311e9)*5.4848/4 /2E6 = .107

The upper bound of measured net currents [3] in the primary passive plates is also about 10% of the plasma current. Currents in the secondary passive plates are not as readily determined from the current vector plot but it is clear that they are lower, consistent with measured data.

```
tarea
 Element Group for which Area is to be Calculated
1
  TOTAL SURFACE AREA OF 4 NODE ELEMENTS IS BEING COMPUTED.
 TOTAL AREA =   5.4848189E-03
 CENTROID X,Y,Z=    1.437300      -0.7918749      -2.6471052E-02 MOMENTS OF INERTIA
 =   0.0000000E+00   1.9485991E-17   1.9029288E-20
 AXISYMMETRIC VOL=   4.9532536E-02
```

Figure 9.2.2-2 Passive Plate Cross Sectional Area

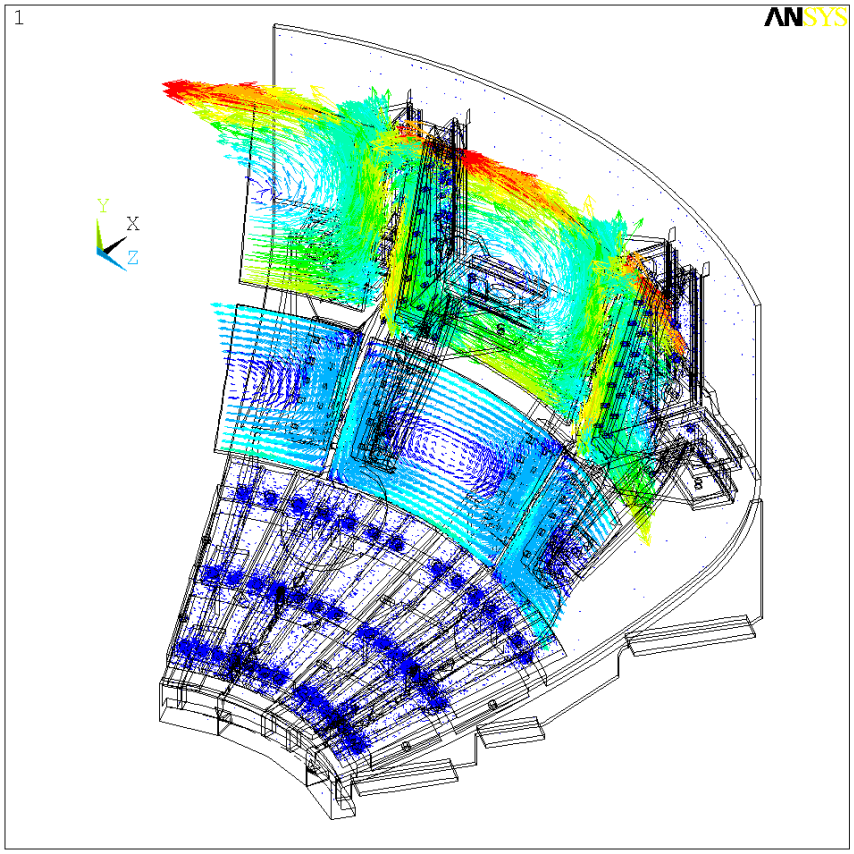

Figure 9.2.2-3

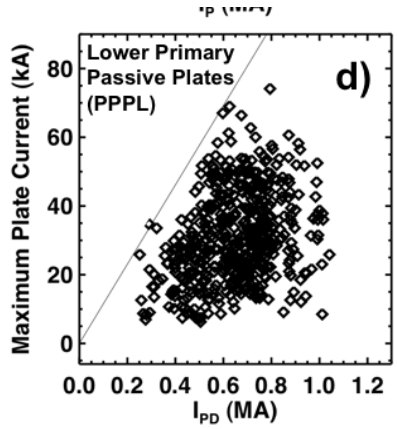

Figure 9.2.2-4 Figure from [3]

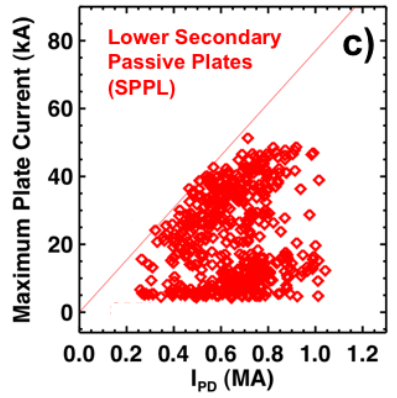

Figure 9.2.2-5 Figure 12 in Ref [3]

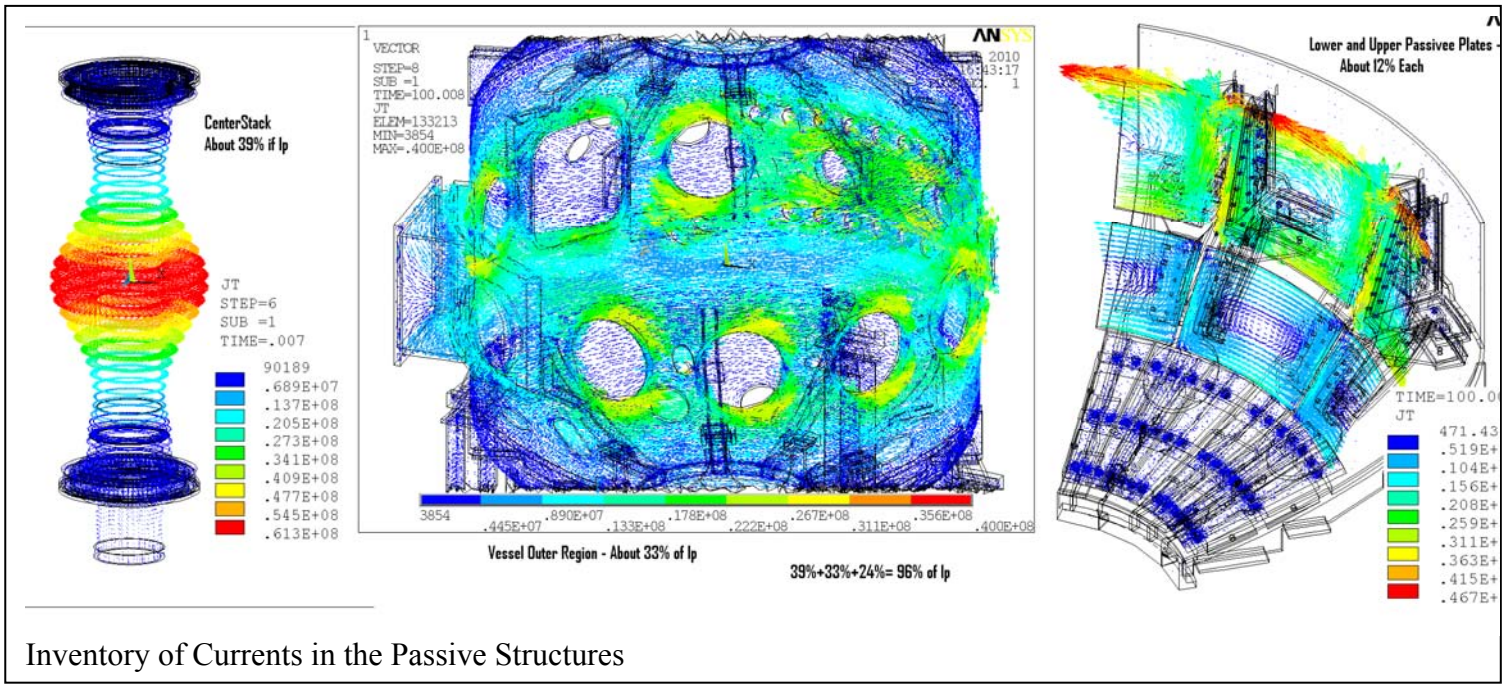

Figure 9.2.2-6 Inventory of Currents in the Passive Structures

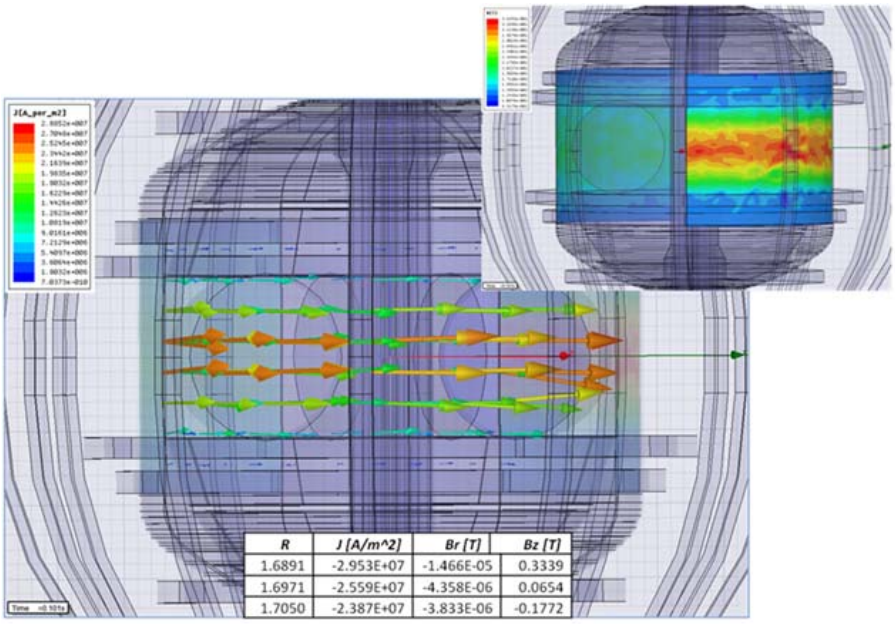

Maxwell 3D vs Opera 2D VV Wall Eddy Current and B Field Results

From Tom Willards Wed meeting Presentation Aug 2010

Figure 9.2.2-7 Maxwell and OPERA Mid-Plane Disruption Current Densities

9.3 Slow Plasma Translations

Slow VDE's sound less severe than quenchs. These are characterized by a translation from the mid-plane to another location. for the most significant of these with respect to the passive plates, the final position at a passive plate. The function of the passive plate is to resist this motion by developing counter currents which "push back" on the plasma. These forces are compressive i.e. push the passive plates back against the vessel. Consequently the tensile loads on the attachments should not be challenged.

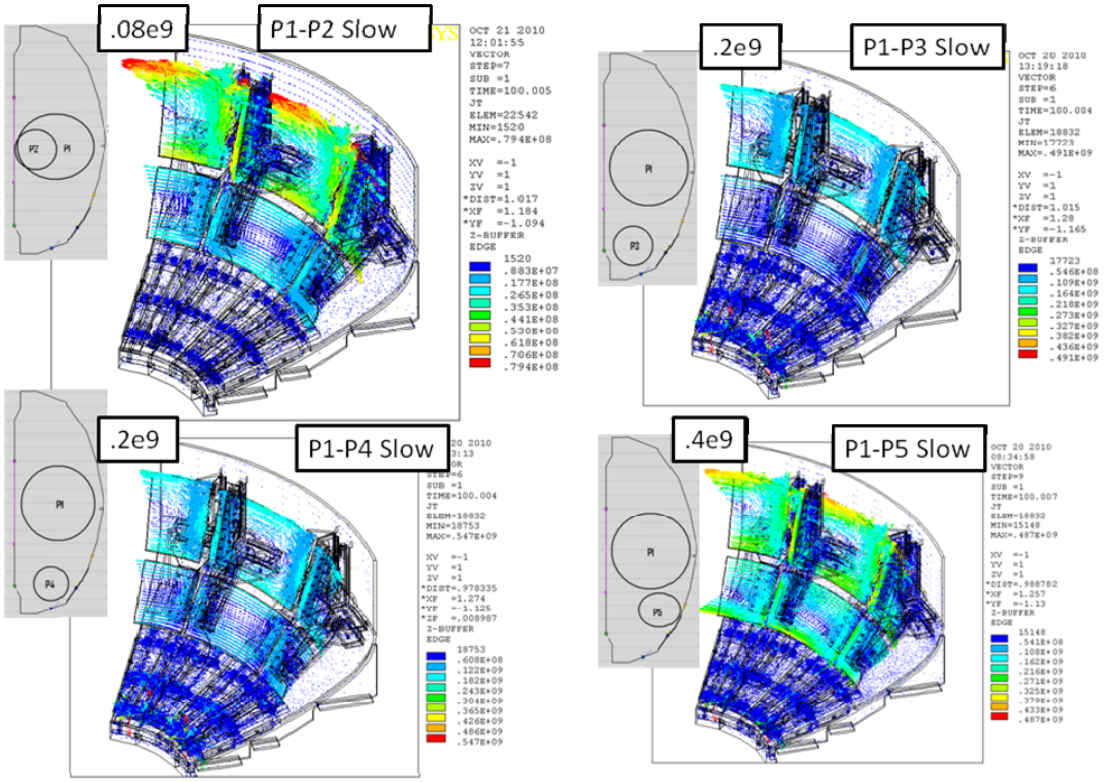

Figure 9.3-1 Comparison of Slow Translation Disruptions

9.3.1 P1-P2 Radial Slow Translation

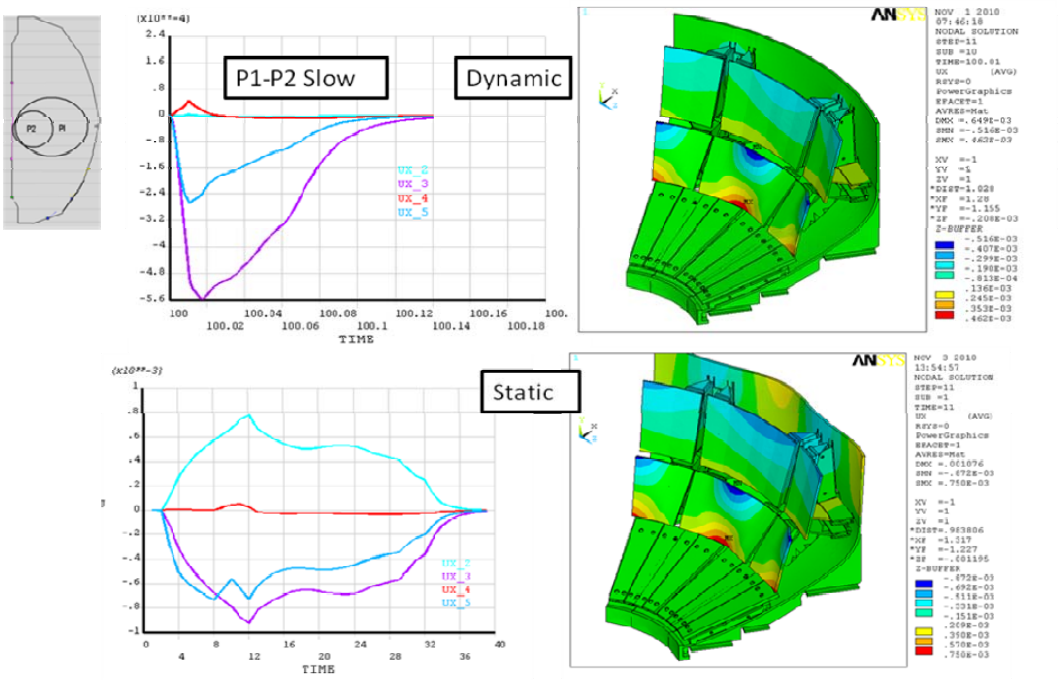

9.3-2 P1-P3 Slow

9.3.3 P1-P4 Slow

From figure 7.3.2, for loading of the secondary passive plate, .the following background fields would be appropriate: Bz=-.5, Br=.18

The following figures are from a run that assumed Bz=1.0, and Br = 0. As of April 21 this is being re-run

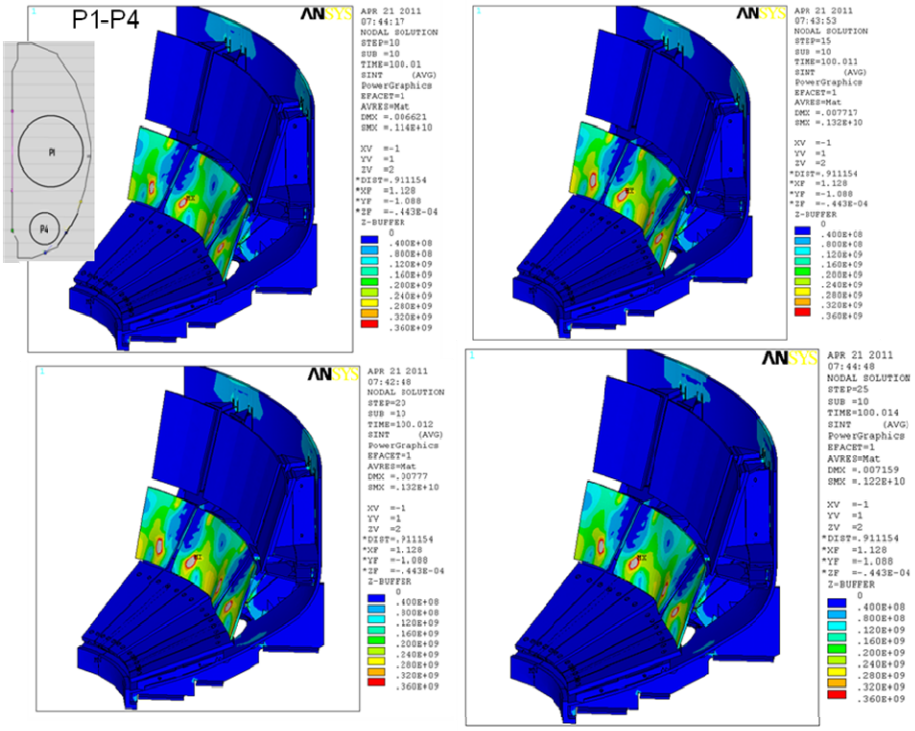

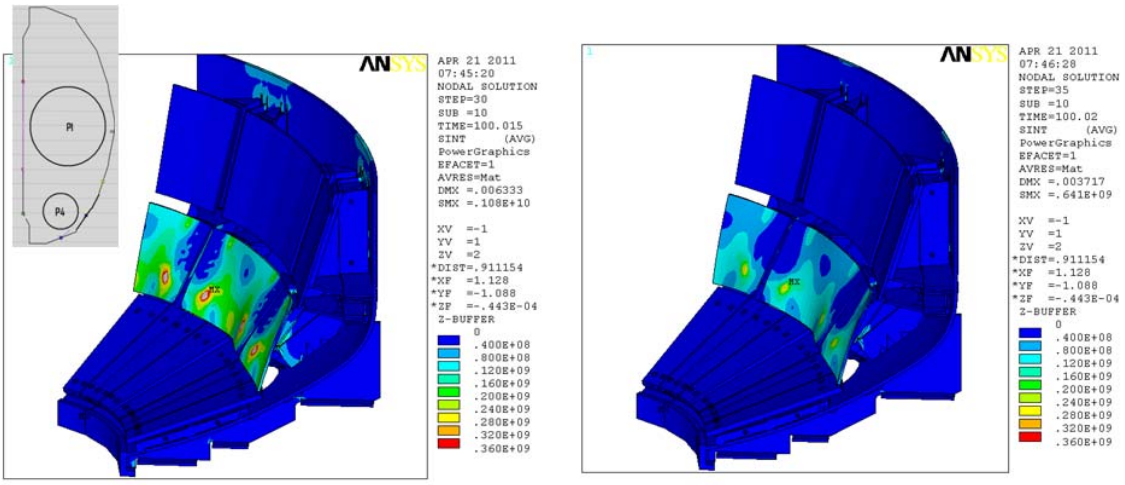

9.3.4 P1- P5 Slow

From figure 7.3.2, the following background fields would be appropriate: Bz=-.5, Br=.18 for loading of the secondary passive plate. .

The following figures are from a run that assumed Bz=1.0, and Br = 0. As of April 21 this is being re-run

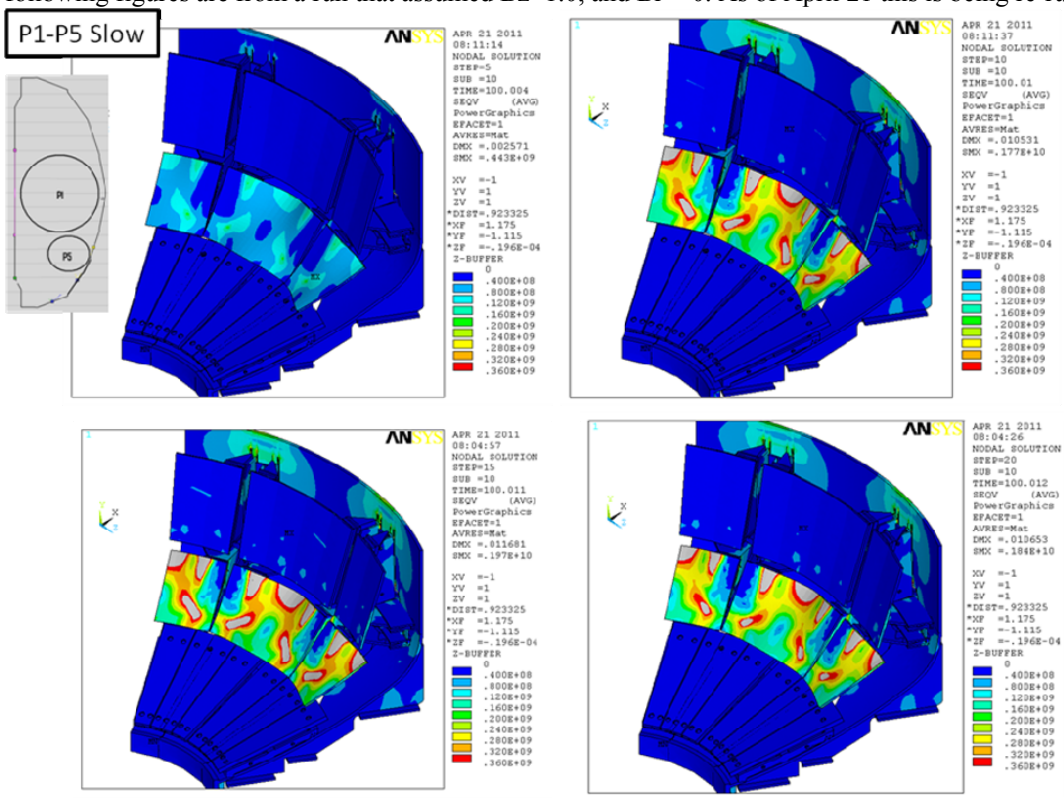

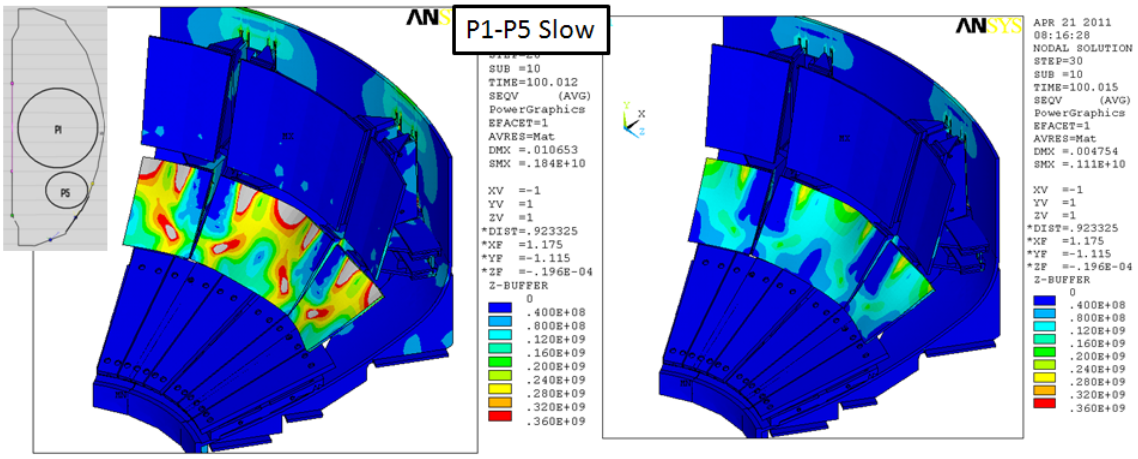

9.4 VDE to Plasma 4 Then Quench

This disruption simulation was expected to produce the largest loads on the lower passive plates and divertor, but it is not quite as severe as the slow translations

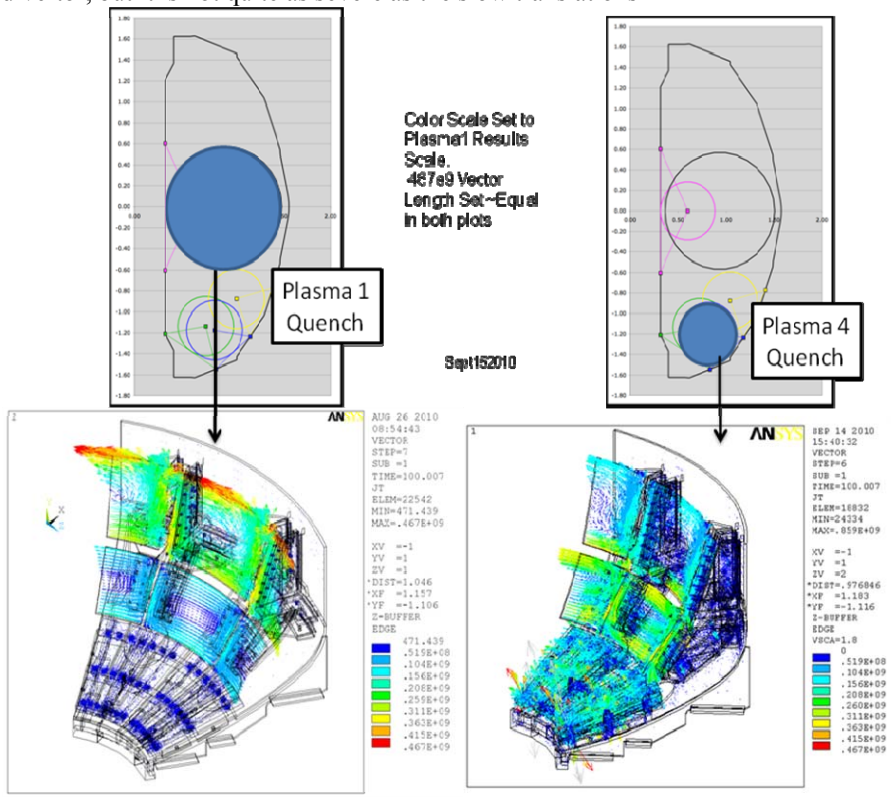

Dynamic Analysis Results
Mid Plane Disruption
Fast Quench of Plasma 1

Dynamic Analysis Results
Disruption Near Secondary Passive Plate
Fast Quench of Plasma 4

Same /Contour Scale as for the Mid Plane Disruption

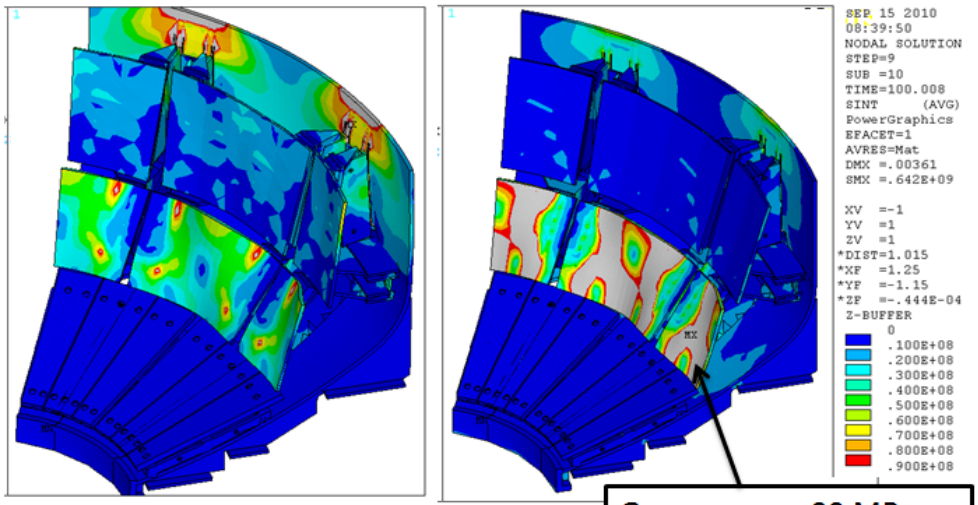

Gray means > 90 MPa

Static Analysis
Fast Quench of Plasma 4

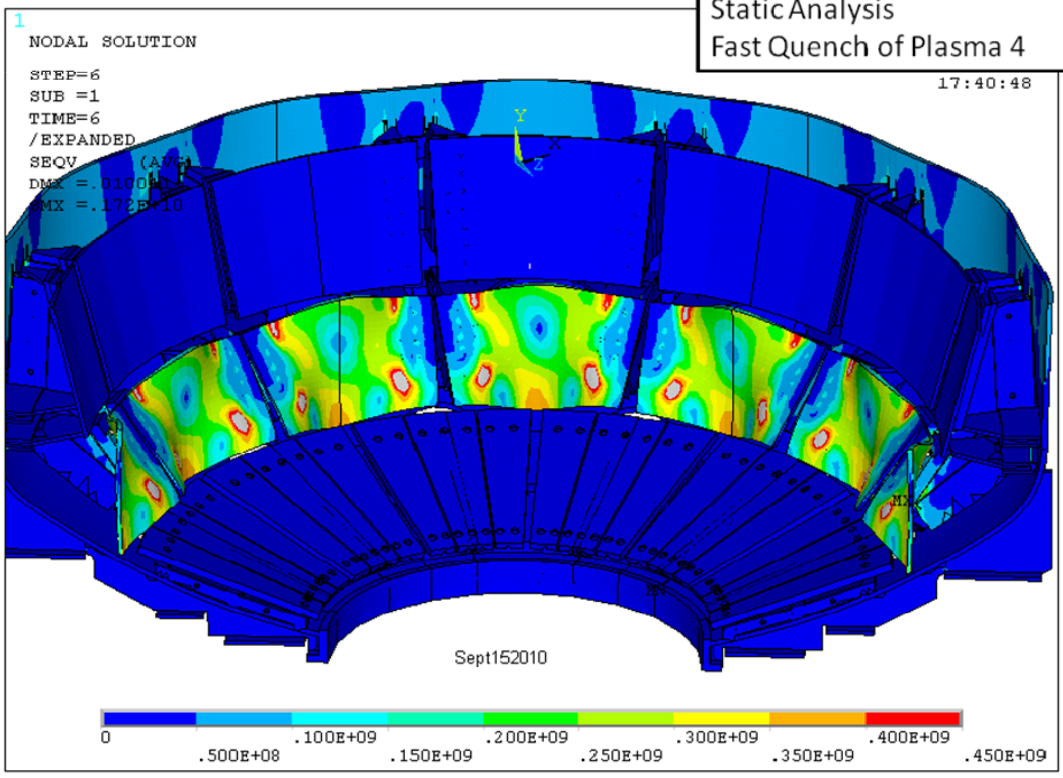

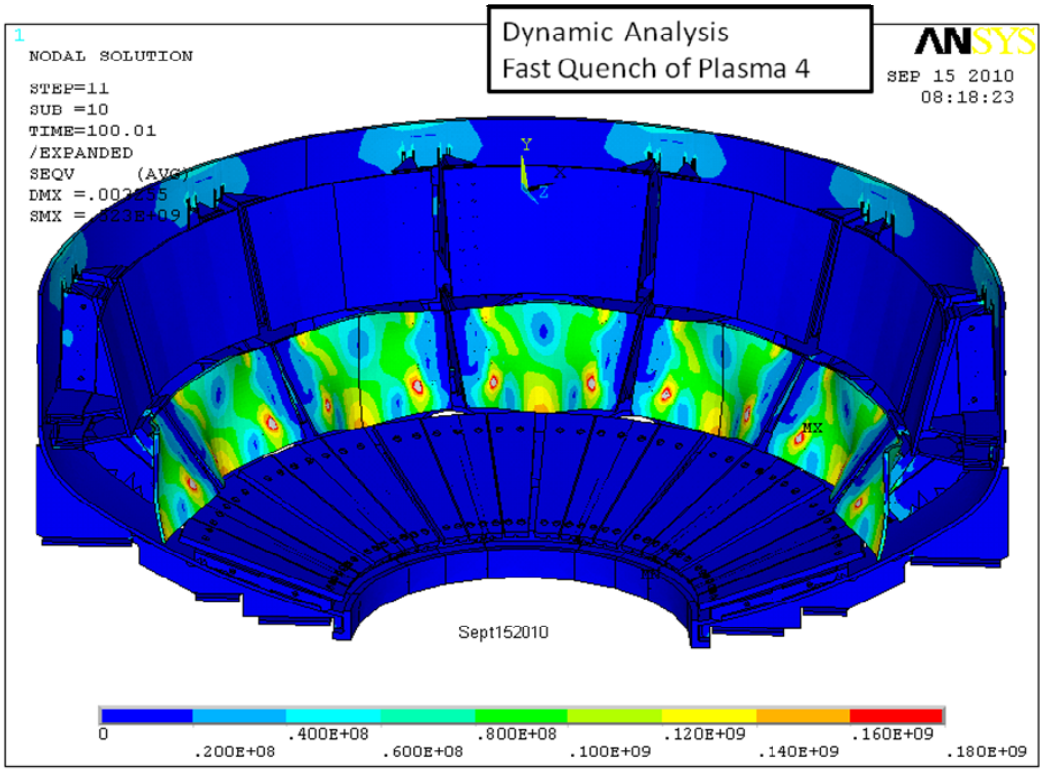
Dynamic Analysis
Fast Quench of Plasma 4
ANSYS
SEP 15 2010
08:18:23
NODAL SOLUTION
STEP=11
SUB =10
TIME=100.01
/EXPANDED
SEQV (AVG)
DMX =.002285
SMX =.823E+09
MX
Sept152010
0
.200E+08
.400E+08
.600E+08
.800E+08
.100E+09
.120E+09
.140E+09
.160E+09
.180E+09

9.5 Bolting Analysis

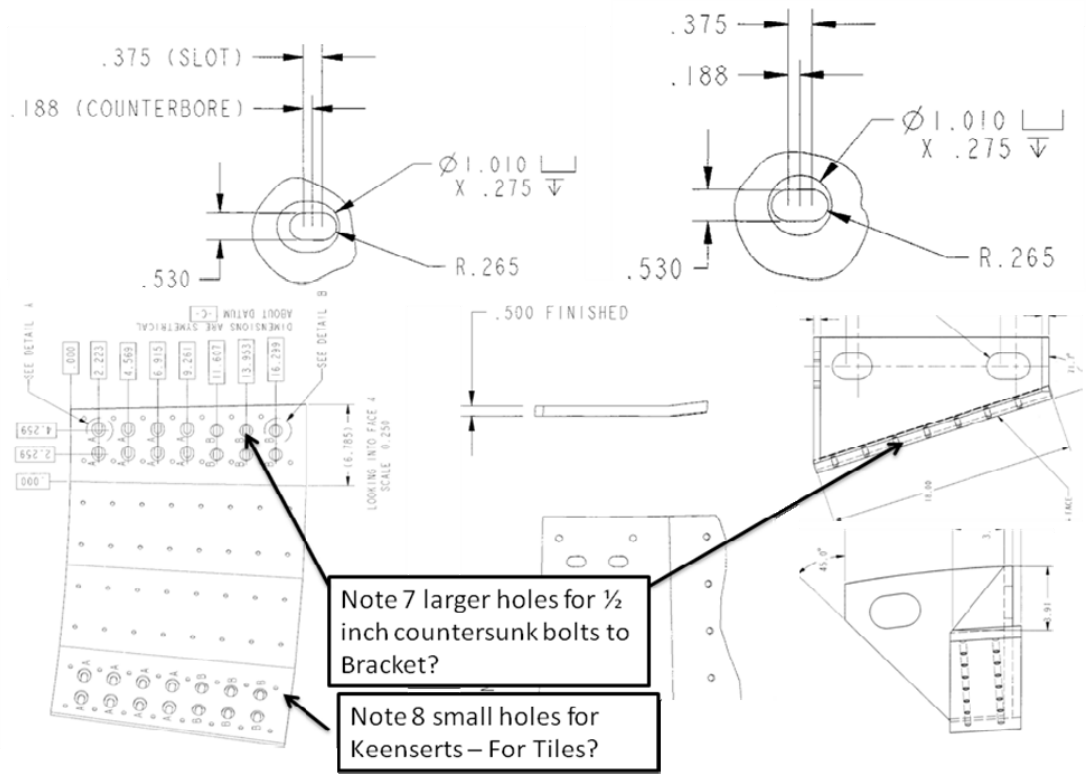

KEENSERT #KNHL420J	STN STL
PRIMARY PASSIVE PLATE	CDA 18150 COPPER
NOMENCLATURE OR DESCRIPTION	MATERIAL

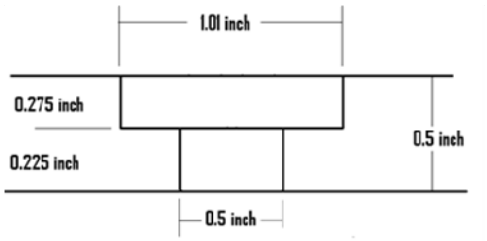

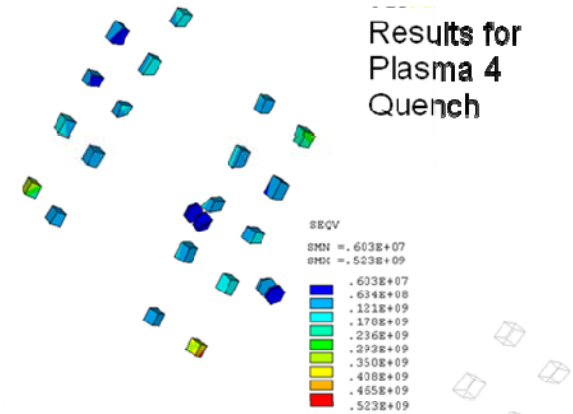

350e6*.01187*.0128*.2248=11954 lbs

Stress Area of a ½ inch bolt is .1416 in^2

Stress in worst corner bolt in the array=84,423psi

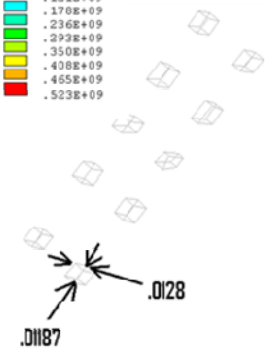

Shear Stress in Passive Plate Counterbore:
=11954/(1.01*pi*.225) = 16744 psi
Equivalent Tresca = 33488 psi = 231 MPa

Tensile Property CuCrZr

Material	Yield (Mpa)	UTS(MPa)
Low strength (L)	78	248
Intermediate strength (I)	199.4	318.6
High strength (H)	297	405.3

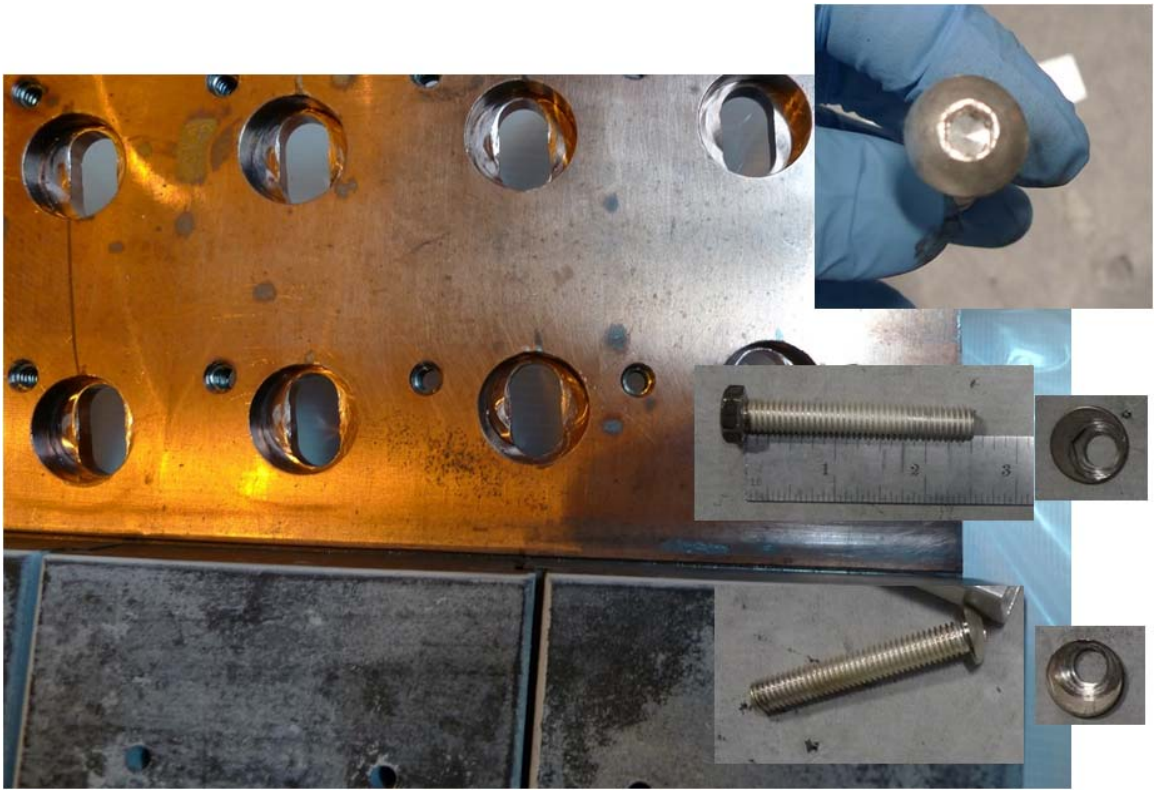

The passive Plates are made of CuCr1Zr UNS.C18150. Chromium Zirconium Copper C18150 is a copper alloy with high electrical conductivity, hardness, and ductility, moderate strength, and excellent resistance to softening at elevated temperatures. The addition of 0.1% zirconium (Zr) and 1.0% chromium (Cr) to copper results in a heat treatable alloy which may be solution treated and subsequently aged to produce these desirable properties.
NSTX Bake-out temperature is 350 degrees C. The softening temperature of properly heat treated C18150 rod exceeds 500°C as compared to unalloyed pure copper which softens at 200°C, and silver bearing coppers which soften at 350°C.

Copper Cr Zr Properties from ref [4]

Material	Yield strength (MPa)	UTS (MPa)	Average over
Low strength (L)	78	248	3
Intermediate strength (I)	199.4	318.6	3
High strength (H)	297	405.3	5

Ref 1, the original NSTX Passive Plate Calculation has slightly lower properties for CuCrZr

Estimate of 5/8 bolt shear load

Each bracket has 12 bolts, each in double shear, shear area =.306in^2
700000 amp halo current*.8m poloidally across the face of the PP *1Tesla toroidal field*1.5 peaking factor/12brackets/12bolts per bracket/2shear planes per bolt = shear load per shear area = 2916N = 655 lbs or 2142 psi shear or 4.2 ksi Tresca

Passive Plate 5/8 bolt Shear Stress Estimate for Halo Loads

- **Estimate of 5/8 bolt shear load**
- **Each bracket has 12 bolts, each in double shear, shear area =.306in^2**
- **700000 amp halo current*.8m poloidally across the face of the PP *1Tesla toroidal field*1.5 peaking factor /12brackets /12bolts per bracket / 2 shear planes per bolt = shear load per shear area = 2916N = 655 lbs or 2142 psi shear or 4.2 ksi Tresca**

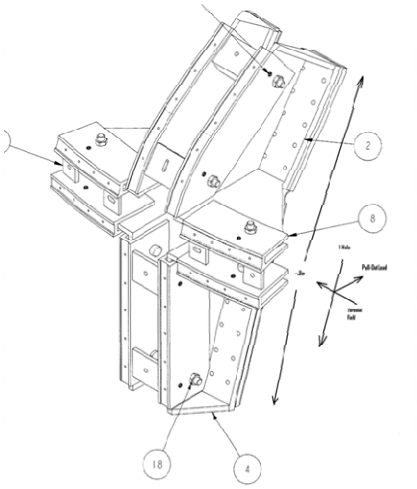

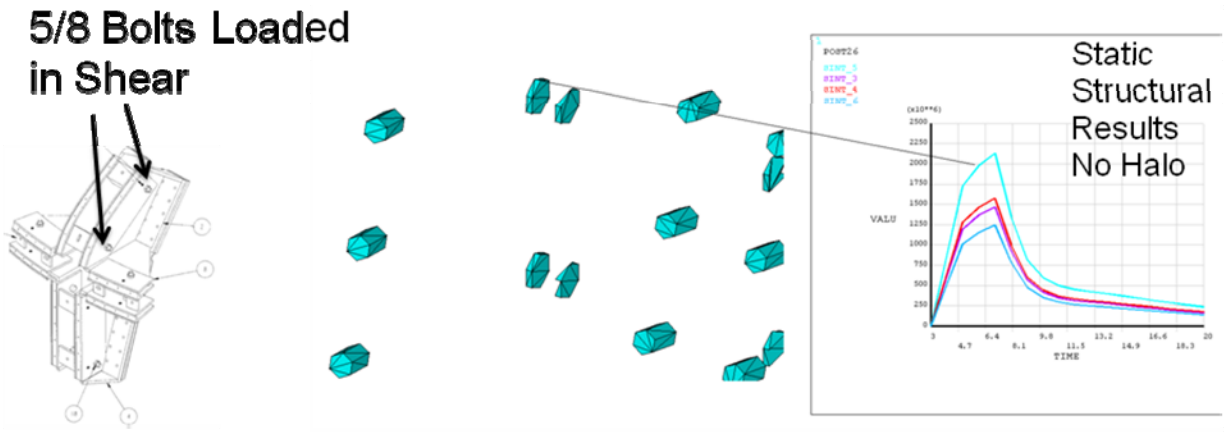

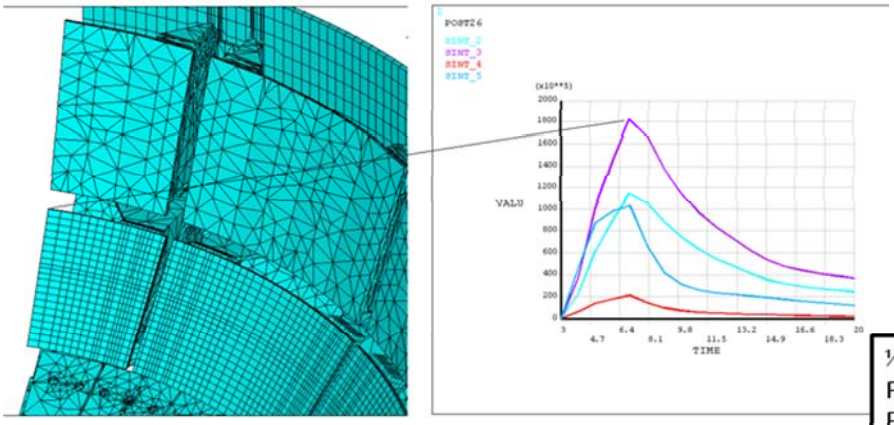

$t5=6.50E-03

$t10=9.00E-03

½ Period= 2.5 millisec, Frequency=1/.005=200 Forcing Function

9.6 Brack Welds

Prior to Making the Welds

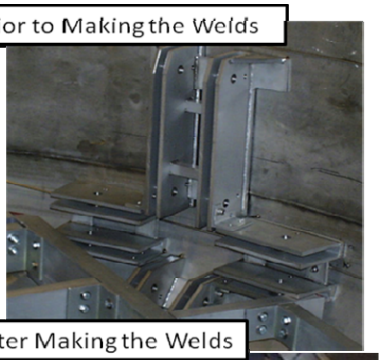

After Making the Welds

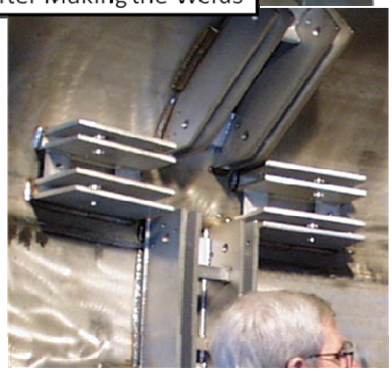

Bracket Welds

From Attachment F Passive Plate Bracket Weld QA Report

From J Boscoe To E Perry

Re: Welding of Vertical Straight (1053) and Vertical Curved Support Brackets (1055)

Because of fit-up - assembly gap issues on the above mentioned components & instructions (verbal) were given per Chrzanowski/Berner to use ¼" thick x ½" wide bridge-transition pieces to overcome these gaps. Due to worries about excessive installation time it was decided that doubling up on weld size ⅜" fillet to ¾" fillet would decrease required weld length by ½ or an increase of weld size from ⅜" fillet to 5/16" fillet would decrease the required weld length by ⅓. Welder - Tig torch accessibility for full length welds up both sides of pieces was also a factor in this decision. The design drawing - weld detail in question is EDB-1051. I believe it was intended for CR 70 to cover this (along with many other modifications - tweaking to original design). This change did not get included on CR 70.

In addition I noticed on inspection of the lower support-brackets that the unwelded portions of the vertical curved brackets #1055 ("bobsleds") are the ⅓ of length including the curved sections. My most recent concern was the remote possibility that this could adversely affect stress calculations

9.7 Frequency Analysis of the Passive Plate Model

The need of performing a modal analysis is reduced by the ability to run full dynamic analyses of the vessel and internal components. In this section, the results of modal analyses of the passive plates are presented for the purpose of aiding in the evaluation of the dynamic load factors that result from the dynamic analysis.

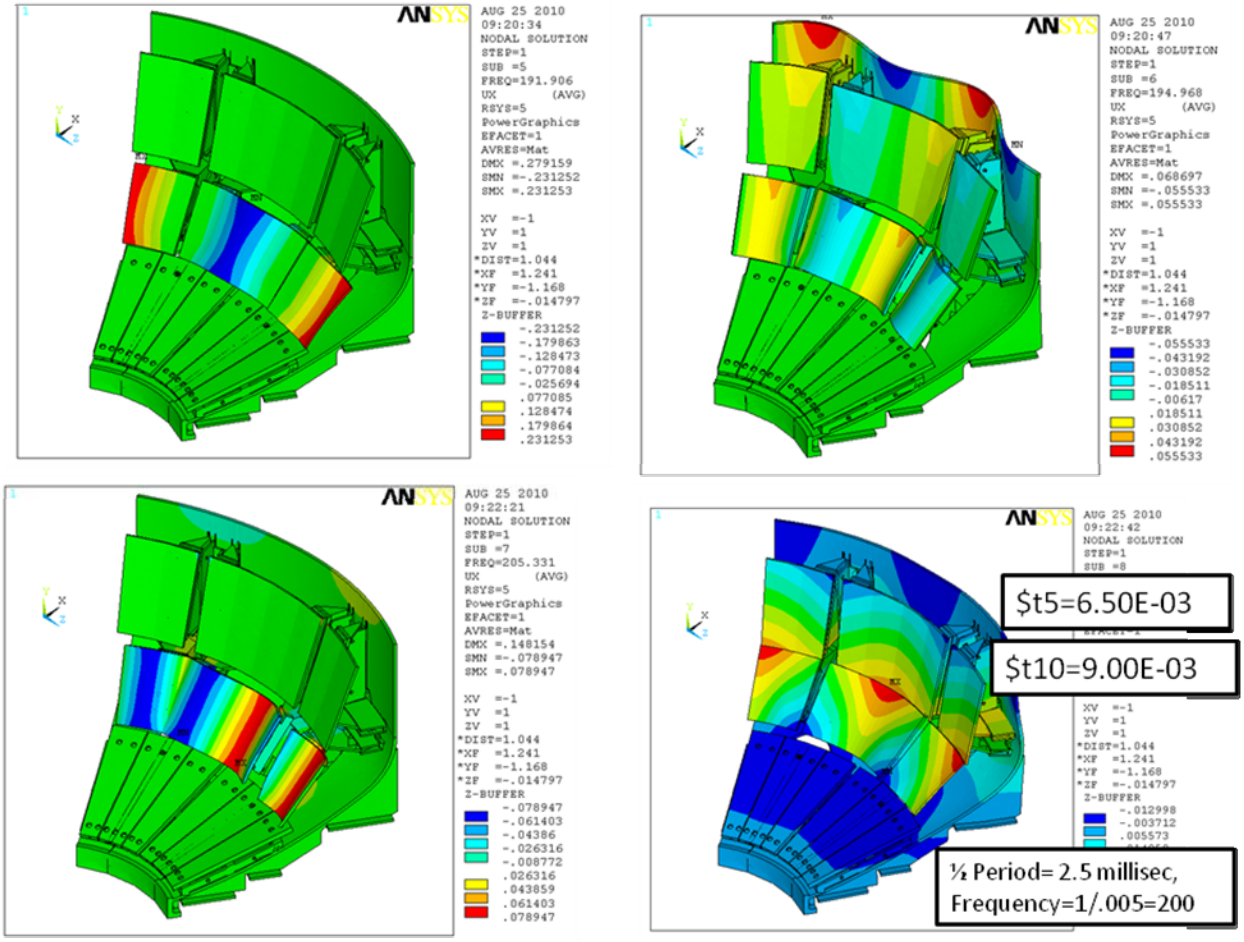

The passive plate frequencies are in the range of the disruption excitation frequency. From this, it would be expected that the dynamic load factors would be greater than one.

Amplification factor, or DLF – Single degree of freedom oscillator with a "truncated" harmonic forcing function. Half a wavelength, or a load pulse of half a period would give a peak DLF of ~1.7 - if the frequency ratio is uncertain. For a high frequency pulsed load acting on a low frequency structure, the dynamic amplification factor is less than one.

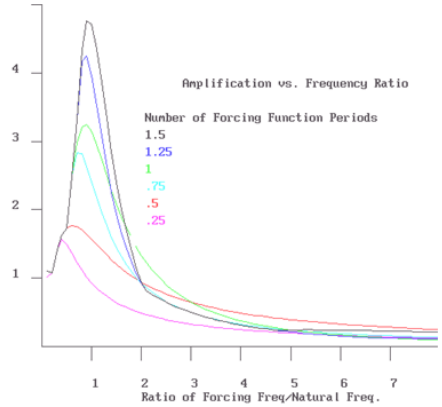

11.0 Centerstack Casing Analysis

11.1 Drawing Excerpts

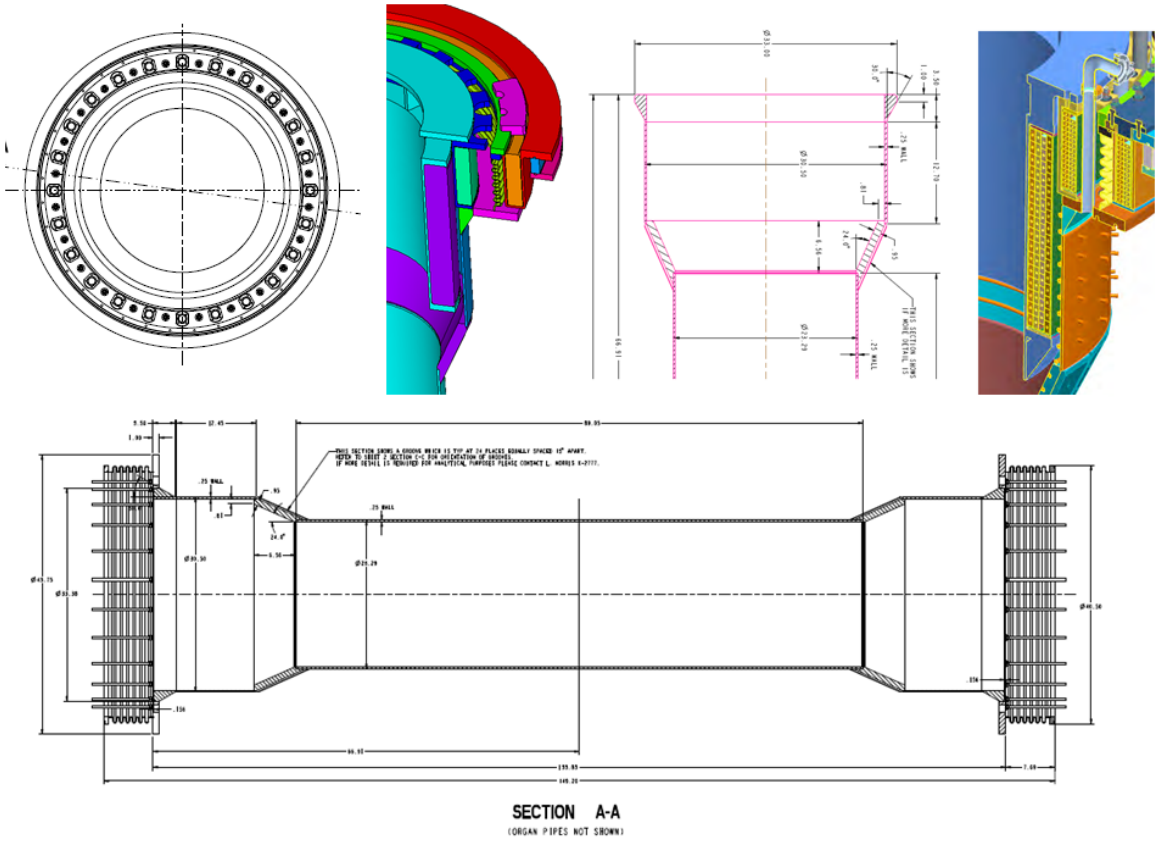

11.2 Inductively Driven Currents and Resulting Forces

Disruption analyses were performed on the centerstack casing using the procedures outlined in this calculation. Inductive eddy current loads have minimal effect on the casing because toroidal currents are induced. These are parallel to the toroidal field which then does not contribute to the Lorentz Loads. Only the poloidal fields and the toroidal currents produce significant loads..

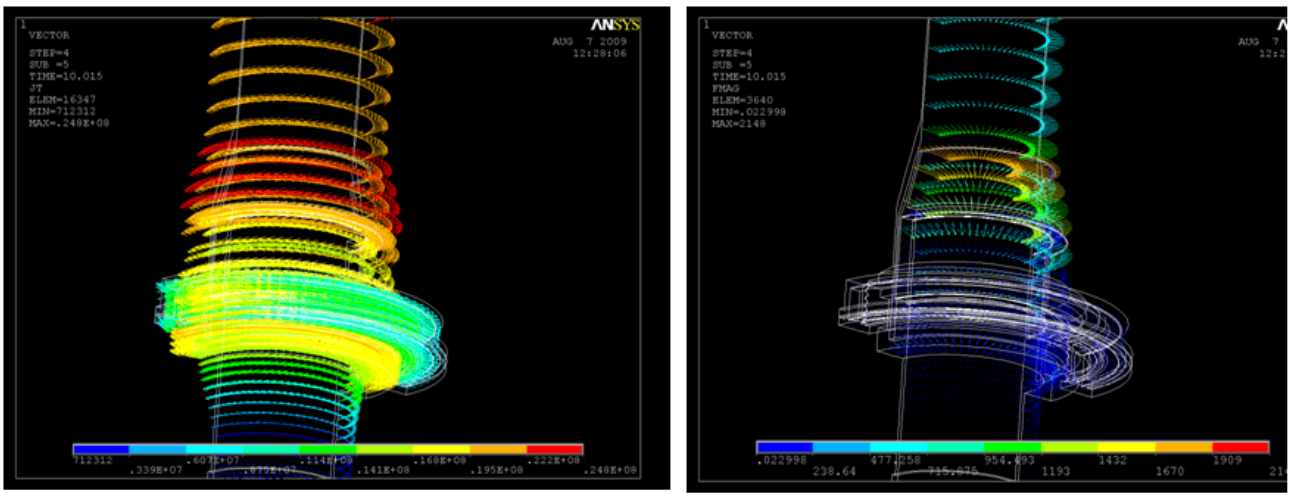

Inductively Driven Disruption Currents in the Casing Forces from Inductively Driven Disruption Currents

Figure 11.2-1 Inductively Currents and Forces from a Mid-Plane Disruption

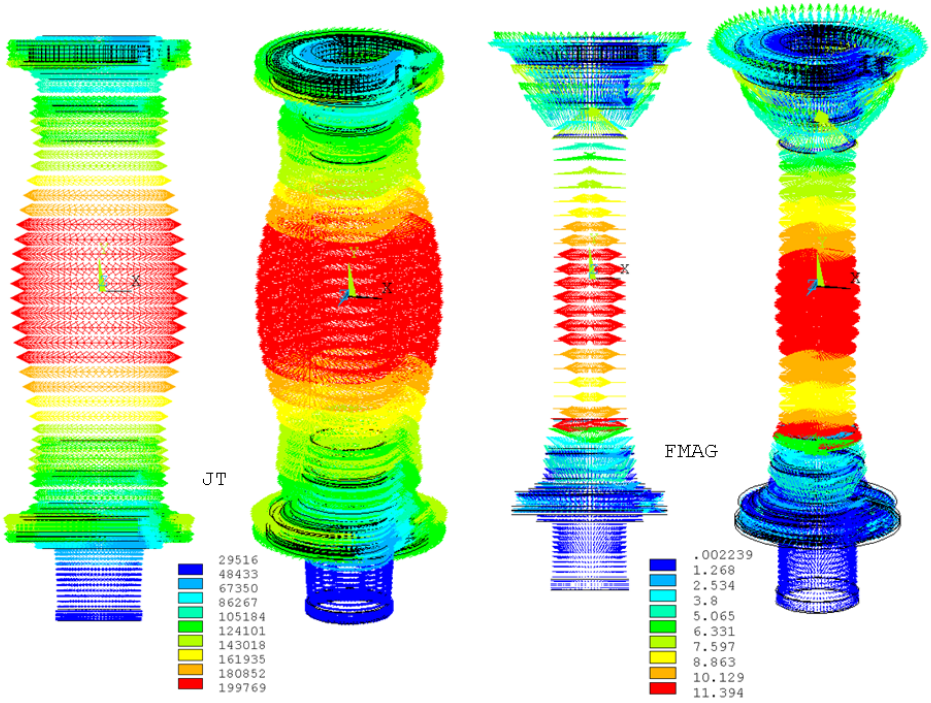

Figure 11.2-2 Inductively Currents and Forces from a Mid-Plane Disruption (April 2011)

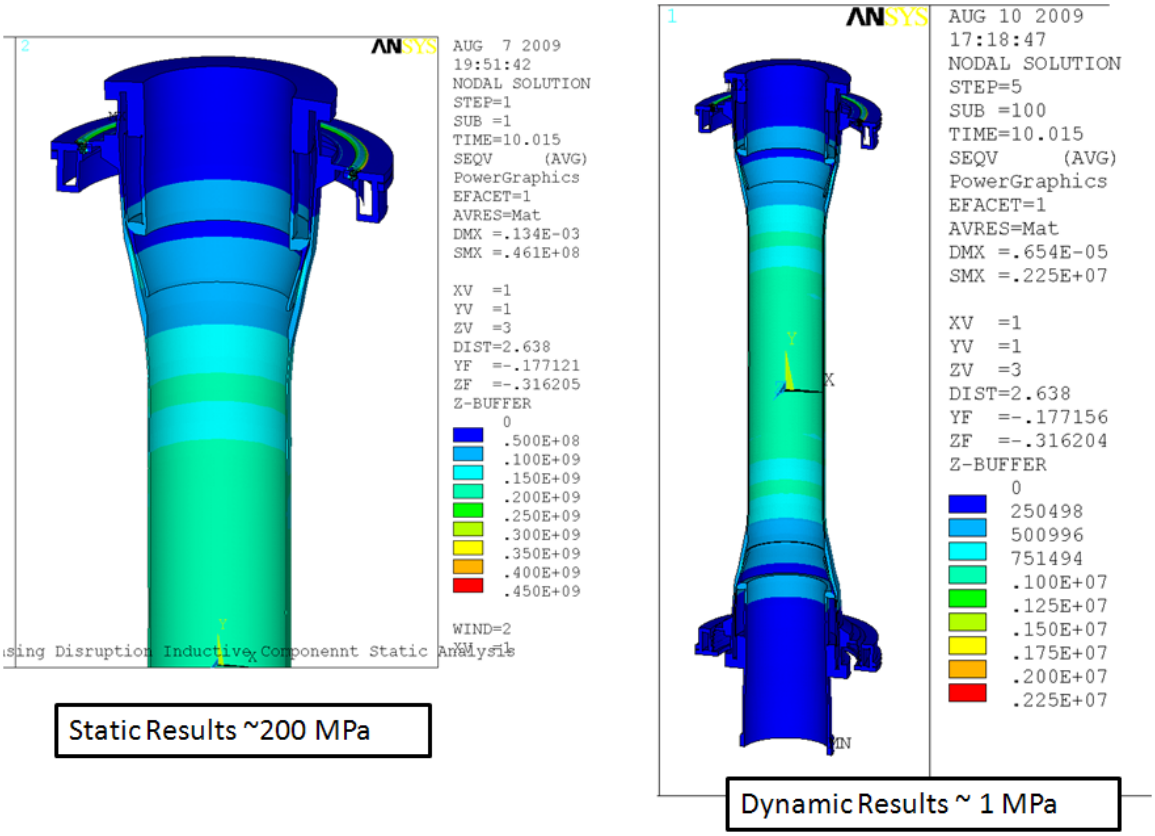

Figure 11.2-3 Stresses Due to Inductively Driven Currents and Forces from a Mid-Plane Disruption

11.3 Halo Currents and Resulting Forces

Halo currents have a large poloidal current component, are not axisymmetric, and potentially produce a large net lateral load. NSTX has some history regarding halo loads. .Neil Pomphrey and Jim Bialek studied the distribution of Halo Currents in NSTX [12]. Their understanding of the current re-distribution is that there is a resistive re-distribution of currents that minimizes the peaking factor or non axisymmetric loading over most of the height of the centerstack casing. . Art Brooks has studied the inductive component of the halo current derived from the poloidal inventory of current s in the plasma. Initially the peaking factor applies because inductive effects oppose resistive redistribution of the currents. In a short time, the currents redistribute resistively and reduce the peaking factor. This work is described in NSTX calculation " Halo Current Analysis of Center Stack" Calculation number NSTX-CALC--133-05-00-April 13, 2010 by Art Brooks [13]. Art Brooks' calculation is the calculation of record for Halo loading.

Halo loading was also investigated along with the inductively driven currents. The following spec is from the CDR Upgrade GRD:

Halo current [MA]	n.a	20%=	35%=	35%=	35%=
		400kA	700kA	700kA	700kA
Halo current entry point (r,z) [m]	n.a	0.3148	0.3148	0.8302	1.1813
		0.6041	-1.2081	-1.5441	-1.2348
Halo current exit point (r,z) [m]	n.a	0.3148	0.8302	1.1813	1.4105
		-0.6041	-1.5441	-1.2348	-0.7713

Addition of the halo currents was done in two ways. The first was to develop a cosine distribution of loads on the centerstack casing. These were then added to the Lorentz loads obtained from the inductively driven

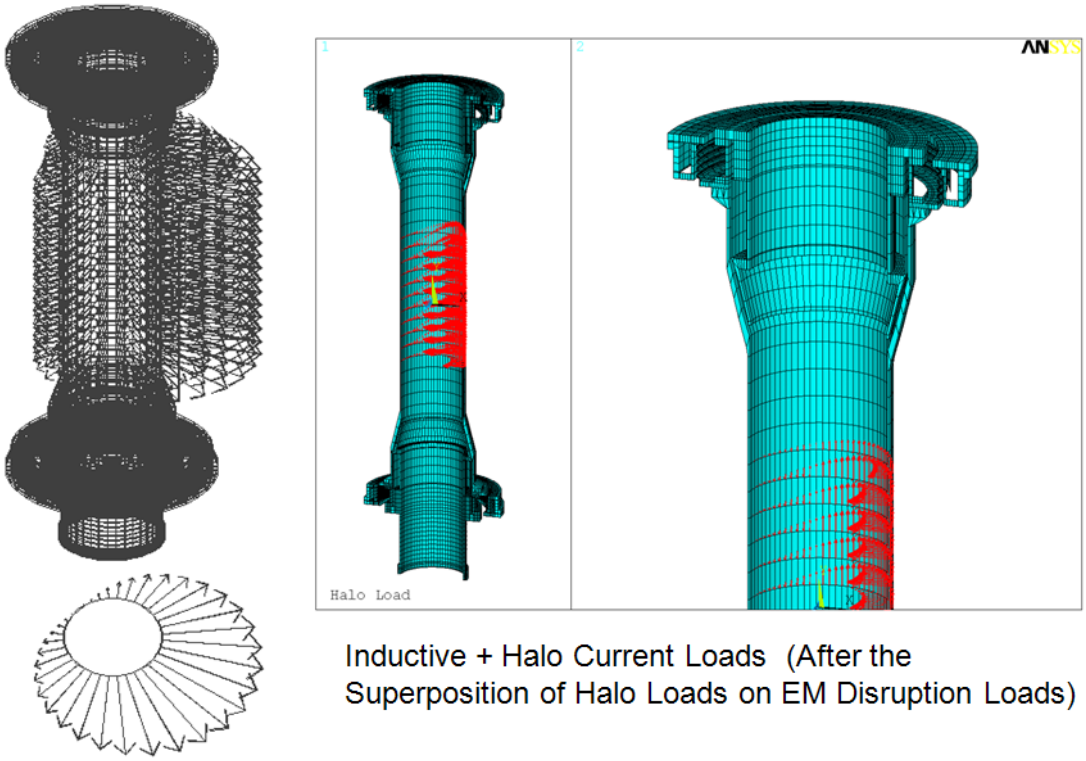

Figure 11.3-1 Disruption Forces, Including Halo Loads

currents/loads in the shell. Halo loads were calculated outside of ANSYS and read in after reading the inductive loads with the LDREAD command, and with FCUM,ALL

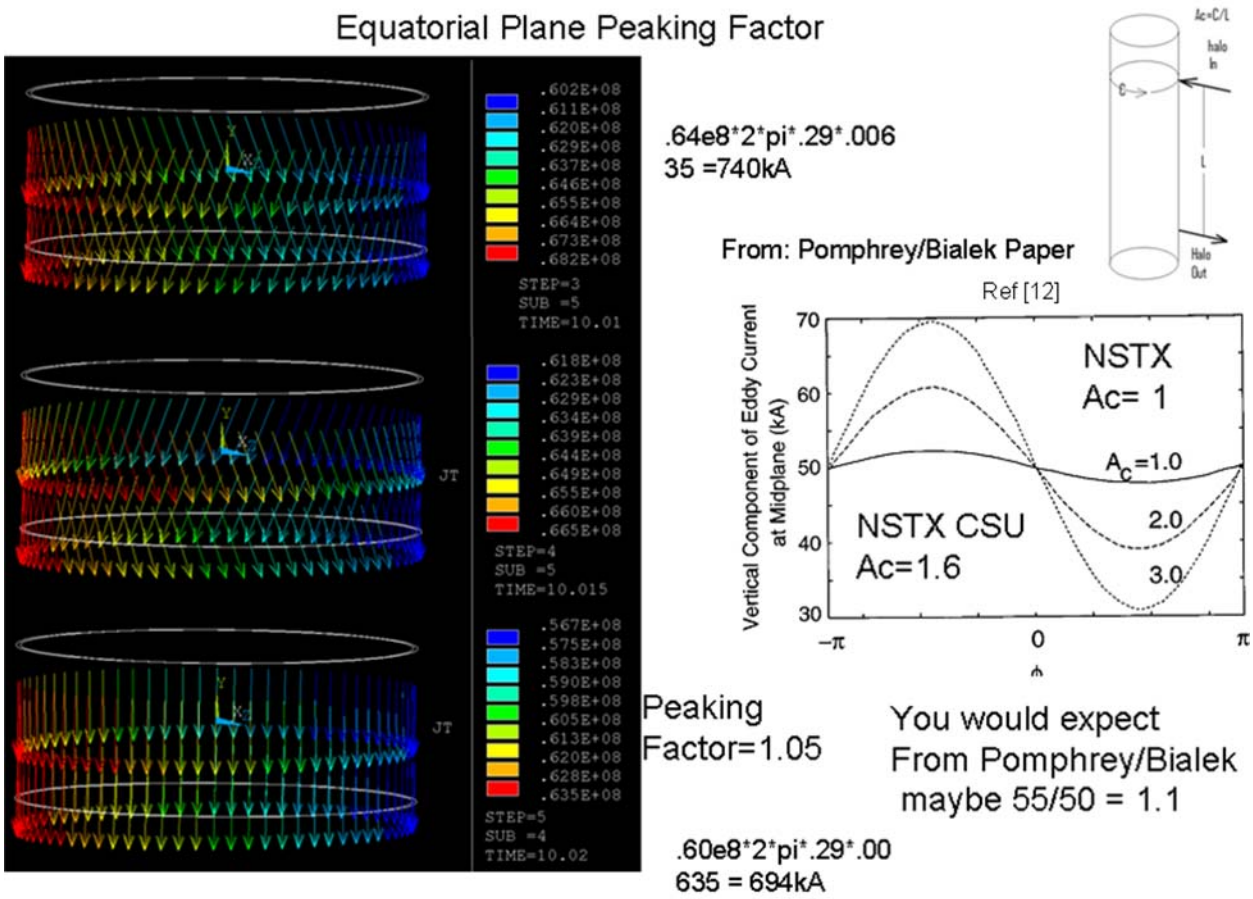

The second way to include halo loading is to introduce the halo currents during the ANSYS electromagnetic simulation in the same way the halo loads were included in the passive plate analyses. This was done, but the work was superseded by a more rigorous treatment by Art Brooks. [13]

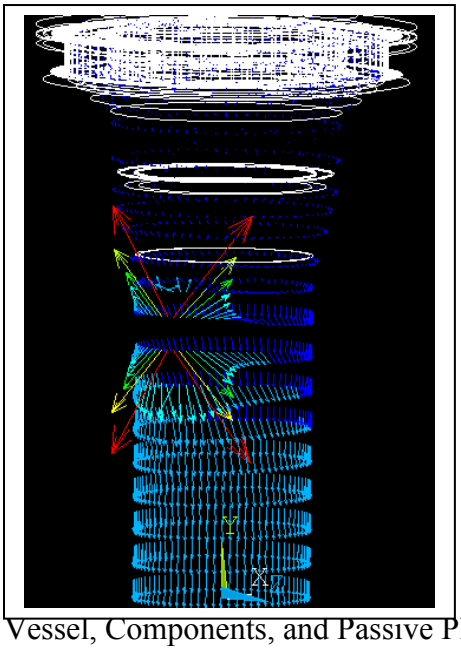

```
BR=130000*12*3*2e-7
*get,nmax,node,,num,max
*do,i,1,nmax
z=nz(i)
x=nx(i)
d,i,ay,vect4(x,z)
d,i,az,-0.5*BR*log(x*x)
*enddo
d,all,ax,0.
f,32437,amps,700000.0
f,18830,amps,-700000.0
lswrite,4
time,10.02
autots,1
deltim,.001,.0005,.002
kbc,0
*dim,vect5,table,81,81,1,x,z,,5
*tread,vect5,'5','txt'
nall
BR=130000*12*3*2e-7
*get,nmax,node,,num,max
```

12.0 Bellows Analysis

The analysis of the bellows is presented in detail in calculation number NSTXU-CALC-133-10-0 by Peter Rogoff. Presented here is the initial analysis of the electromagnetic analysis of the bellows. P. Rogoff's calculation includes the EM analysis and structural analyses for all loading of the bellows. Also Rogoff sizes the convolutions and bellows thicknesses to satisfy the EJMA standards and the NSTX criteria. The finite element model used in the EM calculations derives from Rogoff's NASTRAN plate element model. This was converted to 8 node brick solids that allow use of the procedure developed in this calculation.

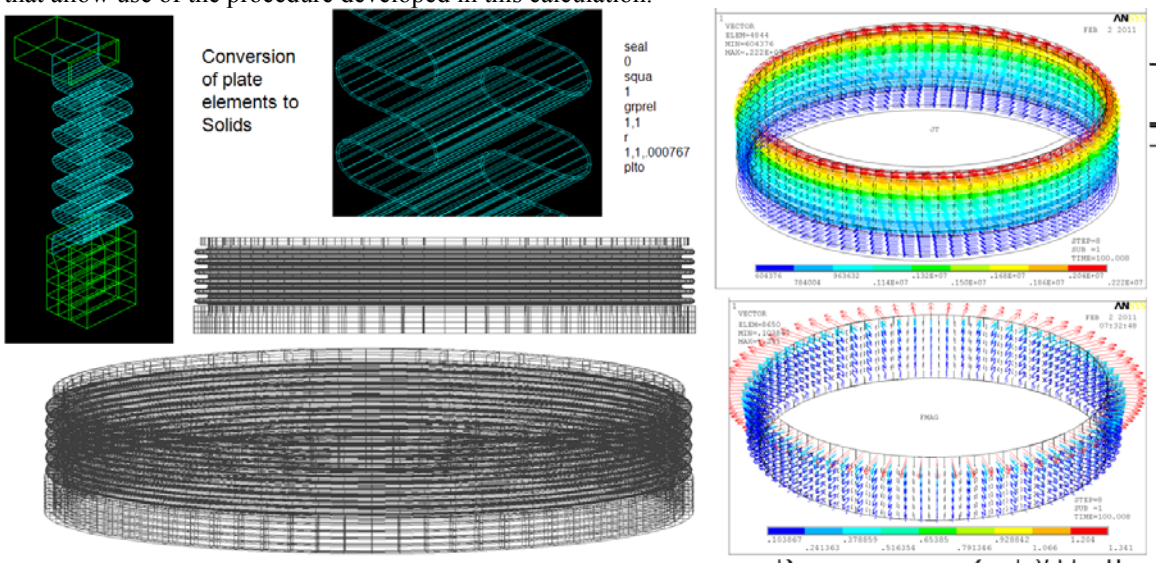

Figure 12.0-1 Bellows mesh (Left) Current Density (Right, Upper) Forces (Right Lower).

13.0 NB Backing Plate Analysis

This is another application of the procedure that is covered in more detail in the calculation of record by Larry Bryant This procedure has been applied to the neutral beam armor plate backing structure, various diagnostic components, and the centerstack casing, using a common set of OPERA disruption VP files.

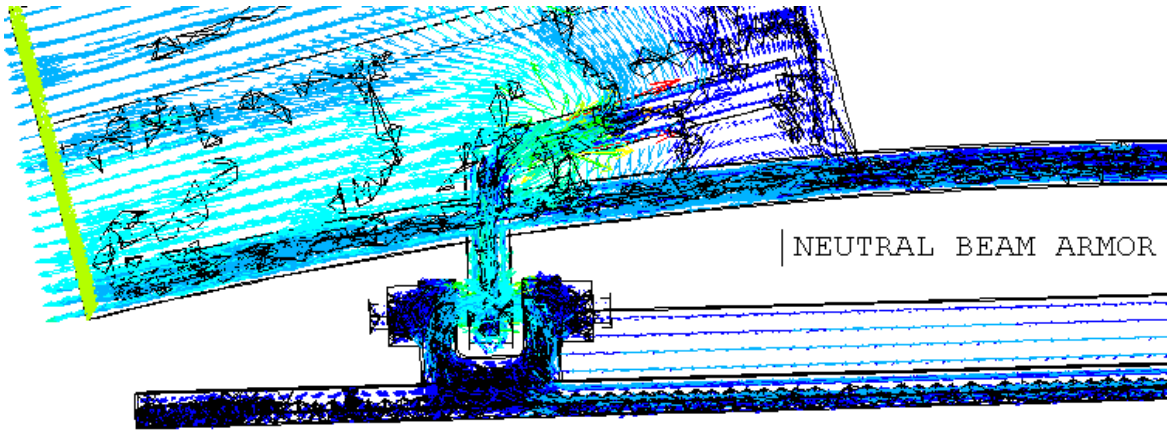

Figure 13.0-1 Current Densities in the Neutral Beam Armor Plate Backing Plate,

14.0 Moly Shield for the TAE antenna

The TAE antenna is a stand alone antenna utilizing five turns of 10 gauge copper wire on stud-mounted Macor standoffs shielded by molybdenum strips. Figure 14-1 shows the position of the antenna and the inset shows some of the details of the TAE corner spoolpieces, and the shield cross sections/ The Moly strips and attachments proposed for shielding of the TAE antenna were sized to experience eddy current forces equivalent to the Moly shields installed over the existing RWM sensor coils (I believe this was analyzed by Art brooks Michael Bell's). The first e-mail included in attachment is calculations for the maximum forces on the moly shields being proposed for the new antenna. We would to either have Michael's calculations checked, or further analysis done as you see appropriate.

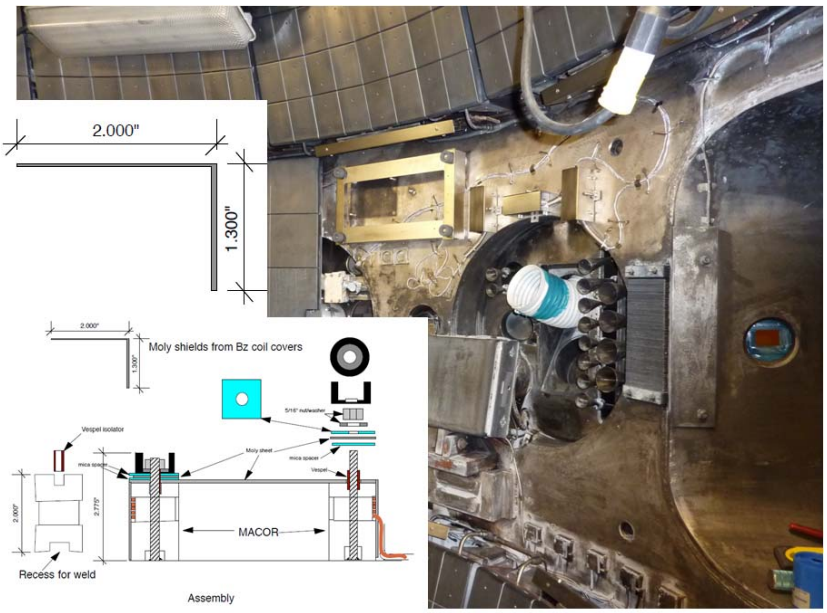

Figure 14.0-1 TAE Antenna with trial mounted shield

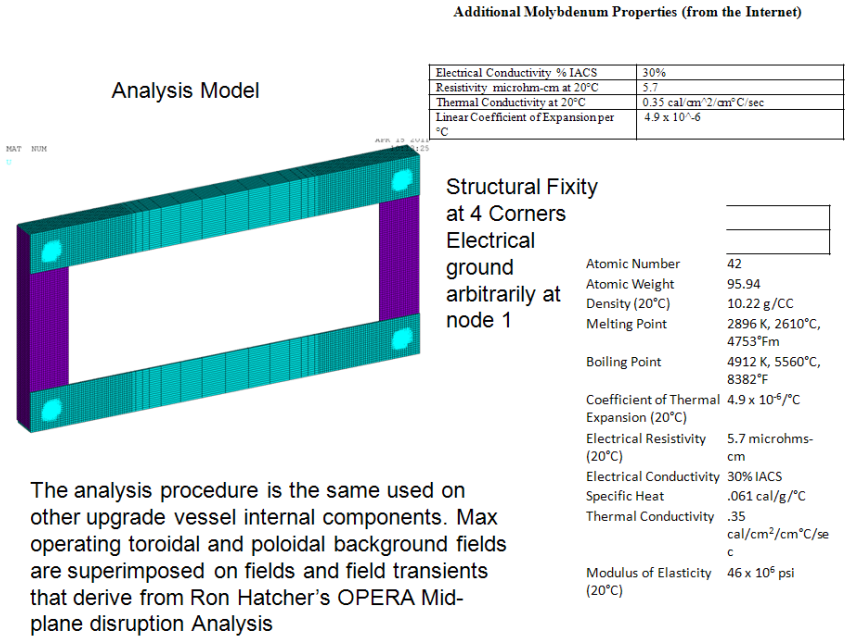

Figure 14.0-2 TAE Antenna Analysis Model

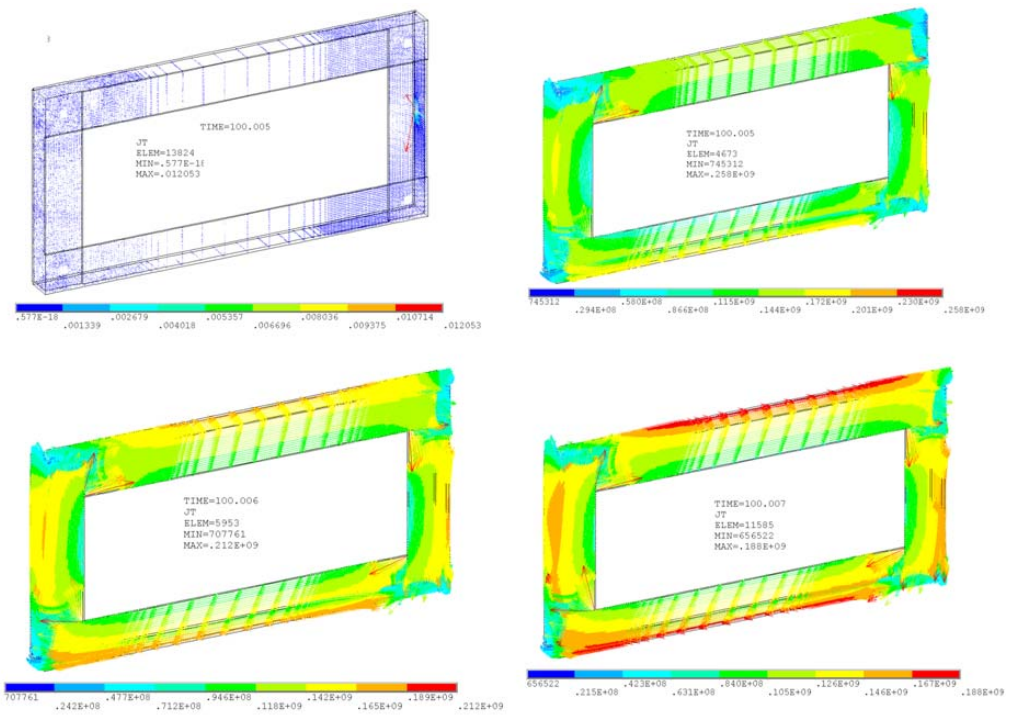

Figure 14.0-1 TAE Antenna with trial mounted shield

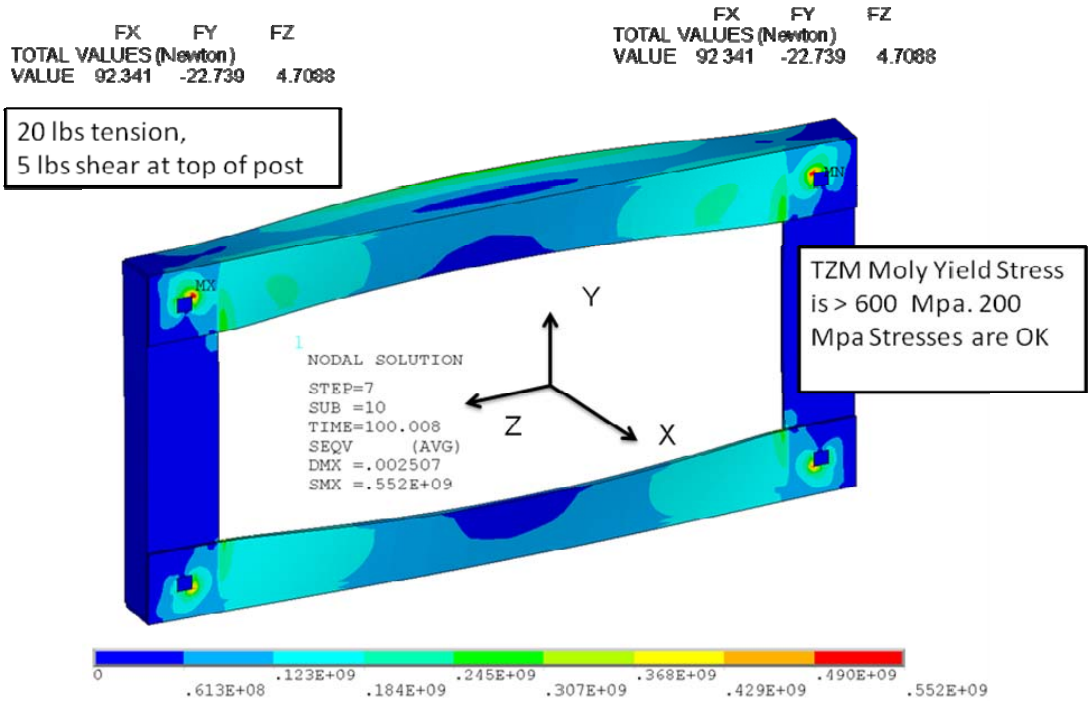

Figure 14.0-3 TAE Antenna Stress and Reaction Results

Appendix A

MACRO FOR GENERATING EDDY CURRENTS

```
!!!(Used for P1-P5 Slow VDE)

/filename,halo2
/prep7
/nerr,1000000,1000000

BackBz =-.5
BackBr = .18
et,1,45
ex,1,200e9     !Vessel
ex,5,117e9     !passive Plates
ex,8,200e9     !Vessel Shell
ex,10,200e9    !Diverto2 Support
ex,11,200e9    !ribs
ex,12,200e9    !PPL Support
ex,13,200e9    !Vessel Bracket
ex,14,200e9    !Vessel Bracket
ex,15,200e9    !Vessel Bracket
ex,17,200e9    !bolts


shpp,off
/input,lowd,mod
!/input,ves2,mod
nummer,node,.000001
nsel,y,-3,-1.8
d,all,all,0.0
nall
eall
csys,5
!nrotate,all
!nsel,y,-15.001,-14.999
!nasel,y,14.999,15.001
!d,all,uy,0.0
nrotate,all
cpdele,all,all
cpcyc,ux,.001,5,0,60,0
cpcyc,uy,.001,5,0,60,0
cpcyc,uz,.001,5,0,60,0
nall
eall
```

```
save

fini

/solu
f,31523,fy,1.0
solve
save
fini
!/exit   ! remove for the electromagnetic part

/filename,elect2
/prep7
/nerr,,99999997,,0,,
resume,halo2,db ! 360 degree model of the vessel, legs, umbrella & passive plates
et,1,97,1  !Center Stack Casing
et,5,97,1 ! vessel, legs and umbrella structure
et,12,97,1 ! passive plates

!ex,1,200e9     !Vessel
!ex,5,117e9     !passive Plates
!ex,8,200e9     !Vessel Shell
!ex,10,200e9    !Diverto2 Support
!ex,11,200e9    !ribs
!ex,12,200e9    !PPL Support
!ex,13,200e9    !Vessel Bracket
!ex,14,200e9    !Vessel Bracket
!ex,15,200e9    !Vessel Bracket
!ex,17,200e9    !bolts

*do,imat,1,20
mp,dens,imat,8950
mp,murx,imat,1.0
mp,rsvx,imat,74.0e-8
*enddo
mp,dens,1,8950 ! vessel, legs and umbrella structure
mp,rsvx,1,74.e-8
mp,dens,20,8950 ! Center Stack Casing Inconel 625
mp,rsvx,20,1.3e-6
mp,dens,5,8950 ! Passive plates
mp,rsvx,5,.85*2.443e-8 ! @400K
mp,dens,6,8950 ! Passive plates
mp,rsvx,6,74e-8
csys,5 ! Opera output is in Cylindrical System
nrotat,all
!nsel,s,loc,z,-3.9342,-3.9215 ! Selects nodes at the base
```

```
nsel,s,loc,z,-100,-1.8
!nasel,y,29.99,30.001
!nasel,y,-30.001,-29.99
d,all,volt,0 ! Constrains the Volts DOF at the Lower CHI/Bellows/Ceramic Break
nall
eall
cpdele,all,all
cpcyc,volt,.001,5,0,60,0
!nsel,y,29.99,30.001
!nasel,y,-30.001,-29.99
!d,all,volt,0 ! Constrains the Volts DOF Vessel Cyc Symm
nsel,all
allsel,all
save
!
fini
/solu
HaloCur=.1/6/4
```

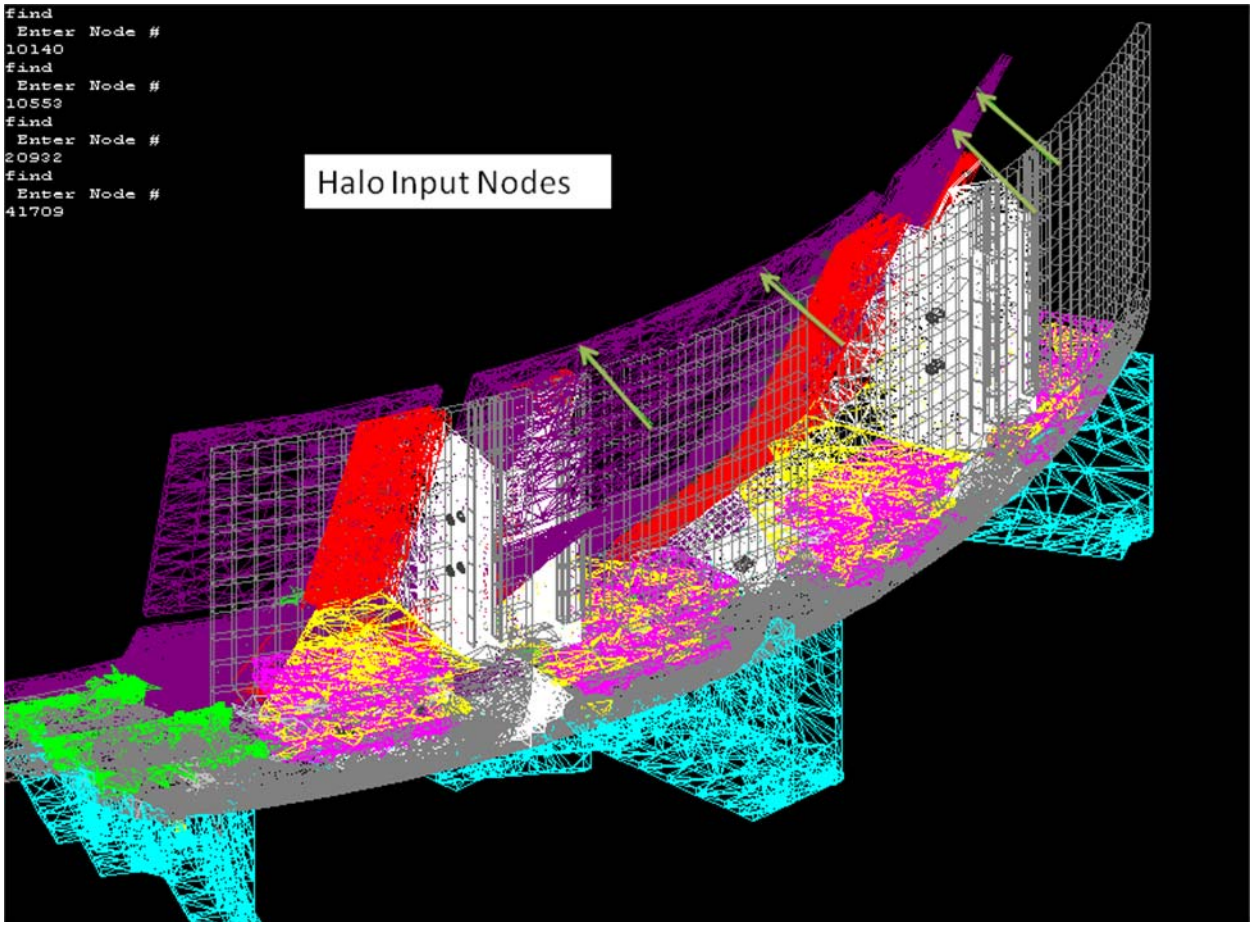


```
nodein1=10140
nodein2=10553
```

nodein3=20932
nodein4=41709
Nodeout=10841
!Output times [s]:
 t1= 0.0
 t2= 1.0E-03
 t3= 2.0E-03
 t4= 3.0E-03
 t5= 4.0E-03
 t6= 5.0E-03
 t7= 6.0E-03
 t8= 7.0E-03
 t9= 8.0E-03
t10= 0.01
t11= 0.01025
t12= 0.0105
t13= 0.01075
t14= 0.011
t15= 0.01125
t16= 0.0115
t17= 0.01175
t18= 0.012
t19= 0.01225
t20= 0.0125
t21= 0.01275
t22= 0.013
t23= 0.01325
t24= 0.0135
t25= 0.01375
t26= 0.014
t27= 0.01425
t28= 0.0145
t29= 0.01475
t30= 0.015
t31= 0.016
t32= 0.017
t33= 0.018
t34= 0.019
t35= 0.02
t36= 0.03
t37= 0.04
t38= 0.05
t39= 0.06
t40= 0.07
t41= 0.08
t42= 0.09

```
t43= 0.1
t44= 0.11
t45= 0.12
t46= 0.13
t47= 0.15
t48= 0.16
t49= 0.17
t50= 0.18
t51= 0.19
t52= 0.2
t53= 0.225
t54= 0.25



BackBz = -.4  !BackBz will be constant every only if BackBr=0. Otherwise it is constant
just on z=z0 to satisfy Div(B)=0
BackBr = -.3
z0=-.6 ! height at which Br is truely radial for Bz & BtR = 0
antype,4
!antype,static
trnopt,full
outres,all,last
autots,1
deltim,1,.5,3
kbc,0

time,.001
lswrite,1

*do,inum,1,44,1
time,t%inum%+100
*dim,vect%inum%,table,81,81,1,x,z,,5 ! Specfies a 81X 81 parameter table

*tread,vect%inum%,'VecPot_case_%inum%','txt' ! Reads the file 1.txt into the table

nall
BR=130000*12*3*2e-7 ! Toroidal current
*get,nmax,node,,num,max
*do,i,1,nmax
z=nz(i)
x=nx(i)

!           Applying Poloidal Fields
!d,i,ay,vect%inum%(x,z) ! Intrepolates and applies the Vector Potential on the node
                !/x removed because Ron's Files have been corrected for 1/r
```

```
d,i,ay,BackBz*x/2-BackBr*(z-z0)+vect%inum%(x,z) ! Intrepolates and applies the
Vector Potential on the node
                !/x removed because Ron's Files have been corrected for 1/r
!d,i,ay,BackBz*x/2-BackBr*(z-z0)! Applies only the background fields
!          Applying the Toroidal Field
d,i,az,-0.5*BR*log(x*x) ! applies vector potential for toroidal magnetic field
*enddo
d,all,ax,0.
*if,inum,gt,7,then
HaloCur=700000./6/4
*endif
*if,inum,gt,10,then
HaloCur=.1/6/4
*endif
f,Nodein1,amps,HaloCur
f,Nodein2,amps,HaloCur
f,Nodein3,amps,HaloCur
f,Nodein4,amps,HaloCur
!f,nodeout,amps,-HaloCur
lswrite,inum+1
*enddo


!
lssolve,1,40,1 ! solves 9 load steps
save
fini
/post1
plnstr,bsum
/exit
```

Appendix B
MACRO FOR STATIC STRUCTURAL ANALYSIS

```
/batch
/filename,struct2
!/pmacro
/nerr,,99999997,,0,,
/prep7
!resume,elect,db  ! resume your model

shpp,off

et,1,45                ! Use appropriate element type numbers
et,5,45
dof,delete
dof,ux,uy,uz
```

```
mp,dens,6,8900

ex,1,200e9     !Vessel
ex,5,117e9     !passive Plates
ex,8,200e9     !Vessel Shell
ex,10,200e9    !Diverto2 Support
ex,11,200e9    !ribs
ex,12,200e9    !PPL Support
ex,13,200e9    !Vessel Bracket
ex,14,200e9    !Vessel Bracket
ex,15,200e9    !Vessel Bracket
ex,17,200e9    !bolts
*do,imat,1,20
mp,dens,imat,8950
mp,prxy,imat,0.3
mp,dens,imat,8900
*enddo

/input,lowd,mod
eusel,mat,90
nelem

csys,5                  ! Use the same coordinate system as the one in magnetic analysis
nrotat,all
      ! Constraints the base of the structure
ddele,all
nsel,z,-3,-1.8
d,all,all,0.0
nsel,z,-1.47,-1.45
nrsel,x,1.5,2
d,all,all,0.0
nall
eall
!nsel,y,-15.001,-14.999
!nasel,y,14.999,15.001
!d,all,uy,0.0
cpdele,all,all
cpcyc,ux,.001,5,0,60,0
cpcyc,uy,.001,5,0,60,0
cpcyc,uz,.001,5,0,60,0
nall
eall
nall
eall
save
```

```
!
fini
/solu
!antype,4      ! Use 4 for dynamic analysis
antype,0     ! Use 0 for static analysis
!outres,all,3     ! writes results every three load steps.  Use smaller # for more resolution

!Output times [s]:
t1=1.00E-03 $t2=5.00E-03$t3=5.50E-03$t4=6.00E-03$t5=6.50E-03$t6=7.00E-
03$t7=7.50E-03$t8=8.00E-03$t9=8.50E-03$t10=9.00E-03
t11=9.50E-03$t12=1.00E-02$t13=1.10E-02$t14=1.20E-02$t15=1.30E-02$t16=1.40E-
02$t17=1.50E-02$t18=1.60E-02$t19=1.70E-02$t20=1.80E-02$t21=1.90E-02
t22=2.00E-02$t23=2.10E-02$t24=2.20E-02$t25=2.30E-02$t26=2.40E-02$t27=2.50E-
02$t28=2.60E-02$t29=2.70E-02$t30=2.80E-02$t31=2.90E-02$t32=3.00E-02
t33=3.50E-02$t34=4.00E-02$t35=4.50E-02$t36=5.00E-02$t37=5.50E-02$t38=6.00E-
02$t39=6.50E-02$t40=7.00E-02$t41=7.50E-02$t42=8.00E-02$t43=8.50E-02
t44=9.00E-02$t45=9.50E-02$t46=1.00E-01$t47=1.50E-01$t48=2.00E-01

!nsubst,100        ! For more finer results use larger #.
!betad,0.005         !Damping
kbc,0
fdele,all,all
lswrite,1

*do,inum,2,40,1
time,t%inum%
fdele,all,all
ldread,forc,inum,,,,elect2,rst,   ! Use the appropriate file name.
lswrite,inum+1
*enddo


!lssolve,4,6,1
lssolve,1,40,1
```

Appendix C
MACRO FOR DYNAMIC STRUCTURAL ANALYSIS

```
!!!(Used for P1-P5 Slow VDE)

/batch
/filename,Dynamic
!/pmacro
/nerr,,99999997,,0,,
/prep7
!resume,elect,db  ! resume your model (If needed to Obtain the Mesh)
```

```
shpp,off

et,1,45                 ! Use appropriate element type numbers
et,5,45
dof,delete
dof,ux,uy,uz

mp,dens,6,8900

ex,1,200e9     !Vessel
ex,5,117e9     !passive Plates
ex,8,200e9     !Vessel Shell
ex,10,200e9    !Divertor Support
ex,11,200e9    !ribs
ex,12,200e9    !PPL Support
ex,13,200e9    !Vessel Bracket
ex,14,200e9    !Vessel Bracket
ex,15,200e9    !Vessel Bracket
ex,17,200e9    !bolts
*do,imat,1,20
mp,dens,imat,8950
mp,prxy,imat,0.3
mp,dens,imat,8900
*enddo

/input,lowd,mod
eusel,mat,90
nelem

csys,5                  ! Use the same coordinate system as the one in magnetic analysis
nrotat,all
      ! Constraints the base of the structure
ddele,all
nsel,z,-3,-1.8
d,all,all,0.0
nsel,z,-1.47,-1.45
nrsel,x,1.5,2
d,all,all,0.0
! restrain vessel around ports
nsel,z,-.468,-.467
d,all,all,0.0
nall
eall
!nsel,y,-15.001,-14.999
!nasel,y,14.999,15.001
```

```
!d,all,uy,0.0
cpdele,all,all
cpcyc,ux,.001,5,0,60,0
cpcyc,uy,.001,5,0,60,0
cpcyc,uz,.001,5,0,60,0
nall
eall
nall
eall
save
!
fini
/solu
antype,4      ! Use 4 for dynamic analysis
!antype,0     ! Use 0 for static analysis
outres,all,1     ! writes results every sub step.  Use smaller # for more resolution
!Output times:
 t1= 0.0
 t2= 1.0E-03
 t3= 2.0E-03
 t4= 3.0E-03
 t5= 4.0E-03
 t6= 5.0E-03
 t7= 6.0E-03
 t8= 7.0E-03
 t9= 8.0E-03
t10= 0.01
t11= 0.01025
t12= 0.0105
t13= 0.01075
t14= 0.011
t15= 0.01125
t16= 0.0115
t17= 0.01175
t18= 0.012
t19= 0.01225
t20= 0.0125
t21= 0.01275
t22= 0.013
t23= 0.01325
t24= 0.0135
t25= 0.01375
t26= 0.014
t27= 0.01425
t28= 0.0145
t29= 0.01475
```

```
t30= 0.015
t31= 0.016
t32= 0.017
t33= 0.018
t34= 0.019
t35= 0.02
t36= 0.03
t37= 0.04
t38= 0.05
t39= 0.06
t40= 0.07
t41= 0.08
t42= 0.09
t43= 0.1
t44= 0.11
t45= 0.12
t46= 0.13
t47= 0.15
t48= 0.16
t49= 0.17
t50= 0.18
t51= 0.19
t52= 0.2
t53 =0.225
t54= 0.25

nsubst,10       ! For more finer results use larger #.
betad,0.005        !Damping
alphd,0.005        !Damping
kbc,0
fdele,all,all
time,.001
lswrite,1
time,100.0
lswrite,2
*do,inum,3,40,1
time,t%inum% + 100
fdele,all,all
ldread,forc,inum,,,,elect2,rst,   ! Use the appropriate file name.
time,t%inum% + 100
lswrite,inum
*enddo


!lssolve,4,6,1
                                        lssolve,1,40,1
```

Appendix D

From Art Brooks:

The Magnetic Potential needed to produce a (near) Uniform Magnetic Field in Cylindrical Coordinates

The magnetic flux density can be expressed in terms of the curl of a vector potential

$$\mathbf{B} = \nabla \times \mathbf{A} \tag{1.1}$$

In cylindrical coordinates equation (1.1) becomes

$$\nabla \times \mathbf{A} = \frac{1}{r}\begin{vmatrix} u_r & u_\theta & u_z \\ \frac{\partial}{\partial r} & \frac{\partial}{\partial \theta} & \frac{\partial}{\partial z} \\ A_r & rA_\theta & A_z \end{vmatrix} \tag{1.2}$$

Which expands to

$$B_r = \frac{1}{r}\left\{\frac{\partial A_z}{\partial \theta} - \frac{\partial (rA_\theta)}{\partial z}\right\}u_r \tag{1.3}$$

$$B_\theta = \frac{1}{r}\left\{\frac{\partial A_r}{\partial z} - \frac{\partial A_z}{\partial r}\right\}ru_\theta \tag{1.4}$$

$$B_z = \frac{1}{r}\left\{\frac{\partial (rA_\theta)}{\partial r} - \frac{\partial A_r}{\partial \theta}\right\}u_z \tag{1.5}$$

The above can be solved for the vector potential for a constant field in any one of the directions. An expression of the total field in terms of vector potential is obtained by superposition. However as will be shown below, while the expressions are linear in A and B, they are coupled in the coordinate directions, so that the presence of a radial field induces a non uniform vertical field. The specified field can be obtained only over a limited range from the field point chosen.

For the 2D field in a plane normal to the z-axis where $B_z = 0$ equation (1.5) can be satisfied by setting $A_r = A_\theta = 0$ so B_r and B_θ becomes functions of A_z only. Then (1.3) and (1.4) become

$$B_r = \frac{1}{r}\frac{\partial (A_z)}{\partial \theta} \tag{1.6}$$

$$B_\theta = -\frac{dA_z}{dr} \tag{1.7}$$

With a 1/r toroidal field $B_\theta = \frac{B_o R_o}{r}$ and $B_r = 0$ we have

$$dA_z = -\frac{B_o R_o}{r} dr \tag{1.8}$$

plus an arbitrary constant which can be set equal to zero.
Integrating both sides of the equation we have

$$A_z = -B_o R_o \ln(r) \tag{1.9}$$

For $B_\theta = 0$ equation (1.4) can be satisfied by setting $A_r = A_z = 0$ so B_r and B_z becomes functions of A_θ only. Then (1.3) and (1.5) become

$$B_r = -\frac{1}{r}\frac{\partial(rA_\theta)}{\partial z} \tag{1.10}$$

$$B_z = \frac{1}{r}\frac{\partial(rA_\theta)}{\partial r} \tag{1.11}$$

For constant B_r assume A_θ is a function of z only and integrate (1.10)

$$\begin{aligned} rA_\theta &= -B_r rz \\ A_\theta &= -B_r z \end{aligned} \tag{1.12}$$

For constant B_z assume A_θ is a function of r only and integrate (1.11)

$$\begin{aligned} rA_\theta &= \frac{B_z r^2}{2} \\ A_\theta &= \frac{B_z r}{2} \end{aligned} \tag{1.13}$$

For constant B_r and B_z we have from summing (1.12) and (1.13)

$$A_\theta = -B_r z + \frac{B_z r}{2} \tag{1.14}$$

Back substituting (1.14) into (1.10) to verify B_r we have

$$\begin{aligned} B_r &= -\frac{1}{r}\frac{\partial}{\partial z}\{-B_r zr + \frac{B_z r^2}{2}\} \\ &= -\frac{1}{r}(-B_z r) \\ &= B_r \text{ everywhere} \end{aligned} \tag{1.15}$$

However for B_z we get

$$
\begin{aligned}
B_z &= \frac{1}{r}\frac{\partial}{\partial r}\{-B_r zr + \frac{B_z r^2}{2}\} \\
&= \frac{1}{r}(-B_r z + B_z r) \\
&= B_z - B_r \frac{z}{r} \\
&= B_z \text{ only on the plane z= 0}
\end{aligned}
\tag{1.16}
$$

```
fini
/clear
!
! Test of producing B field from vector potential in cylindrical coordinates
!
BtR=1.  ! Telsa-meters   $Br=1
z0=0.5  ! height at which Br is truely radial for Bz & BtR = 0
Bz=1 ! Bz will be constant every only if Br=0. Otherwise it is constant just on z=z0 to
satisfy Div(B)=0
!
! Choose if y is up ('no' leaves z up)
!
yup='yes'
*if,yup,eq,'yes',then
csys,5
wpcsys,-1,5
*else
csys,1
*endif
!
/prep7
et,1,97,0
mp,murx,1,1.
cylind,.5,1.5,-1,1,0,90
esize,.1
vmesh,all!
!
! apply 1/R toroidal field, constant Bz field and near constant Br field
!  using magnetic vector potential thru body
!
nrotat,all ! into cyclindrical cord sys (1 for z up, 5 for y up)
d,all,ax,0.
!
*get,nmax,node,,num,max
*do,i,1,nmax
rr=nx(i)
zz=nz(i)
d,i,az,-.5*BtR*log(rr*rr)
d,i,ay,Bz*rr/2-Br*(zz-z0)
*enddo
!
fini
/solu  $solve  $fini
/post1
/WIND,ALL,OFF   $/WIND,1,LTOP  $/WIND,2,RTOP  $/WIND,3,LBOT  $/WIND,4,RBOT
/view,1,1  $/view,2,,1  $/view,3,,,1  $/view,4,1,1,1  $/vscale,1,.25,1
plvect,b,,,,vect,,on
```

Appendix E
Background Poloidal Fields…(By J. Boales&R. Hatcher)

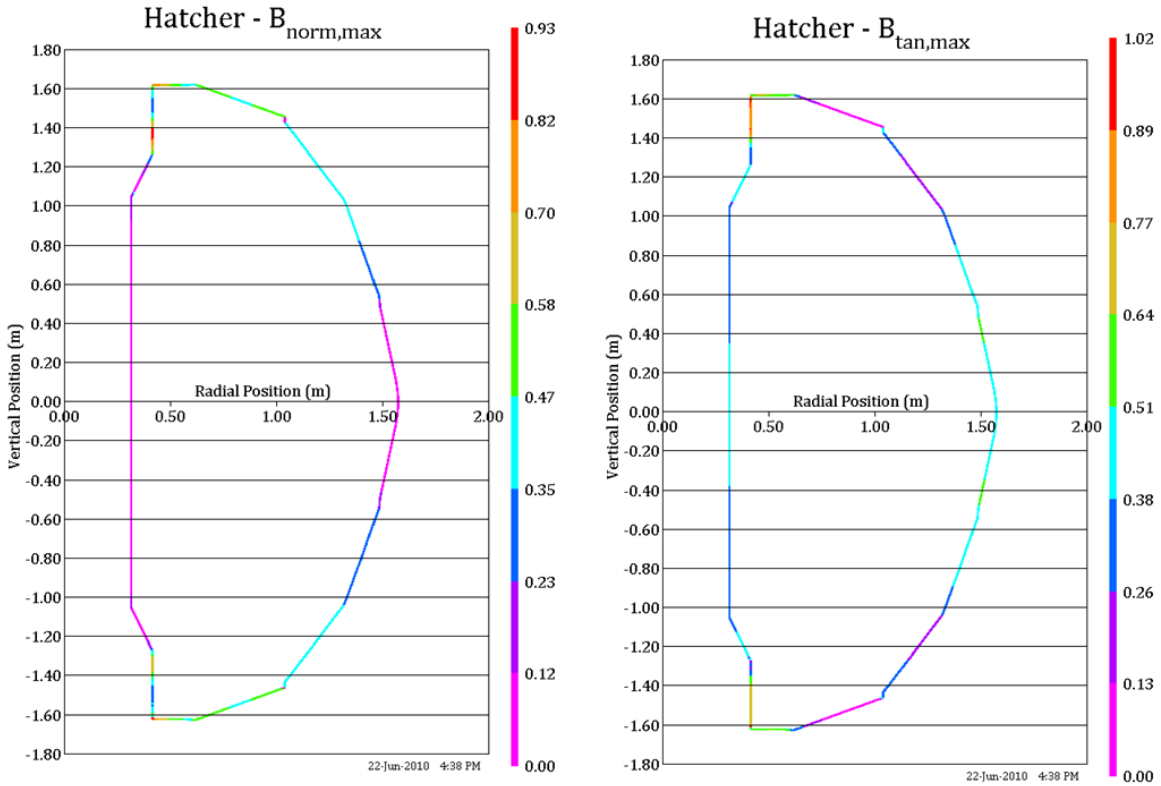

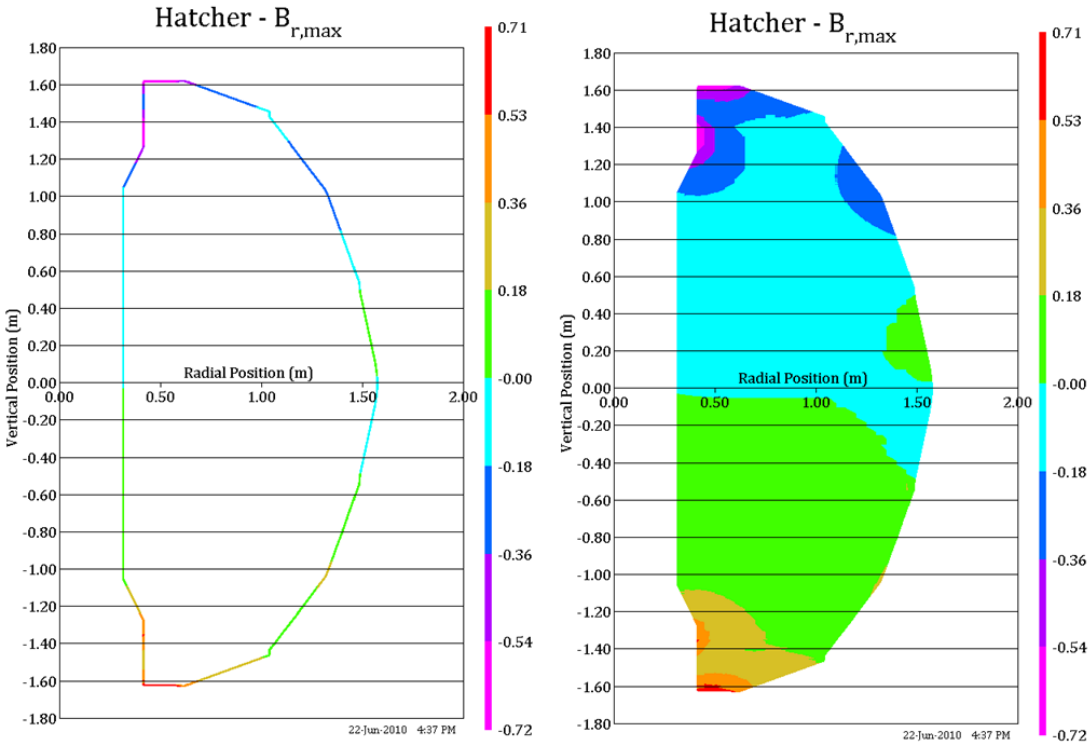

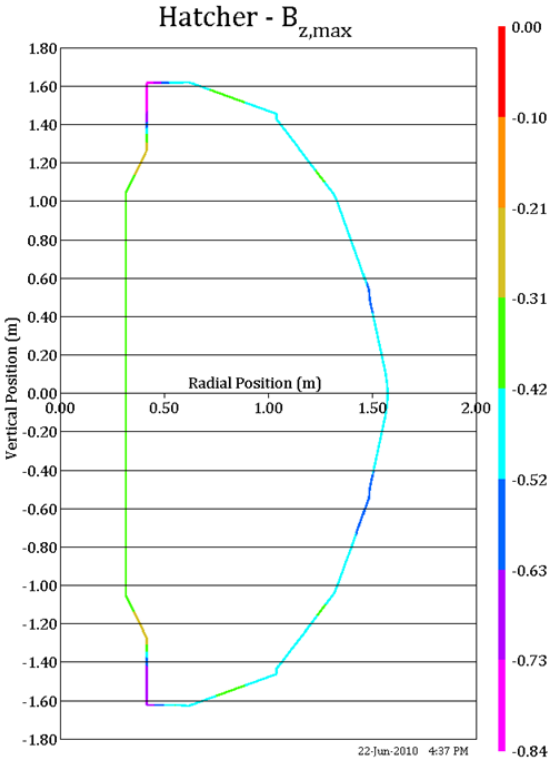
Hatcher - $B_{z,max}$
Vertical Position (m)
Radial Position (m)
0.00
0.50
1.00
1.50
2.00
1.80
1.60
1.40
1.20
1.00
0.80
0.60
0.40
0.20
0.00
-0.20
-0.40
-0.60
-0.80
-1.00
-1.20
-1.40
-1.60
-1.80
0.00
-0.10
-0.21
-0.31
-0.42
-0.52
-0.63
-0.73
-0.84
22-Jun-2010 4:37 PM

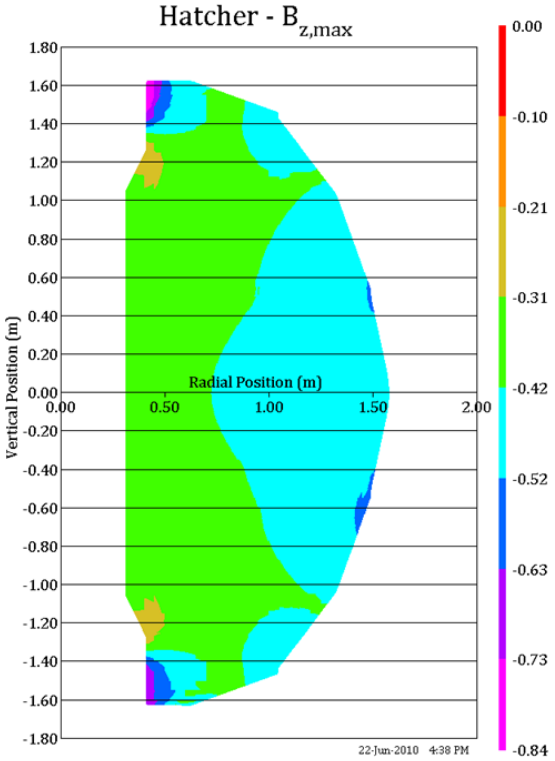
Hatcher - $B_{z,max}$
Vertical Position (m)
Radial Position (m)
0.00
0.50
1.00
1.50
2.00
1.80
1.60
1.40
1.20
1.00
0.80
0.60
0.40
0.20
0.00
-0.20
-0.40
-0.60
-0.80
-1.00
-1.20
-1.40
-1.60
-1.80
0.00
-0.10
-0.21
-0.31
-0.42
-0.52
-0.63
-0.73
-0.84
22-Jun-2010 4:38 PM

Attachment F
Passive Plate Bracket Weld QA Report

From J Boscoe To E Perry

Re: Welding of Vertical Straight (1053) and Vertical Curved Support Brackets (1055).

Because of fit-up - assembly gap issues on the above mentioned components ~~&~~ instructions (verbal) were given per Chrzanowski/Barnes to use 1/4" thick x 1/2" ~~gerwedge~~ wide bridge-transition pieces to overcome these gaps Due to worries about excessive installation time it was decided that doubling up on weld size, 1/8" fillet to 1/4" fillet would decrease required weld length by 1/2, or an increase of weld size from 1/8" fillet to 3/16" fillet would decrease the required weld length by 1/3. Welder - Tig torch accessibility for full length welds up both sides of pieces were also a factor in this decision. The design drawing - weld detail in question is EDB-1051. I believe it was intended for CR 70 to cover this (along with many other modifications - tweaking to original design). This change did not get included on CR 70.

In addition I noticed on inspection of the lower support-brackets that the unwelded portions of the vertical curved brackets #1055 ("bobsleds") are the 1/3 of length including the curved sections. My most recent concern was the remote possibility that this could adversely affect stress calculations

Attachement G
email from Michael Belll
On Mar 29, 2011, at 9:43 PM, Michael G. Bell wrote:

Masa,
You asked me to send you some estimates for the maximum forces that could affect the moly shields on the proposed *AE antenna.
The shields are L-shaped pieces of molybdenum sheet 0.040" thick that are 2" wide on one side and 1.3" wide on the other (data from drawing B-9D11037 and from Lane Roquemore). This cross-section is the same as that of the new moly shields fixed over the 24 RWM B_p coils just behind the graphite tiles at the top or bottom of the lower and upper passive plates, respectively. The two horizontal shields will span a distance
of 16" and the verticals will span 8" between their mounting studs.

When we were designing the moly shields for the B_pol sensors, Jim Bialek did a calculation of the eddy current induced in them by rapid changes in the poloidal field, such as during a disruption. He considered the case of a poloidal field of 0.8T disappearing in 3ms, which is a worst case. In this case, the eddy currents in the normal face of the shield reached a maximum of 2.8kA, limited by the resistance (i.e. determined by the rate of change of the flux, not the total flux change). The largest face of the shield (2" x 17.5") has an area of of about 0.023m^2, so the dipole moment induced in the shield is less than 2.8kA x 0.23m^2 = 64A.m^2. I then plugged these numbers into my code which
calculates the force and torque on a magnetic
dipole in NSTX. The worst case forces I calculated were 20N, less than 5 lbf, and the torque 25 N.m, i.e. 18 ft.lbf. Given that each of these is divided between two 1/4" bolts welded to the vessel and Macor standoffs 1.5" in diameter, these worst-case loads are not excessive. We had concluded the same thing when we analyzed their
use on the RWM sensors.

The calculation above assumed that the eddy currents flowed in the shields independently because they are insulated from each other at the corners. If all the insulators failed, then eddy currents could circulate in the loop formed by all four shields which has an area of 17.5" x 9.5" ‰ 0.1m^2. This could intercept a radial field up to 0.1T maximum for a total flux of 10mWb. I estimate that this loop has an inductance of about 1µH and a resistance of about 1m‡ for an L/R time of 1ms. If the field disappeared in 3ms (conservative), the induced current would be ~3kA (resistance limited). The radial force on each horizontal element due to a vertical field of 0.8T would then be about 1000N, about 220lbf (one would be pushed towards and one pulled away from the wall). The radial force on the vertical elements crossing the TF would be less than half this. These forces are much greater, but they should be within the capability of the shields and mounts to withstand. They also require that all four insulators fail to zero resistance and they result from truly awesome disruptions. I have suggested to Lane that we make the insulators between the shields out ot two layers of Micamat with the inner layer undercut so that any lithium condensing on the shields would have to bridge 4 gaps of about a millimeter to complete the circuit.

I believe that the risk of mechanical faiure of the proposed antenna due to eddy-current forces is low.

Michael
--

Michael Bell
Princeton Plasma Physics Laboratory
Email: MBell@pppl.gov
Mail: MS34, P.O. Box 451, Princeton, NJ 08543-0451 U.S.A.
Phone: +1-609-243-3282
FAX: +1-609-243-2874